

Durham E-Theses

Charming Decays And How To Calculate Them

CHRISTOS VLAHOS

How to cite:

VLAHOS, CHRISTOS (2022) Charming Decays And How To Calculate Them. Doctoral thesis, Durham University.

Use policy

The full-text may be used and/or reproduced, and given to third parties in any format or medium, without prior permission or charge, for personal research or study, educational, or not-for-profit purposes provided that:

- a full bibliographic reference is made to the original source
- a <https://etheses.durham.ac.uk/id/eprint/14454/> is made to the metadata record in Durham E-Theses
- the full-text is not changed in any way

The full-text must not be sold in any format or medium without the formal permission of the copyright holders.

Please consult the [full Durham E-Theses policy](#) for further details.

Charming Decays And How To Calculate Them

Christos Vlahos

A Thesis presented for the degree of
Doctor of Philosophy



Institute for Particle Physics Phenomenology
Department of Physics
Durham University
United Kingdom

May 2022

Charming Decays And How To Calculate Them

Christos Vlahos

Submitted for the degree of Doctor of Philosophy

May 2022

Abstract: In this work we focus on the phenomenology of the charm system, more specifically the description of D-mixing and the lifetimes of the D^0 , D^+ and D_s^+ meson. We start with a brief introduction of flavour physics and the role the charm quark plays in the Standard Model (SM). Then, we focus on more specialised techniques like the Weak Effective Theory (WET) and the Heavy Quark Effective theory (HQET) as well as the Heavy Quark Expansion (HQE), a framework built to express inclusive decays of heavy hadrons as a series of local operators. We continue with the description of the neutral meson mixing system in general before focusing on the D^0 case and discuss the peculiarities arising that make its theoretical description more difficult than the B system. We propose two different methods of tackling these issues and show that we can get results in the ballpark of the experimental measurements. Then, we move to the calculations of the D mesons lifetimes. Including the recently calculated Darwin operator contribution and D_s^+ Bag parameters, we present updated results for the total and semi-leptonic decay rates and their ratios. We conclude that after comparing our results with experimental measurements by the LHCb, Belle II and BESIII collaborations we can describe inclusive decays of charm mesons in the HQE framework albeit with large theoretical uncertainties. Finally, we suggest how this work could continue in the future and what new measurements would be needed to get more precise results.

Contents

Abstract	3
List of Figures	7
List of Tables	11
1 Introduction	17
1.1 The Standard Model	17
1.1.1 QCD	19
1.1.2 Electroweak Theory	19
1.2 Flavour Physics	23
1.2.1 CKM	23
1.2.2 Charm Quark and the GIM Mechanism	27
1.3 Rest of the Thesis	30
2 Theoretical Methods in Flavour Physics	33
2.1 Effective Theories	33
2.1.1 Weak Effective Theory	34
2.1.2 Heavy Quark Effective Theory	44
2.2 Heavy Quark Expansion	52

3	D-Mixing	61
3.1	Introduction to Neutral Meson Mixing	61
3.2	Mixing Observables	65
3.3	D-Mixing	68
3.4	HQE in D-Mixing	69
3.5	Alternative scale setting	75
4	Lifetimes of D Mesons	81
4.1	Introduction	81
4.2	Total Decay Rates	86
4.3	Determination of Non-perturbative Parameters	103
4.4	Numerical Results	107
5	Conclusion	119
A	Numerical Input to Chapter 4	123
B	LO Analytic Expressions for $\mathcal{C}_3^{(q_1\bar{q}_2)}$, $\mathcal{C}_G^{(q_1\bar{q}_2)}$ and $\mathcal{C}_{\rho_D}^{(q_1\bar{q}_2)}$	125
C	Derivation of $\Delta C = 0$ matrix elements in HQET	129
D	Calculation of Spectator Effects for Γ_{12} and $\Gamma(D)$	133
	Bibliography	149

List of Figures

1.1	The unitarity triangle for the first line of Equation (1.2.13)	27
1.2	Box diagrams contributing to the K^0 mixing amplitude (left) and $K_L \rightarrow \mu^+ \mu^-$ amplitude (right). The coupling in each vertex is included so that the colour matches the quark lines.	30
2.1	Tree level diagrams contributing to the process $c \rightarrow s \bar{u}$ in the full theory (left) and the effective theory (right). In the process from left to right the W boson has been integrated out and a four-quark operator has been created instead.	34
2.2	One-loop QCD correction diagrams in the SM. Gluon lines are shown in red. Their symmetric counterparts are not shown here.	35
2.3	The quark propagator and the heavy quark-gluon vertex in the HQET framework	46
3.1	The box diagrams contributing to D-mixing.	62

- 3.2 (a) Diagrams describing the mixing of neutral D mesons via intermediate $s\bar{s}$, $s\bar{d}$, $d\bar{s}$ and $d\bar{d}$ states in the “full” theory at LO-QCD (left) and NLO-QCD (right). The crossed circles denote the insertion of $\Delta C = 1$ operators of the effective Hamiltonian describing the charm-quark decay. The dependence on the renormalisation scale μ_1 in the Wilson coefficients cancels against the μ_1 dependence of the QCD corrections. (b) Diagram describing mixing of neutral D mesons at NLO-QCD in the HQE. The full dot indicates the insertion of $\Delta C = 2$ operators. The dependence on the renormalisation scale μ_2 cancels out between the QCD corrections to the diagram and the matrix elements of the corresponding $\Delta C = 2$ operators. 72
- 3.3 Scale dependence of $|\Gamma_{12}|$ at LO-QCD (blue) and NLO-QCD (orange) 76
- 3.4 Scale dependence of $|\Gamma_{12}^{ss}|$ at LO-QCD (blue) and NLO-QCD (orange) 76
- 3.5 Comparison of the ϵ dependence of Ω at LO-QCD (blue) and NLO-QCD (pink) for different values of μ : the central lines corresponds to $\mu = m_c$ while the other lines to $\mu = 1$ GeV and $\mu = 2m_c$. In the label of each plot are stated the scheme used, the dimension-six operator basis and the values of the non-perturbative matrix elements. 79
- 4.1 The diagrams describing contributions to the HQE in Equation (2.2.25). The crossed circles denote the $\Delta C = 1$ operators Q_i of the effective Hamiltonian while the squares denote the local $\Delta C = 0$ operators \mathcal{O}_i and $\tilde{\mathcal{O}}_i$. The two-loop and the phase space enhanced one-loop diagrams correspond respectively to the two-quark operators \mathcal{O}_i and to the four-quark operators $\tilde{\mathcal{O}}_i$ in the HQE. 88
- 4.2 Scale dependence of the Wilson coefficient combination $\mathcal{N}_a = 3C_1^2 + 3C_2^2 + 2C_1C_2$ 89
- 4.3 Scale dependence of the coefficient of the chromomagnetic operator. 92
- 4.4 Scale dependence of the coefficient of the Darwin operator. 93

4.5	Spectator quark effects in the HQE expansion: WE (left), PI (middle) and WA (right).	93
4.6	Diagrams describing the eye-contractions.	94
4.7	A comparison of the HQE prediction for the charm observables in the kinetic scheme (blue) with the corresponding experimental data (green).115	

List of Tables

2.1	Terms included in the perturbative expansion of the Wilson coefficients calculation.	37
3.1	Numerical results of Γ_{12}/M_{12} for B_s and B_d meson mixing after applying the ϵ renormalisation scale setting.	80
4.1	Status of the experimental determinations of the lifetime and the semi-leptonic branching fractions of the lightest charmed mesons ($D^q \in \{D^0, D^+, D_s^+\}$). All values are taken from the PDG [1] apart from the semi-leptonic D_s^+ -meson decays which were recently measured by the BESIII Collaboration [2].	82
4.2	Numerical values of the strong coupling α_s evaluated at different scales and different loop order, obtained using the RunDec package [3].	82
4.3	Comparison of the Wilson coefficients at NLO-QCD (LO-QCD) for different values of μ_1	87
4.4	Numerical values of $\Gamma_3^{\text{LO}} = \Gamma_3^{(0)}$ and $\Gamma_3^{\text{NLO}} = \Gamma_3^{(0)} + \alpha_s(m_c)/(4\pi)\Gamma_3^{(1)}$ using different schemes for the c -quark mass. The uncertainties are obtained by varying the renormalisation scale μ_1 between 1 GeV and 3 GeV.	90
4.5	Comparison of the combinations $C_{\text{WE,PI,WA}}^{S,O}$, respectively at LO- and NLO-QCD, for different values of the renormalisation scale μ_1	97

4.6	Dimension-six contributions to D -meson decay widths (see Equation (4.2.43)) (in ps^{-1}) and split up into LO-QCD and NLO-QCD corrections within different mass schemes and both in VIA and using the HQET SR for Bag parameters.	99
4.7	Dimension-seven contributions to D -meson decay widths (see Equation (4.2.58)) in ps^{-1} within VIA in the kinetic mass scheme.	102
4.8	Different determinations of $\mu_\pi^2(B)$ available in the literature.	103
4.9	Values of $\rho_D^3(H)$ for B and D mesons in VIA and using HQET SR for Bag parameters for three different choices of α_s in Equation (4.3.12).	106
4.10	Central values of the charm observables in different quark mass schemes using VIA for the matrix elements of the 4-quark operators compared to the corresponding experimental values (last column).	108
4.11	Central values of the charm observables in different quark mass schemes using HQET sum rule results [4,5] for the matrix elements of the 4-quark operators compared to the corresponding experimental values (last column).	109
4.12	HQE predictions for all the ten observables in the kinetic scheme (second column), using HQET SR results for the Bag parameters. The first uncertainty is parametric, the second and third uncertainties are due to μ_1 - and μ_0 -scales variation, respectively. The results are compared with the corresponding experimental measurements (third column).	110
A.1	Numerical input used in our analysis.	123
A.2	Numerical values of the HQET Bag parameters [4,5] evaluated through a traditional HQET sum rule at $\mu_0 = 1.5 \text{ GeV}$. The B_i^q and ϵ_i^q include the corresponding δ_i^{qq} and the column with δ_i^{ss} has been removed because it only exists in the sum with the valence parts, whereas δ_i^{qq} are present because we have $\delta_i^{ud/du}$	124

Declaration

The work in this thesis is based on research carried out in the Department of Physics at Durham University. No part of this thesis has been submitted elsewhere for any degree or qualification.

The contents of Chapter 3 are based upon joint research with my supervisor Prof. Alexander Lenz and fellow PhD candidate (now Dr) Maria Laura Piscopo and is presented in [6]. This work was also published as conference proceedings for CHARM 2020 [7].

The contents of Chapter 4 are based upon joint work with Daniel King, Prof. Alexander Lenz, Maria Laura Piscopo, Dr Thomas Rauh and Dr Aleksey Rusov and is presented in [8], currently under review. My work in this project was programming all terms contributing to the inclusive decay of D mesons and independently carrying out the numerical analysis.

Copyright © 2022 Christos Vlahos.

The copyright of this thesis rests with the author. No quotation from it should be published without the author's prior written consent and information derived from it should be acknowledged.

Acknowledgements

First and foremost, I would like to thank my supervisor Alex Lenz for his constant guidance and advice over the last three and a half years. His expertise in physics and his advice in general have made me grow from a student to a researcher. I would also like to thank Frank Krauss for his supervision over the first year as well as Valya Khoze for taking the official role of my supervisor during the last year when Alex left Durham, enabling me to continue and finish my work. I must also extend my thanks to IPPP for giving me this chance to continue my studies and to STFC for funding my work.

One of the greatest aspects of my work has been the collaboration with great people that helped me improve and grow. Therefore, I would like to thank Maria Laura Piscopo, Aleksey Rusov, Danny King and Thomas Rauh for a very enjoyable collaboration. I need to extend my thanks to everyone at the IPPP for creating such an amazing atmosphere at work. In particular, I would like to thank Kevin, Andrew, Parisa, Joe, Maria Laura, Henry, Marian and Alan who shared an office with me. IPPP has one of the best public outreach teams and it has been my honour being part of it. It has been really fun and very rewarding at the same time.

Beyond work, I would like to thank Ustinov College for welcoming me. The college system is one of the things that make student life in Durham so special and I was glad I was part of such a wonderful and diverse community. Therefore, I would like to thank Glenn McGregor and all the staff that is working hard to make Ustinov an

amazing home for everyone. I also need to thank Anna Gangi and all the porters. They have been incredibly helpful all these years to not only just me but everyone in college. During my time living in college I had many flatmates. I would like to thank them all for being a great company and making my experience in Durham even better. I can not name them all here but I would like to specifically mention Tom, Dori, Scarlett, Matt, Connor, Rachel and Ryan for making all these months during the pandemic go by with lots of fun.

I consider myself lucky being part of the Ustinov GCR. For three years I was involved with an incredible group of people trying to make college experience as special as possible for all Ustinovians. While in Ustinov, I had the chance to meet my girlfriend Vera who I thank for her love and support in the last three years and for pushing me to always become better (and for introducing me to Ultimate Frisbee).

There are two clubs that I had the pleasure of being a part of and will always have close to my heart; the Ustinov Basketball Club and the Spin Doctors. I do not have the space to thank everyone separately but I would like to thank Kevin, Giorgio and Alberto for being constantly on the court with me playing ball and for our endless discussions as well as Vera, Diane and Jake for freezing out together on the pitch in the middle of winter throwing the disk.

Finally I would like to thank my parents for their support over all the years I have been in academia and in UK and my sister Ioanna for being there for me whenever I needed her, including proofreading this thesis.

Chapter 1

Introduction

Particle physics tries to describe the fundamental particles of the Universe and their interactions. The ultimate goal is the development of a theory that can explain all physical observations at a small scale. Although we are not there yet, after decades of research and discoveries we have a working theory that describes three of the four (known) fundamental forces, and the currently known particle content. This is the Standard Model (SM) of particle physics. In the rest of the chapter we will introduce the SM and we will discuss in particular some specific features of it that are the basis of the work developed in the remainder of the thesis.

1.1 The Standard Model

The SM is the culmination of many years of developing theories trying to explain the laws of physics at the smallest scales. Mathematically it is defined as a quantum field theory (QFT) with its dynamics described by the SM Lagrangian, \mathcal{L}_{SM} . Historically one could say that the first part of the SM was the development of Quantum Electrodynamics (QED), a theory that describes electromagnetism at the quantum level. This was achieved by the work of many physicists like Dirac [9], Feynman [10–12], Schwinger [13, 14] and Tomonaga [15]. Since then many more steps

were taken towards the SM, including the development of QCD [16–18], the development of a weak theory [19, 20], its unification with QED [20–22], and the Higgs mechanism [23–25].

The Lagrangian of the SM is given by

$$\begin{aligned}
 \mathcal{L}_{SM} &= -\frac{1}{4}F_{\mu\nu}F^{\mu\nu} \\
 &+ \bar{\psi}\not{D}\psi \\
 &- \bar{\psi}_i y_{ij} \psi_j H + h.c. \\
 &+ |D_\mu H|^2 - V(H) ,
 \end{aligned} \tag{1.1.1}$$

where the RHS terms are the self-interactions of the gauge fields, the kinetic terms of the fermions and their interactions with the gauge fields, the interactions of the fermions with the Higgs field and the kinetic term and self-interactions of the Higgs field. The gauge symmetry of the SM is

$$SU(3)_c \times SU(2)_L \times U(1)_Y \rightarrow SU(3)_c \times U(1)_{EM} , \tag{1.1.2}$$

where the $SU(3)_c$ is the gauge symmetry of QCD (c stands for the colour charge) and $SU(2)_L \times U(1)_Y$ is the symmetry of the electroweak sector (L stands for left chirality and Y for the weak hypercharge). The arrow shows the spontaneous symmetry break of the electroweak symmetry to $U(1)_{EM}$ (EM stands for electromagnetism). Furthermore the SM is symmetric under the Poincare group. In the end, all renormalisable terms that obey the gauge and Poincare symmetries are included in Equation (1.1.1).

The particle content of the SM can be split into matter (fermions), force mediators (vector bosons) and the Higgs boson (scalar boson) that is responsible for giving mass to particles. In the next two sections we will look into the separate parts of the SM and present them in more detail.

1.1.1 QCD

Quantum Chromodynamics (QCD) is the non-abelian (i.e. its generators do not commute) gauge theory that describes the strong nuclear force with gauge group $SU(3)_c$. The $SU(N)$ group has $(N^2 - 1)$ generators, so in the QCD case we have 8 generators denoted as T^a . The colour label c can take the ‘values’ *red*, *blue*, and *green* (these have nothing to do with the actual colours of the visible EM spectrum). The strong force is mediated via the gluon particle. Since there are 8 generators in the gauge group, there are 8 gluons too. If we isolate the pure QCD terms from Equation (1.1.1) we get:

$$\mathcal{L}_{QCD} = -\frac{1}{4}F_{\mu\nu}^a F_a^{\mu\nu} + \bar{\psi}_i(i\not{D}_{ij} - m\delta_{ij})\psi_j, \quad (1.1.3)$$

where the mass term originates from the Yukawa term of the SM Lagrangian. Under the $SU(3)_c$ group the quark fields lie in the fundamental representation while the gluons lie in the adjoint. The field strength tensor in QCD reads

$$F_{\mu\nu}^a = \partial_\mu A_\nu^a - \partial_\nu A_\mu^a + g_s f^{abc} A_\mu^b A_\nu^c, \quad (1.1.4)$$

where A_μ^a is the gluon field and a runs from 1 to 8, g_s is the coupling constant of QCD and f^{abc} are the structure constants of the gauge group that satisfy $[T^a, T^b]_{ij} = if^{abc}T_{ij}^c$. Note that f^{abc} vanishes for abelian groups such as $U(1)$ in QED. In that case the field strength tensor is reduced to the first two terms of Equation (1.1.4). As a consequence the gluons self-interact while the photon does not.

1.1.2 Electroweak Theory

The rest of the SM Lagrangian describes the electroweak theory and the Higgs mechanism through which the symmetry $SU(2)_L \times U(1)_Y$ spontaneously breaks to $U(1)_{EM}$ and the fermions and the weak gauge bosons obtain their mass. As the subscript L indicates, the electroweak sector distinguishes between left and right handed fermions (theoretically proposed by [26] and experimentally verified by [27]).

This experimentally observed parity violation can be theoretically demonstrated by putting left handed fermions in the doublet representation of $SU(2)$ while the right handed are singlets. The field strength tensors of this theory are

$$W_{\mu\nu}^\alpha = \partial_\mu W_\nu^\alpha - \partial_\nu W_\mu^\alpha + g_1 \epsilon^{abc} W_\mu^b W_\nu^c, \quad (1.1.5)$$

$$B_{\mu\nu} = \partial_\mu B_\nu - \partial_\nu B_\mu, \quad (1.1.6)$$

where the first line describes the field strength tensors of the weak force (notice the similarity to the QCD one, where the structure constant is now simply the Levi-Civita tensor) and the second line is the $U(1)_Y$ field strength tensor. W_μ^a are the three gauge boson fields of the $SU(2)_L$ theory and B_μ is the boson field of the $U(1)_Y$ theory. Mass terms for the gauge bosons can not be simply added, since they are not gauge invariant. However, the weak interaction seems to have a very short range indicating very massive mediators. How do the W and Z bosons (and the fermions of course) obtain their mass?

This is where the Higgs mechanism comes into play, causing the spontaneous symmetry breaking of the electroweak symmetry group as mentioned above. All that is needed is the addition of a complex scalar field with a certain potential term.

The Higgs field is introduced as an $SU(2)_L$ doublet,

$$H = \begin{pmatrix} \phi^+ \\ \phi^0 \end{pmatrix}, \quad (1.1.7)$$

where the ϕ^+, ϕ^0 are complex scalar fields. The potential is given by

$$V(H) = \mu^2 (H^\dagger H) + \lambda (H^\dagger H)^2, \quad (1.1.8)$$

where for $\mu^2 < 0$ there is a non-trivial minimum of the Higgs potential at

$$\langle H \rangle = \frac{v}{\sqrt{2}} = \sqrt{\frac{-\mu^2}{2\lambda}}. \quad (1.1.9)$$

Due to this non-zero VEV the Higgs field breaks the electroweak symmetry down to the $U(1)_{EM}$. Expanding the Higgs field from Equation (1.1.7) around the VEV we get

$$H = \begin{pmatrix} 0 \\ \frac{v+h}{\sqrt{2}} \end{pmatrix}, \quad (1.1.10)$$

where h is the scalar field associated with the Higgs boson. Below we will shortly show how the Higgs mechanism gives the gauge bosons their masses. For the fermion case, see Section 1.2.1.

Gauge Boson Masses

The mass of the W and Z bosons comes from the third line of Equation (1.1.1) and more specifically the $|D_\mu H|^2$ term. To see it clearly we use Equation (1.1.10) to expand the covariant derivative

$$D_\mu = \partial_\mu - ig_1 W_\mu^a \frac{\sigma^a}{2} - ig_2 Y_L B_\mu, \quad (1.1.11)$$

where g_1 , g_2 and Y_L are the coupling for the $SU(2)_L$ interaction, the coupling of the $U(1)_Y$ interaction, and the weak hypercharge respectively. For the mass terms we keep only the terms proportional to v^2 as the terms including the field h are associated with interactions of the Higgs boson with the W and Z bosons. So the mass terms are

$$\begin{aligned} \mathcal{L}_{gauge-mass} &= \left| \frac{-i}{2\sqrt{2}} \begin{pmatrix} g_2 B_\mu + g_1 W_\mu^3 & g_1 W_\mu^1 - ig_1 W_\mu^2 \\ g_1 W_\mu^1 + ig_1 W_\mu^2 & g_2 B_\mu - g_1 W_\mu^3 \end{pmatrix} \begin{pmatrix} 0 \\ v \end{pmatrix} \right|^2 \\ &= \frac{v^2}{8} (g_1^2 (W^1)^2 + g_2^2 B^2 + g_1^2 (W^2)^2 + g_1^2 (W^3)^2 - 2g_1 g_2 B^\mu W_\mu^3). \end{aligned} \quad (1.1.12)$$

Now we rewrite the above equation by defining 4 new fields, as linear combinations of the old ones

$$\begin{aligned} W_\mu^\pm &= \frac{1}{\sqrt{2}} (W_\mu^1 \mp iW_\mu^2), \\ Z_\mu &= c_w W_\mu^3 - s_w B_\mu, \end{aligned} \quad (1.1.13)$$

$$A_\mu = s_w W_\mu^3 + c_w B_\mu ,$$

where $s_w = \sin \theta_w$, $c_w = \cos \theta_w$ and $\theta_w = \tan^{-1} \left(\frac{g_2}{g_1} \right)$ widely known as the weak angle, first introduced by Glashow [20]. We recognise this new basis as the fields of the actual W and Z bosons as well as the photon. In fact, in this basis the photon remains massless as it should and we get

$$\begin{aligned} m_W &= \frac{g_1 v}{2} , \\ m_Z &= \frac{v}{2} \sqrt{g_1^2 + g_2^2} , \end{aligned}$$

as the masses of the weak bosons.

Fermion couplings

For the fermion couplings we will use the mass basis introduced above for the gauge fields, thus rewriting the covariant derivative

$$D_\mu = \partial_\mu - \frac{ig_1}{2\sqrt{2}} (W_\mu^+ \sigma^+ + W_\mu^- \sigma^-) - \frac{ig_1}{\cos \theta_w} \left(\frac{\sigma^3}{2} - \sin^2 \theta_w Q \right) Z_\mu - ieQA_\mu , \quad (1.1.14)$$

where $Q = \frac{\sigma^3}{2} + Y$ and corresponds to the electric charge, $\sigma^\pm = \sigma^1 \pm i\sigma^2$, and e the electron charge satisfying $e = g_1 \sin \theta_w$. Now if we consider the kinetic part of the SM Lagrangian regarding the quarks and expand it to separated terms we get

$$\mathcal{L} = \bar{Q}_L (i\not{D}) Q_L + \bar{u}_R (i\not{D}) u_R + \bar{d}_R (i\not{D}) d_R , \quad (1.1.15)$$

where $Q_L = \begin{pmatrix} u_L \\ d_L \end{pmatrix}$. After substituting Equation (1.1.14) we obtain

$$\mathcal{L} = \bar{Q}_L (i\not{\partial}) Q_L + g_1 \left(W_\mu^+ J_{W,Q}^{\mu+} + W_\mu^- J_{W,Q}^{\mu-} + Z_\mu J_{Z,Q}^\mu \right) + e A_\mu J_{A,Q}^\mu , \quad (1.1.16)$$

where

$$J_{W,Q}^{\mu+} = \frac{1}{\sqrt{2}} \bar{u}_L \gamma^\mu d_L ,$$

$$\begin{aligned}
J_{W,Q}^{\mu-} &= \frac{1}{\sqrt{2}} \bar{d}_L \gamma^\mu u_L , \\
J_{Z,Q}^\mu &= \frac{1}{\cos^2 \theta_W} \left[\left(\frac{1}{2} - \frac{2}{3} \sin^2 \theta_W \right) \bar{u}_L \gamma^\mu u_L + \left(-\frac{1}{2} + \frac{1}{3} \sin^2 \theta_W \right) \bar{d}_L \gamma^\mu d_L \right. \\
&\quad \left. - \frac{2}{3} \sin^2 \theta_W \bar{u}_R \gamma^\mu u_R + \frac{1}{3} \sin^2 \theta_W \bar{d}_R \gamma^\mu d_R \right] , \\
J_{A,Q}^\mu &= \frac{2}{3} \bar{u} \gamma^\mu u - \frac{1}{3} \bar{d} \gamma^\mu d .
\end{aligned} \tag{1.1.17}$$

1.2 Flavour Physics

In Section 1.1.2 we mentioned how the left handed fermions can be expressed as doublets of the $SU(2)_L$, i.e

$$Q_L = \begin{pmatrix} u_L \\ d_L \end{pmatrix} , \quad L_L = \begin{pmatrix} \nu_e \\ e_L \end{pmatrix} .$$

Here the quark doublet Q_L consists of two component Dirac spinors of the up and down quark with weak isospin $+1/2$ and $-1/2$ respectively. The lepton doublet L_L consists of two Dirac spinors of the neutrino and the lepton with weak isospin $+1/2$ and $-1/2$ respectively. It was later discovered that there are two more (heavier) copies of these doublets and in total we have three generations of fermions. Flavour physics studies specifically these different types of fermions and their interactions.

1.2.1 CKM

The way fermions obtain their masses is encoded in the Yukawa interaction term [28] (third line of Equation (1.1.1)) since terms of the form $m_Q (\bar{Q}_L Q_R + \bar{Q}_R Q_L)$ would not be gauge invariant under $SU(2)_L$. The Yukawa Lagrangian for the interaction of fermions with the Higgs field is

$$\mathcal{L}_{Yukawa} = \bar{\mathbf{Q}}_L \hat{Y}^u \tilde{H} \mathbf{u}_R + \bar{\mathbf{Q}}_L \hat{Y}^d H \mathbf{d}_R + h.c. , \tag{1.2.1}$$

where $\overline{\mathbf{Q}}_L$ has three components (as many generations of fermions) and each component is an $SU(2)_L$ doublet i.e.

$$Q_{1,L} = \begin{pmatrix} u_L \\ d_L \end{pmatrix} ; \quad Q_{2,L} = \begin{pmatrix} c_L \\ s_L \end{pmatrix} ; \quad Q_{3,L} = \begin{pmatrix} t_L \\ b_L \end{pmatrix} . \quad (1.2.2)$$

$\hat{Y}^{u,d}$ are the complex Yukawa coupling matrices of the up- and down-type quarks. Finally, $\mathbf{u}_R, \mathbf{d}_R$ are three-dimensional vectors of the right hand spinors of the up and down-type quarks respectively. Notice also that in order to give the masses to the quarks we need to introduce a modified Higgs field that depends on the original one:

$$\tilde{H} = i\sigma_2 H^* . \quad (1.2.3)$$

Now, if we replace the Higgs field with its expression in Equation (1.1.10) and keep only the terms proportional to its VEV we get:

$$\mathcal{L}_{Yukawa} \supset \frac{v}{\sqrt{2}} \overline{\mathbf{u}}_L \hat{Y}^u \mathbf{u}_R + \frac{v}{\sqrt{2}} \overline{\mathbf{d}}_L \hat{Y}^d \mathbf{d}_R + h.c. . \quad (1.2.4)$$

which looks like fermion mass terms. The Yukawa matrices in general do not need to be diagonal. However, in order to get diagonal mass terms we will need to rotate the basis of the quark eigenstates. The way to do this is to apply the singular value decomposition and change from the weak eigenstate basis to the mass eigenstate one. To do so we perform the transformation

$$\begin{aligned} \mathbf{u}_{L,R} &\rightarrow U_{L,R}^u \mathbf{u}_{L,R} \\ \mathbf{d}_{L,R} &\rightarrow U_{L,R}^d \mathbf{d}_{L,R} \end{aligned} \quad (1.2.5)$$

where the matrices $U_{1,2}$ are unitary. In order for the Lagrangian terms to remain unchanged the mass matrices need to transform accordingly

$$M^u = \frac{v}{\sqrt{2}} \hat{Y}^u \rightarrow \frac{v}{\sqrt{2}} (U_L^u)^\dagger \hat{Y}^u U_R^u = \begin{pmatrix} m_u & & \\ & m_c & \\ & & m_t \end{pmatrix} ,$$

$$M^d = \frac{v}{\sqrt{2}} \hat{Y}^d \rightarrow \frac{v}{\sqrt{2}} (U_L^d)^\dagger \hat{Y}^d U_R^d = \begin{pmatrix} m_d & & \\ & m_s & \\ & & m_b \end{pmatrix}. \quad (1.2.6)$$

Now we can see how this transformation changes the neutral and charged currents of Equation (1.1.18). The combinations $\bar{q}_{L,R} \gamma^\mu q_{L,R}$ remain unchanged under the change of basis. So the neutral currents remain as they are with the mass eigenstates. The charged current however changes. See for example the W^+ current:

$$J_{W,Q}^{\mu+} \rightarrow \bar{\mathbf{u}}_L (U_L^u)^\dagger \gamma^\mu U_L^d \mathbf{d}_L = \bar{\mathbf{u}}_L V_{CKM} \gamma^\mu \mathbf{d}_L, \quad (1.2.7)$$

where we have introduced the Cabibbo-Kobayashi-Maskawa (CKM) matrix as

$$V_{CKM} \equiv (U_L^u)^\dagger U_L^d. \quad (1.2.8)$$

In exactly the same way we can show the transformation of the negative charged current, with the hermitian CKM matrix. Although the CKM matrix could theoretically be diagonal, it has been shown experimentally that it is not. These non-diagonal elements are responsible for the interactions between the different generations of quarks.

Historically the CKM matrix was first proposed as a 2×2 matrix in 1963 by Cabibbo [29]. However, ten years later the current form of the matrix was expanded to its current form by Kobayashi and Maskawa [30] (even before the c, b, t quarks were discovered). A general $n \times n$ complex matrix has $2n^2$ parameters. Using its unitarity property, the number of free parameters is reduced to n^2 and if we discard unphysical phases we end up with $n(n-1)/2$ real parameters and $(n-1)(n-2)/2$ phases. In case of the SM with 3 generations of quarks this leaves 3 real parameters and 1 phase. The complex phase is the source of CP violation in the SM. This is something that can only happen with at least 3 generations of quarks, as for $n=2$

no complex phase is possible. The current CKM matrix can be written in detail as

$$V_{CKM} = \begin{pmatrix} V_{ud} & V_{us} & V_{ub} \\ V_{cd} & V_{cs} & V_{cb} \\ V_{td} & V_{ts} & V_{tb} \end{pmatrix} = \begin{pmatrix} 0.974 & 0.225 & 0.004 - 0.001i \\ -0.225 - 0.0i & 0.974 - 0.0i & 0.042 \\ 0.006 - 0.001i & -0.041 - 0.0i & 0.999 \end{pmatrix}, \quad (1.2.9)$$

where the CKM elements are calculated based on input from the CKMfitter group [31] (note that numbers are rounded and errors are omitted here). As we can see, the diagonal elements are dominant (and close to 1) but the non-diagonal are still non-zero. This implies that a quark is more likely to decay to same generation quark (e.g. $t \rightarrow b$), than “jump” between generations¹.

CKM Parametrization

There are two widely used ways of parametrizing the CKM matrix. The first one parametrizes the CKM elements in terms of three angles, θ_{23}, θ_{12} and θ_{13} and one phase δ_{13} as

$$V_{CKM} = \begin{pmatrix} c_{12}c_{13} & s_{12}c_{13} & s_{13}e^{-i\delta_{13}} \\ -s_{12}c_{23} - c_{12}s_{23}s_{13}e^{i\delta_{13}} & c_{12}c_{23} - s_{12}s_{23}s_{13}e^{i\delta_{13}} & s_{23}c_{13} \\ s_{12}s_{23} - c_{12}c_{23}s_{13}e^{i\delta_{13}} & -c_{12}s_{23} - s_{12}c_{23}s_{13}e^{i\delta_{13}} & c_{23}c_{13} \end{pmatrix}, \quad (1.2.10)$$

where $s_{ij} = \sin \theta_{ij}$ and $c_{ij} = \cos \theta_{ij}$. This is called the Standard Parametrization [32].

The other parametrization is an approximation that is based on the experimental hierarchy $s_{13} \ll s_{23} \ll s_{12} \ll 1$ by introducing the parameter $\lambda \approx V_{us}$ and perform a Taylor expansion in this parameter. There are 3 more parameters (A, ρ, η) introduced defined as

$$\begin{aligned} s_{12} &= \lambda = \frac{|V_{us}|}{\sqrt{|V_{ud}|^2 + |V_{us}|^2}}, \\ s_{23} &= A\lambda^2 = \lambda \left| \frac{V_{cb}}{V_{us}} \right|, \end{aligned} \quad (1.2.11)$$

¹Only if the decay is possible, e.g. a b quark is most likely to decay in a c quark and not a t .

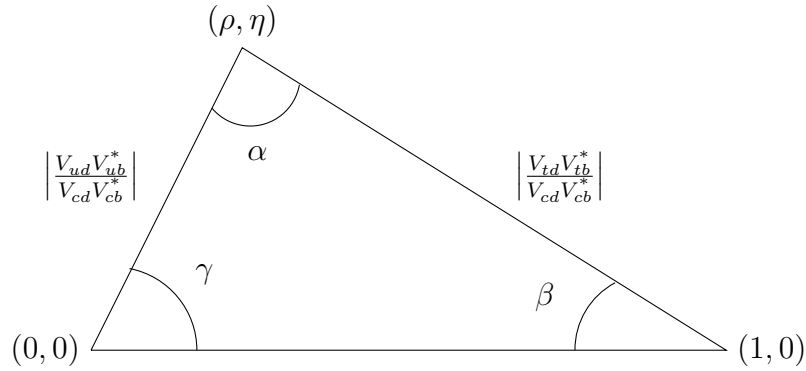


Figure 1.1: The unitarity triangle for the first line of Equation (1.2.13)

$$s_{13}e^{i\delta_{13}} = V_{ub}^* = A\lambda^3(\rho + i\eta) .$$

Up to $\mathcal{O}(\lambda^4)$ the CKM matrix becomes

$$V_{CKM} = \begin{pmatrix} 1 - \frac{1}{2}\lambda^2 & \lambda & A\lambda^3(\rho - i\eta) \\ -\lambda & 1 - \frac{1}{2} & A\lambda^2 \\ A\lambda^3(1 - \rho - i\eta) & -A\lambda^2 & 1 \end{pmatrix} + \mathcal{O}(\lambda^4) . \quad (1.2.12)$$

This is the Wolfenstein parametrization [33]. The unitarity of the CKM matrix gives rise to three orthogonality conditions

$$\begin{aligned} B_d : \quad & V_{ud}V_{ub}^* + V_{cd}V_{cb}^* + V_{td}V_{tb}^* = 0 , \\ K : \quad & V_{ud}V_{us}^* + V_{cd}V_{cs}^* + V_{td}V_{ts}^* = 0 , \\ B_s : \quad & V_{us}V_{ub}^* + V_{cs}V_{cb}^* + V_{ts}V_{tb}^* = 0 , \end{aligned} \quad (1.2.13)$$

where the first one can be depicted as a triangle in the (ρ, η) plane as shown in Figure 1.1. These equations can be used in studies of neutral meson mixing and other calculations simplifying them significantly without affecting the result.

1.2.2 Charm Quark and the GIM Mechanism

In this section we give a short historical review of the prediction of the charm quark leading to its experimental discovery and its implications in the Glashow-Iliopoulos-Maiani (GIM) mechanism [34].

Before the proposal of a fourth quark, the quark model consisted of a triplet $q = \begin{pmatrix} u \\ d \\ s \end{pmatrix}$ and the Eightfold way was explaining the known meson and baryon states very well [35,36]. Considering only the quark content, the weak interaction current was written as

$$\begin{aligned} J^\mu &= \bar{u}\gamma^\mu(1 - \gamma_5)d' + h.c. = \bar{q}\gamma^\mu(1 - \gamma_5)\mathcal{C}q + h.c. , \\ d' &= \cos\theta_C d + \sin\theta_C s , \\ \mathcal{C} &= \begin{pmatrix} 0 & \cos\theta_C & \sin\theta_C \\ 0 & 0 & 0 \\ 0 & 0 & 0 \end{pmatrix} , \end{aligned} \tag{1.2.14}$$

where θ_C is the Cabibbo angle and $\mathcal{C}, \mathcal{C}^\dagger$ can be recognised as the raising and lowering generators of the weak SU(2) group. The third generator is given by their commutator and is not diagonal. Because of that this model allowed for Flavour Changing Neutral Currents (FCNC) at tree level, something that was not suggested by data. Another issue was arising when Glashow proposed his unification of the electroweak theory in 1961 [20]. It could only be applied to leptons as it would require the quarks to form SU(2) doublets, which was not possible with the quark content found till then.

That was the case till 1970 when Glashow, Iliopoulos and Maiani introduced their solution to suppressed $\Delta S = 1, 2$ neutral currents. Their model required a fourth quark with electric charge of $+2/3$ which was named charm quark. The introduction of this new particle would change Equation (1.2.15) by adding

$$\begin{aligned} J_c^\mu &= \bar{c}\gamma^\mu(1 - \gamma_5)s' + h.c. , \\ s' &= -\sin\theta_C d + \cos\theta_C s . \end{aligned} \tag{1.2.15}$$

This way the matrix \mathcal{C} becomes:

$$\mathcal{C} = \begin{pmatrix} 0 & 0 & \cos \theta_C & \sin \theta_C \\ 0 & 0 & -\sin \theta_C & \cos \theta_C \\ 0 & 0 & 0 & 0 \\ 0 & 0 & 0 & 0 \end{pmatrix} ; \quad q = \begin{pmatrix} u \\ c \\ d \\ s \end{pmatrix}. \quad (1.2.16)$$

Now the third generator associated with the Z boson is diagonal and FCNCs are forbidden at tree level. How does it help with the $\Delta S = 1, 2$ amplitudes though? Two examples of such processes are the amplitudes $K_L \rightarrow \mu^+ \mu^-$ and $K^0 \rightarrow \bar{K}^0$ respectively. From these amplitudes it was known experimentally that [1]

$$\begin{aligned} \frac{\Gamma(K_L \rightarrow \mu^+ \mu^-)}{\Gamma(K^+ \rightarrow \mu^+ \bar{\nu}_\mu)} &= 2.60 \times 10^{-9}, \\ M_{K_L} - M_{K_S} &= 3.484 \times 10^{-12} \text{ MeV}, \end{aligned}$$

where $M_{K_{L,S}}$ are the masses of the long-lived and short-lived mass eigenstate of K^0 (which are linear combinations of the K^0, \bar{K}^0 mesons). Now the problem with the three quark theory is that the diagrams contributing to these observables (shown in Figure 1.2 in red) predict a much higher value. With the GIM mechanism though and the introduction of the charm quark for every diagram in Figure 1.2 (shown in blue) we get a second one where the u -quark is replaced by a c -quark. Notice however the total sign of the coupling being opposite to the diagrams with the u -quark line. In the case of $m_u = m_c$ the total amplitude would vanish. Now that the masses are different, the amplitude is proportional to $\alpha^2 \frac{m_c^2 - m_u^2}{M_W^2}$ where α is the fine structure constant. As we can see the sum of the two diagrams is very suppressed. In the same way, GIM mechanism helps with the $\Delta S = 1$ amplitudes. In Chapter 3 we will see how the GIM mechanism affects the mixing of D^0 meson with its antiparticle and makes theoretical predictions very hard.

Although the charm quark was predicted in 1970, it was only confirmed experimentally in 1974, independently in SLAC and BNL by teams led by Burton Richter [37]

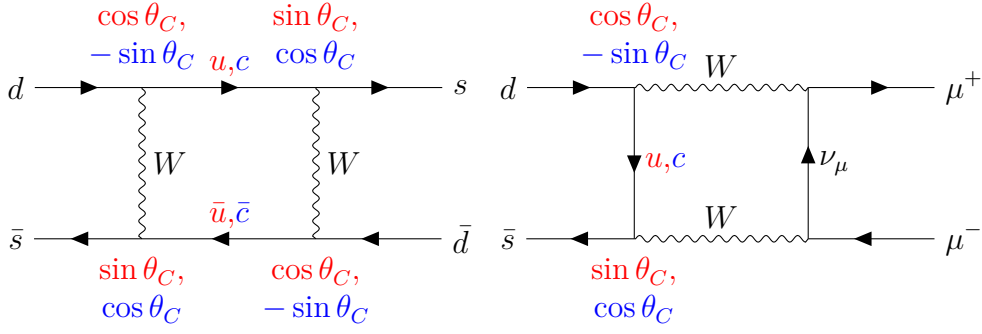


Figure 1.2: Box diagrams contributing to the K^0 mixing amplitude (left) and $K_L \rightarrow \mu^+ \mu^-$ amplitude (right). The coupling in each vertex is included so that the colour matches the quark lines.

and Samuel Ting [38] respectively. The two teams observed a new resonance with peak at around 3.1 GeV which was identified as a bound state of $c\bar{c}$, more widely known as “Charmonium”.

1.3 Rest of the Thesis

In this introductory chapter we presented the basics of the Standard Model. We also focused on the flavour physics part of the SM and how the quarks interact with each other and gain their masses. Finally we explained the importance of the discovery of the charm quark through the GIM mechanism.

The remainder of this thesis splits into 4 more chapters. In Chapter 2 we introduce some more specialised tools like Effective Theories and the Heavy Quark Expansion framework. These topics play a very important role in the work done in the following chapters and we try to present the reasoning behind them and their basic properties.

In Chapter 3 we discuss the system of $D^0 - \bar{D}^0$ oscillations. We present the basic formalism of neutral meson mixing and focus on the theoretical difficulties the $D^0 - \bar{D}^0$ system shows. Moreover, we present a new point of view regarding the renormalisation scheme applied traditionally in these calculations. Using this new method we show that it is possible to get theoretical predictions in agreement with

the current experimental values, alas with large theoretical uncertainties.

In Chapter 4 we focus on the lifetimes of D mesons, more specifically D^0 , D^+ and D_s^+ and how we can calculate them in the Heavy Quark Expansion framework. We conduct a very thorough study including two recently calculated contributions, the Darwin term for the decay of the charm quark and the Bag parameters of the D_s^+ meson. We also show the effect that these new results have in other observables like lifetime ratios and semi-leptonic decays and their ratios.

Finally, in Chapter 5 we summarise the work presented in the previous chapters and comment on the effect these results can have for future work. We will also point to the pieces missing in order to get better theoretical predictions and how attainable this is in the near future. In Appendices A-D we include supplementary material, like numerical input, example calculations and relevant proofs of equations used in the previous chapters.

Chapter 2

Theoretical Methods in Flavour Physics

In this chapter we will present some key concepts that are crucial in the study of flavour physics. We will start by presenting the Weak Effective Theory (WET) that simplifies our calculations at a lower energy scale by integrating out heavier particles. In this theory we will present some key calculations that will be used throughout the rest of the thesis. Next we will move to some more specialised methods, introducing the Heavy Quark Effective Theory (HQET) and the Heavy Quark Expansion (HQE) that are used to approximate the state of hadrons that include at least one heavy quark in low energies and enables us to study their inclusive decays (e.g. hadron lifetimes, mixing decay width).

2.1 Effective Theories

Effective Field Theories (EFTs) are a very powerful tool when you are interested in calculating a process at a lower energy scale. Essentially you use only the theory that is relevant to your energy regime and you “integrate out” higher degrees of freedom. In this section we will introduce two examples of EFTs; the Weak Effective Theory (WET) and the Heavy Quark Effective Theory (HQET). These two are examples of

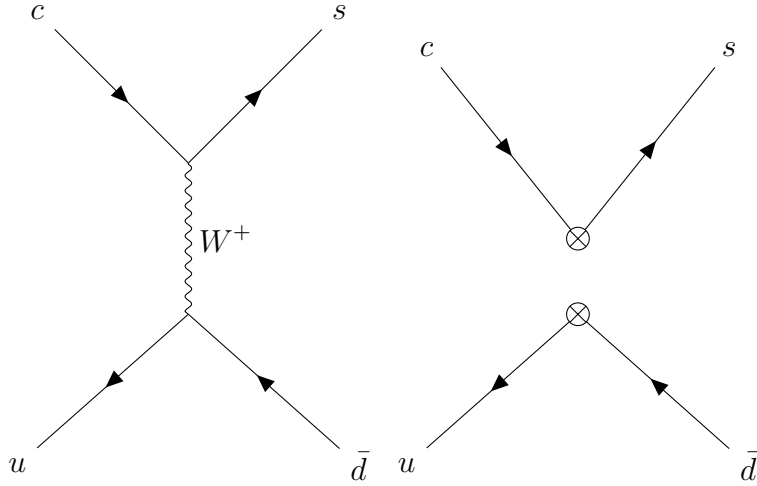


Figure 2.1: Tree level diagrams contributing to the process $c \rightarrow s u \bar{d}$ in the full theory (left) and the effective theory (right). In the process from left to right the W boson has been integrated out and a four-quark operator has been created instead.

a top down approach where you take a theory that works in a higher energy scale (the SM in this case) and you integrate out the degrees of freedom higher than your energy. What is left is an EFT that describes the “full” theory in this lower energy.

2.1.1 Weak Effective Theory

Matching

The weak decays of hadrons are driven by weak interactions of the quarks. However, the quarks bind into hadrons at an energy scale of ~ 1 GeV while the weak interaction has a much bigger scale ($M_{W,Z} \approx 80 - 90$ GeV). In order to develop a low energy theory of the weak interaction we can employ the Operator Product Expansion (OPE) [39, 40]. To describe this method we will consider the decay $c \rightarrow s u \bar{d}$ which happens through a W^+ boson as shown in the left diagram of Figure 2.1. In this section we will follow the same procedure as [41, 42]

The amplitude of this process at tree level is given by

$$A^{full,(0)} = i \frac{ig_1 V_{cs}^*}{2\sqrt{2}} \frac{ig_1 V_{ud}}{2\sqrt{2}} \frac{(\bar{s}^i \gamma^\mu (1 - \gamma_5) c^i) (\bar{u}^j \gamma_\mu (1 - \gamma_5) d^j)}{k^2 - M_W^2}, \quad (2.1.1)$$

where k^2 is the momentum transfer through the W boson, the indices i, j show the

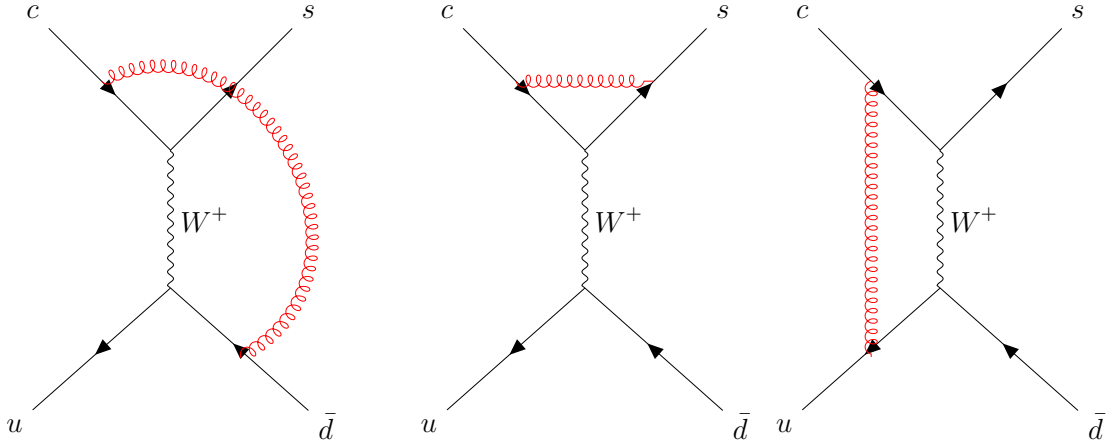


Figure 2.2: One-loop QCD correction diagrams in the SM. Gluon lines are shown in red. Their symmetric counterparts are not shown here.

colour charge of the fields, and the superscript (0) indicates the calculation is at tree level. We can expand the denominator of Equation (2.1.1) in powers of k^2/M_W^2 since $k^2 \ll M_W^2$. By doing so we rewrite

$$A^{full,(0)} = i \frac{G_F}{\sqrt{2}} V_{cs}^* V_{ud} (\bar{s}^i c^i)_{V-A} (\bar{u}^j d^j)_{V-A} + \mathcal{O}(k^2/M_W^2) \quad (2.1.2)$$

where

$$\frac{G_F}{\sqrt{2}} = \frac{g_1^2}{8M_W^2}. \quad (2.1.3)$$

We have also used the notation $V - A$ which indicates the vector-axial vector current i.e. $(\bar{q}_1 q_2)_{V-A} \equiv \bar{q}_1 \gamma^\mu (1 - \gamma_5) q_2$. The expression in Equation (2.1.2) is represented by the diagram on the right side of Figure 2.1. What if we also include QCD corrections to the diagrams of Figure 2.1? In this case we will also need to calculate the one-loop diagrams of Figure 2.2. The corresponding diagrams in the effective theory are identical to the “full” theory ones, but with the W propagator contracted to a point, just like in the right diagram one of Figure 2.1. So far at tree-level we have seen only one operator arising $Q_1 \equiv (\bar{s}^i c^i)_{V-A} (\bar{u}^j d^j)_{V-A}$. If we include the QCD corrections though, a second operator arises with a different colour structure. This operator can be expressed as $Q_2 \equiv (\bar{s}^i c^j)_{V-A} (\bar{u}^j d^i)_{V-A}$.² With these two operators we can build

²The notation of Q_1, Q_2 is just a convention and in the literature they can appear interchangeable.

our effective Hamiltonian:

$$\mathcal{H}_{eff} = \frac{G_F}{\sqrt{2}} V_{cs}^* V_{ud} (C_1 Q_1 + C_2 Q_2) , \quad (2.1.4)$$

where C_1, C_2 are called Wilson coefficients and can be considered as the couplings of the effective vertices (e.g. the crossed circles in the right diagram of Figure 2.1). The central aspect of this OPE is that low energy (long distance) and high energy (short distance) effects are split into the matrix elements of these operators and the coefficients respectively. Both of these quantities depend on an energy scale μ which is the threshold of the above separation. However this parameter is unphysical and so observables should be μ independent. This is achieved through the cancellation of the μ dependence of $C_i(\mu)$ and $\langle Q_i \rangle(\mu)$ at every order in the perturbative series.

If we calculate the effective amplitude at tree level (right diagram of Figure 2.1) we get the expression

$$A^{eff,(0)} = i \frac{G_F}{\sqrt{2}} V_{cs}^* V_{ud} (C_1 \langle Q_1 \rangle^{tree} + C_2 \langle Q_2 \rangle^{tree}) , \quad (2.1.5)$$

where $\langle Q_i \rangle^{tree}$ is the tree level matrix element of the operator Q_i . By requiring $A^{full,(0)} = A^{eff,(0)}$ we immediately get the values of the Wilson coefficients at LO:

$$C_1 = 1 + \mathcal{O}(\alpha_s) , \quad C_2 = 0 + \mathcal{O}(\alpha_s) . \quad (2.1.6)$$

As we mentioned earlier, the point of an EFT is to allow us to calculate quantities at a smaller energy scale than the one of the full theory, simplifying the process as we remove higher degrees of freedom that are not present in such energies. However, after calculating the Wilson coefficients with their dependence on the matching scale we still have one more thing to do. If we calculate the coefficients at a specific (n^{th}) order, we will include corrections up to $\mathcal{O}(\alpha_s^n)$ terms. In these calculations though we will also get large logarithms of the form $\ln(\mu_{match}/\mu_{calc})$ where μ_{match} is the matching scale of the full and effective theories and μ_{calc} is the energy scale of our calculation. Since typically the calculation scale is much smaller than the

matching ones, these logarithms become quite big and spoil the convergence of the series. This problem can be solved by using the renormalisation group equations (RGE) to sum these logarithms order by order. In Table 2.1 we can see specifically what terms are included at each order. The results we show below correspond to a LO+LL order (LL stands for Leading Logarithms). This means we perform the matching at one-loop level and keep only leading logarithmic corrections of order $\alpha_s \cdot \ln$. In order to obtain the QCD corrections to the Wilson coefficients we need

	LL	NLL	NNLL	$N^3\text{LL}$
tree-level	1	-	-	-
1-loop	$\alpha_s \ln$	α_s	-	-
2-loop	$\alpha_s^2 \ln^2$	$\alpha_s^2 \ln$	α_s^2	-
3-loop	$\alpha_s^3 \ln^3$	$\alpha_s^3 \ln^2$	$\alpha_s^3 \ln$	α_s^3

Table 2.1: Terms included in the perturbative expansion of the Wilson coefficients calculation.

to calculate the diagrams of Figure 2.2 and their corresponding ones in the EFT. In the following calculations we will assume massless external quark and off-shell momentum p such that $p^2 < 0$ [41]. These assumptions will not change the result for the Wilson coefficients but will simplify the calculation. We start with the results for the full theory:

$$\begin{aligned}
A_1^{full,(1)} &= \int \frac{d^d l}{(2\pi)^d} \left[\left(\bar{s}^j \frac{ig_1}{\sqrt{2}} \gamma^\mu \frac{1 - \gamma_5}{2} \frac{i(\not{p} + \not{l})}{(p+l)^2} ig_s T_{ji}^\alpha \gamma^\rho c^i \right) \right. \\
&\quad \left. \left(\bar{u}^k ig_s T_{kl}^\alpha \gamma^\sigma \frac{i(\not{p} + \not{l})}{(p+l)^2} \frac{ig_1}{\sqrt{2}} \gamma^\nu \frac{1 - \gamma_5}{2} d^l \right) \frac{-ig_{\mu\nu}}{l^2 - M_W^2} \frac{-ig_{\rho\sigma}}{l^2} V_{cs}^* V_{ud} \right] \\
&= -\frac{iG_F}{\sqrt{2}} V_{cs}^* V_{ud} (\bar{s}^j c^i)_{V-A} (\bar{u}^k d^l)_{V-A} \frac{1}{2} \left(\delta_{jl} \delta_{ik} - \frac{1}{N_C} \delta_{ji} \delta_{kl} \right) \frac{\alpha_s}{4\pi} \ln \frac{M_W^2}{-p^2} \\
&= -\frac{iG_F}{2\sqrt{2}} V_{cs}^* V_{ud} \frac{\alpha_s}{4\pi} \ln \frac{M_W^2}{-p^2} \left(\langle Q_2 \rangle^{tree} - \frac{1}{N_C} \langle Q_1 \rangle^{tree} \right), \tag{2.1.7} \\
A_2^{full,(1)} &= \int \frac{d^d l}{(2\pi)^d} \left[\left(\bar{s}^j \frac{ig_1}{\sqrt{2}} \gamma^\mu \frac{1 - \gamma_5}{2} \frac{i(\not{p} - \not{l})}{(p-l)^2} ig_s T_{ji}^\alpha \gamma^\rho c^i \right) \right. \\
&\quad \left. \left(\bar{u}^k \frac{ig_1}{\sqrt{2}} \gamma^\nu \frac{1 - \gamma_5}{2} \frac{i(\not{p} + \not{l})}{(p+l)^2} ig_s T_{kl}^\alpha \gamma^\sigma d^l \right) \frac{-ig_{\mu\nu}}{l^2 - M_W^2} \frac{-ig_{\rho\sigma}}{l^2} V_{cs}^* V_{ud} \right]
\end{aligned}$$

$$\begin{aligned}
&= \frac{iG_F}{\sqrt{2}} V_{cs}^* V_{ud} (\bar{s}^j c^i)_{V-A} (\bar{u}^k d^l)_{V-A} \frac{1}{2} \left(\delta_{jl} \delta_{ik} - \frac{1}{N_C} \delta_{ji} \delta_{kl} \right) \frac{\alpha_s}{4\pi} \ln \frac{M_W^2}{-p^2} \\
&= \frac{iG_F}{\sqrt{2}} V_{cs}^* V_{ud} \frac{\alpha_s}{4\pi} \ln \frac{M_W^2}{-p^2} \left(\langle Q_2 \rangle^{tree} - \frac{1}{N_C} \langle Q_1 \rangle^{tree} \right), \tag{2.1.8}
\end{aligned}$$

$$\begin{aligned}
A_3^{full,(1)} &= \int \frac{d^d l}{(2\pi)^d} \left[\left(\bar{s}^j i g_s T_{jm}^\alpha \gamma^\rho \frac{i(\not{p} - \not{l})}{(p-l)^2} \frac{i g_1}{\sqrt{2}} \gamma^\mu \frac{(1-\gamma_5)}{2} \frac{i(\not{p} - \not{l})}{(p-l)^2} i g_s T_{mi}^\alpha \gamma^\sigma c^i \right) \right. \\
&\quad \left. \left(\bar{u}^k \frac{i g_1}{\sqrt{2}} \gamma^\nu \frac{1-\gamma_5}{2} d^k \right) \times \frac{i g_{\mu\nu}}{M_W^2} V_{cs}^* V_{ud} \frac{-i g_{\rho\sigma}}{l^2} \right] \\
&= -\frac{iG_F}{\sqrt{2}} V_{cs}^* V_{ud} \frac{\alpha_s}{4\pi} \delta_{ij} (\bar{s}^j c^i)_{V-A} (\bar{u}^k d^k)_{V-A} C_F \left(\frac{1}{\epsilon} + \ln \frac{m_u^2}{-p^2} \right) \\
&= -\frac{iG_F}{\sqrt{2}} V_{cs}^* V_{ud} \frac{\alpha_s}{4\pi} \left[C_F \left(\frac{1}{\epsilon} + \ln \frac{\mu^2}{-p^2} \right) \right] \langle Q_1 \rangle^{tree}, \tag{2.1.9}
\end{aligned}$$

where the indices 1, 2, 3 correspond to the diagrams of Figure 2.2 from left to right and the superscript (1) indicates the calculations are at one-loop level. In the second step of the above calculations we have kept only the terms that correspond to LO+LL accuracy, discarding the rest and we have used the following identities:

$$T_{ij}^\alpha T_{kl}^\alpha = \frac{1}{2} \left(\delta_{il} \delta_{jk} - \frac{1}{N_C} \delta_{ij} \delta_{kl} \right), \tag{2.1.10}$$

$$T_{ij}^\alpha T_{jk}^\alpha = C_F \delta_{ik}, \tag{2.1.11}$$

where $C_F = (N_C^2 - 1)/2N_C$ and N_C is the number of QCD colours ($N_C = 3$ here and so $C_F = 4/3$).

If we add all the diagrams together (the symmetric diagrams give the exact same result) we get

$$\begin{aligned}
A^{full} &= A^{full,(0)} + 2 \left(A_1^{full,(1)} + A_2^{full,(1)} + A_3^{full,(1)} \right) \\
&= -\frac{iG_F}{\sqrt{2}} V_{cs}^* V_{ud} \left(\left[1 + \frac{\alpha_s}{4\pi} \left(2C_F \left(\frac{1}{\epsilon} + \ln \frac{\mu^2}{-p^2} \right) + \frac{3}{N_C} \ln \frac{M_W^2}{-p^2} \right) \right] \langle Q_1 \rangle^{tree} \right. \\
&\quad \left. + \frac{\alpha_s}{4\pi} \left(-3 \ln \frac{M_W^2}{-p^2} \right) \langle Q_2 \rangle^{tree} \right). \tag{2.1.12}
\end{aligned}$$

The corresponding results in the EFT are

$$A_1^{eff,(1)} = -\frac{iG_F}{\sqrt{2}}V_{cs}^*V_{ud}\frac{\alpha_s}{4\pi}\left[\left(\frac{1}{\epsilon} + \ln\frac{\mu^2}{-p^2}\right)\frac{C_1}{2N_C}\langle Q_1\rangle^{tree} + \left(\frac{1}{\epsilon} + \ln\frac{\mu^2}{-p^2}\right)\left(C_F C_2 + \frac{C_1}{2}\right)\langle Q_2\rangle^{tree}\right], \quad (2.1.13)$$

$$A_2^{eff,(1)} = -\frac{iG_F}{\sqrt{2}}V_{cs}^*V_{ud}\frac{\alpha_s}{4\pi}\left[\left(\frac{1}{\epsilon} + \ln\frac{\mu^2}{-p^2}\right)\left(\frac{C_2}{2} + C_F C_1\right)\langle Q_1\rangle^{tree} + \left(\frac{1}{\epsilon} + \ln\frac{\mu^2}{-p^2}\right)\left(-\frac{C_2}{2N_C}\right)\langle Q_2\rangle^{tree}\right], \quad (2.1.14)$$

$$A_3^{eff,(1)} = -\frac{2iG_F}{\sqrt{2}}V_{cs}^*V_{ud}\frac{\alpha_s}{4\pi}\left[\left(\frac{1}{\epsilon} + \ln\frac{\mu^2}{-p^2}\right)\left(\frac{C_1}{2N_C} - C_2\right)\langle Q_1\rangle^{tree} + \left(\frac{1}{\epsilon} + \ln\frac{\mu^2}{-p^2}\right)\left(\frac{C_2}{N_C} - C_1\right)\langle Q_2\rangle^{tree}\right]. \quad (2.1.15)$$

As previously if we put all contributions together (and include symmetric diagrams that give the same result) we get

$$\begin{aligned} A^{eff} &= A^{eff,(0)} + 2\left(A_1^{eff,(1)} + A_2^{eff,(1)} + A_3^{eff,(1)}\right) \\ &= \frac{-iG_F}{\sqrt{2}}V_{cs}^*V_{ud}\left(A_1\langle Q_1\rangle^{tree} + B_1\langle Q_2\rangle^{tree}\right), \end{aligned} \quad (2.1.16)$$

where

$$A_1 = \left[\left(1 + \frac{\alpha_s}{4\pi}\left(\frac{1}{\epsilon} + \ln\frac{\mu^2}{-p^2}\right)\right)\left(2C_F + \frac{3}{N_C}\right)C_1 - 3\frac{\alpha_s}{4\pi}\left(\frac{1}{\epsilon} + \ln\frac{\mu^2}{-p^2}\right)C_2\right], \quad (2.1.17)$$

$$B_1 = \left[\left(1 + \frac{\alpha_s}{4\pi}\left(\frac{1}{\epsilon} + \ln\frac{\mu^2}{-p^2}\right)\right)\left(2C_F + \frac{3}{N_C}\right)C_2 - 3\frac{\alpha_s}{4\pi}\left(\frac{1}{\epsilon} + \ln\frac{\mu^2}{-p^2}\right)C_1\right].$$

Comparing the SM and the EFT result we get the results for the Wilson coefficients

$$C_1 = 1 - \frac{\alpha_s}{4\pi}\frac{3}{N_C}\left(\frac{1}{\epsilon} + \ln\frac{\mu^2}{M_W^2}\right)$$

$$C_2 = -\frac{\alpha_s}{4\pi} 3 \left(\frac{1}{\epsilon} + \ln \frac{\mu^2}{M_W^2} \right). \quad (2.1.18)$$

Looking at Equations (2.1.17) and (2.1.18) we see the main objective of the OPE which is the factorisation into short- and long-distance effects. Ignoring the divergent terms which we will deal with in the next section the expressions of the Wilson coefficients and the matrix elements are of the form

$$\left(1 + \frac{\alpha_s}{4\pi} \ln \frac{M_W^2}{\mu^2} \right) \quad \left(1 + \frac{\alpha_s}{4\pi} \ln \frac{\mu^2}{-p^2} \right), \quad (2.1.19)$$

respectively. Multiplying the two to calculate the amplitude we get

$$\left(1 + \frac{\alpha_s}{4\pi} \ln \frac{M_W^2}{\mu^2} \right) \left(1 + \frac{\alpha_s}{4\pi} \ln \frac{\mu^2}{-p^2} \right) = \left(1 + \frac{\alpha_s}{4\pi} \ln \frac{M_W^2}{-p^2} \right) + \mathcal{O}(\alpha_s^2), \quad (2.1.20)$$

which are the logarithmic terms we get in the full theory. So indeed the OPE splits the effects using the unphysical scale μ as a threshold.

Operator and Coefficient Renormalisation

If we look at Equations (2.1.12) and (2.1.17) we see some divergent terms. The ones that are common in both equations cancel during the matching procedure (they are not present in Equation (2.1.18)). Independently they could also be removed by renormalising the quark fields. For the remaining ones we will have to renormalise the bare Q_i operators. To separate between the bare and renormalised operators we will indicate the first ones with the superscript (0). We write

$$Q_i^{(0)} = \hat{Z}_{ij} Q_j \quad \implies \quad \langle Q_i \rangle^{(0)} = Z_q^{-2} \hat{Z}_{ij} Q_j, \quad (2.1.21)$$

where \hat{Z} is a 2×2 matrix and Z_q is the renormalisation constant for the quark field which removes the common divergencies of the two theories. The matrix Z can be easily identified as

$$\hat{Z} = 1 + \frac{\alpha_s}{4\pi} \frac{1}{\epsilon} \begin{pmatrix} 3/N_C & -3 \\ -3 & 3/N_C \end{pmatrix}. \quad (2.1.22)$$

Inserting these updated matrix elements in Equation 2.1.17 we can extract the renormalised Wilson coefficients:

$$\begin{aligned} C_1 &= 1 + \frac{\alpha_s}{4\pi} \frac{3}{N_C} \ln \frac{M_W^2}{\mu^2} , \\ C_2 &= -3 \frac{\alpha_s}{4\pi} \ln \frac{M_W^2}{\mu^2} . \end{aligned} \quad (2.1.23)$$

The same result would be obtained if instead of the operators we decide to renormalise the coefficients. In that case we can write

$$C_i^{(0)} = \hat{Z}_{ij}^c C_j , \quad (2.1.24)$$

and the effective Hamiltonian can be rewritten as

$$\frac{1}{\frac{G_F}{\sqrt{2}} V_{cs}^* V_{ud}} \mathcal{H}_{eff} = C_i^{(0)} Q_i(q^{(0)}) = Z_q^2 \hat{Z}_{ij}^c C_j Q_i . \quad (2.1.25)$$

To get the effective amplitude we write

$$A^{eff} \equiv \langle \mathcal{H}_{eff} \rangle = Z_q^2 \hat{Z}_{ij}^c C_j \langle Q_i \rangle^{(0)} , \quad (2.1.26)$$

while by using the operator renormalisation we get

$$A^{eff} = Z_q^2 \hat{Z}_{ji}^{-1} C_j \langle Q_i \rangle^{(0)} , \quad (2.1.27)$$

and by comparing the two expressions we find

$$\hat{Z}_{ij}^c = \hat{Z}_{ji}^{-1} . \quad (2.1.28)$$

Renormalisation Group Equations

As we mentioned earlier it is not wise to simply set the μ scale to a value and calculate the Wilson coefficients at that energy. The reason is the arising of large logarithms that can spoil the perturbative expansion. In this section we will see how we can perform a resummation of these logarithmic terms.

We start with the statement that \mathcal{H}_{eff} can not depend on the scale μ . That would

mean

$$\frac{d}{d \ln \mu} \mathcal{H}_{eff} = \frac{d}{d \ln \mu} (C_i Q_i) = 0 \implies \frac{dC_i(\mu)}{d \ln \mu} Q_i(\mu) = -C_i(\mu) \frac{dQ_i(\mu)}{d \ln \mu}. \quad (2.1.29)$$

Additionally, we can use that the bare fields should be scale independent to get

$$\frac{dQ_i^{(0)}}{d \ln \mu} = 0 \implies \hat{Z}_{ij}(\mu) \frac{dQ_j(\mu)}{d \ln \mu} = - \left(\frac{d\hat{Z}_{ij}(\mu)}{d \ln \mu} \right) Q_j(\mu). \quad (2.1.30)$$

The above equation can be rewritten in matrix form as

$$\frac{d\vec{Q}(\mu)}{d \ln \mu} = \hat{\gamma} \vec{Q}(\mu), \quad (2.1.31)$$

where $\hat{\gamma} = \hat{Z}^{-1}(\mu) \frac{d}{d \ln \mu} \hat{Z}(\mu)$. The matrix $\hat{\gamma}$ is defined as the anomalous dimension matrix. Applying Equation (2.1.30) on Equation (2.1.29) we get the RGE for the Wilson coefficients

$$\frac{d\vec{C}(\mu)}{d \ln \mu} = \hat{\gamma}^T \vec{C}. \quad (2.1.32)$$

To solve this equation we will need to define the β function of QCD as

$$\beta(\alpha_s) = \frac{1}{2} \frac{d\alpha_s(\mu)}{d \ln \mu} = -\epsilon \alpha_s - \beta_0 \frac{\alpha_s^2}{4\pi} + \mathcal{O}(\alpha_s^3), \quad (2.1.33)$$

where $\beta_0 = \frac{11N_C - 2f}{3}$ and f is the number of active flavours. Applying this we can calculate the $\hat{\gamma}$ matrix giving

$$\hat{\gamma} = \frac{\alpha_s}{4\pi} \begin{pmatrix} -6/N_C & 6 \\ 6 & -6/N_C \end{pmatrix}. \quad (2.1.34)$$

Applying Equation (2.1.33) we can solve the RGE for the Wilson coefficients and get

$$\vec{C}(\mu) = \hat{U}^{(5)}(\mu, M_W) \vec{C}(M_W) \quad (2.1.35)$$

where the superscript (5) indicates the 5 active flavours between the scales M_W and m_b . The evolution matrix \hat{U} is given by

$$\hat{U}(\mu, M_W) = \exp \left[\int_{\alpha_s(M_W)}^{\alpha_s(\mu)} d\alpha \frac{\hat{\gamma}^T(\alpha)}{2\beta(\alpha)} \right]. \quad (2.1.36)$$

Substituting the expressions for $\hat{\gamma}, \beta$ we get

$$\vec{C}(\mu) = \exp \left[-\frac{\hat{\gamma}^{(0)T}}{2\beta_0} \ln \left(\frac{\alpha_s(\mu)}{\alpha_s(M_W)} \right) \right] \vec{C}(M_W) . \quad (2.1.37)$$

Notice that this solution is valid for energies up to m_b . For lower energies (as we will need for this thesis) we will need to perform another matching of the 5-flavour effective theory and the 4-flavour one, integrating out the heavy b quark. Then we can apply the 4-flavour evolution matrix to the new initial conditions at m_b . This process has to be followed every time we go to lower energies and need to integrate out heavier degrees of freedom.

If one wants to consider more generally the decay of the charm quark then the effective Hamiltonian of Equation (2.1.4) can be extended with the addition of the penguin operators $Q_3 - Q_6$

$$\begin{aligned} Q_3 &= (\bar{u}_i c_i)_{V-A} \sum_q (\bar{q}_j q_j)_{V-A} , \\ Q_4 &= (\bar{u}_i c_j)_{V-A} \sum_q (\bar{q}_j q_i)_{V-A} , \\ Q_5 &= (\bar{u}_i c_i)_{V-A} \sum_q (\bar{q}_j q_j)_{V+A} , \\ Q_6 &= (\bar{u}_i c_j)_{V-A} \sum_q (\bar{q}_j q_i)_{V+A} , \end{aligned} \quad (2.1.38)$$

where the q index runs for all quark flavours and $(\bar{q}q)_{V+A} = \bar{q}\gamma^\mu(1+\gamma_5)q$. In the rest of the thesis the Wilson coefficients used are also taking into account these QCD penguins since we are looking into inclusive decays of the charm quark. We will also consider two-loop corrections. A good review of this calculation can be found in [41, 42]

In conclusion, the procedure to calculate the Wilson coefficients at the charm mass scale can be summarised in the following steps:

- Calculate the matching conditions at $\mu = M_W$ for all the operators of the effective Hamiltonian. For this we would need to calculate the corresponding

diagrams both in full and effective theory and do the matching.

- Remove the remaining divergencies by performing the appropriate renormalisation.
- Sum over the logarithmic corrections at the considered order by using the RGE. For this, we would need to calculate the anomalous dimension matrix at the required order.
- Derive the evolution matrix and run down the scale to m_b . Above we give the result for the LO+LL calculation.
- From there, we will need to match a 5-flavour EFT to a 4-flavour EFT integrating out the bottom quark i.e.

$$\vec{C}^{(4)}(m_b) = \hat{M}(m_b)\vec{C}^{(5)}(m_b) . \quad (2.1.39)$$

The matrix \hat{M} needs to be determined in a similar matching process. This matrix can be found in [43].

- We then apply the 4-flavour evolution matrix to this matching condition and run down to $\mu = m_c$, i.e

$$\vec{C}^{(4)}(\mu) = \hat{U}^{(4)}(\mu, m_b)\vec{C}^{(4)}(m_b) . \quad (2.1.40)$$

2.1.2 Heavy Quark Effective Theory

One of the main properties of QCD that is unique to it, is the confinement property, i.e. colour-charged particles are not allowed to be observed and they have to combine themselves to colour singlet states which are called hadrons. Thus, hadron dynamics are governed by the confinement scale or QCD scale $\Lambda_{QCD} \approx 0.2$ GeV. At such a low energy scale however the running coupling α_s is larger than 1 and hence can not be expanded over. As a result, perturbative QCD can not be applied in this case but it is still possible to calculate hadronic matrix elements by considering certain

approximations. HQET [44–51] can be applied to hadrons that contain one heavy quark Q i.e $m_Q \gg \Lambda_{QCD}$. Excluding the top quark which decays before hadronization, heavy quarks can be assumed to be the bottom with $m_b \approx 4.18$ GeV (in the \overline{MS} scheme) and the charm with $m_c \approx 1.27$ GeV (again in the \overline{MS} scheme). In such an approximation the hadron can be simulated as a heavy quark softly interacting with the light constituents. In the remaining of the section we will show how we can describe such a system mathematically and how under this assumption the QCD Lagrangian changes to the HQET one, giving a new set of Feynman rules.

The rest of the section follows the reviews [52–54]. In HQET the heavy quark can be assumed to be almost on-shell, resulting in the following expression of its momentum

$$P_Q^\mu = m_Q v^\mu + k^\mu, \quad (2.1.41)$$

where the LHS corresponds to the heavy quark momentum and v^μ is the velocity four-vector of the hadron with $v^2 = 1$. k^μ is the residual momentum which is of order Λ_{QCD} and comes from the interactions of the heavy quark with the lighter degrees of freedom. If we use Equation (2.1.41) we can rewrite the QCD quark propagator as

$$\begin{aligned} \frac{i}{\not{P}_Q - m_Q + i\epsilon} &= \frac{i}{m_Q \not{v} + \not{k} - m_Q + i\epsilon} \\ &= \frac{i}{v \cdot k + i\epsilon} \left(\frac{1 + \not{v}}{2} \right) + \mathcal{O}\left(\frac{k}{m_Q}\right), \end{aligned} \quad (2.1.42)$$

where the operator $\frac{1+\not{v}}{2}$ can be understood as a positive-energy projection operator.

In the same way we can define a negative-energy projection operator

$$P_\pm = \frac{1 \pm \not{v}}{2}, \quad (2.1.43)$$

satisfying the projection identities

$$\begin{aligned} P_\pm^2 &= P_\pm, \\ P_\pm P_\mp &= 0. \end{aligned} \quad (2.1.44)$$

$$\begin{aligned}
 & \begin{array}{c} i \text{---} \longrightarrow \text{---} j \\ a, \alpha \end{array} = \frac{1}{v \cdot k} \frac{1 + \not{\psi}}{2} \delta_{ji} \\
 & \begin{array}{c} i \text{---} \longrightarrow \text{---} j \\ \text{---} \text{---} \text{---} \\ \text{---} \text{---} \text{---} \end{array} = ig_s T_{ij}^\alpha v^a
 \end{aligned}$$

Figure 2.3: The quark propagator and the heavy quark-gluon vertex in the HQET framework

By using that $P_+ \gamma^\mu P_+ = P_+ v^\mu P_+$ we can also rewrite the gluon vertex $ig_s T^\alpha \gamma^\mu$ as $ig_s T^\alpha v^\mu$ up to leading order in $1/m_Q$.

The parametrisation of the QCD heavy quark field can be written (using the projection operators) as

$$Q(x) = e^{-im_Q v \cdot x} \left(h_v(x) + H_v(x) \right), \quad (2.1.45)$$

where the two effective quark fields are defined as

$$\begin{aligned}
 h_v(x) &= e^{im_Q v \cdot x} \frac{1 + \not{\psi}}{2} Q(x), \\
 H_v(x) &= e^{im_Q v \cdot x} \frac{1 - \not{\psi}}{2} Q(x),
 \end{aligned} \quad (2.1.46)$$

and satisfy the equations

$$\begin{aligned}
 P_+ h_v(x) &= h_v(x) = \not{\psi} h_v(x) \\
 P_- H_v(x) &= H_v(x) = -\not{\psi} H_v(x)
 \end{aligned} \quad (2.1.47)$$

The large component $h_v(x)$ annihilates a heavy quark with velocity v while the small one $H_v(x)$ creates a heavy antiquark with velocity v . The exponential prefactor in Equation (2.1.45) subtracts $m_Q v$ from the heavy quark momentum so that the effective quark fields contain only small effects of $\mathcal{O}(k)$. By looking at Equation (2.1.46) we can see that effects from $h_v(x)$ are produced at leading order (because of the presence of P_+ in the effective propagator) while effects from $H_v(x)$ are included as $1/m_Q$ corrections.

If we consider only the large component of the heavy quark field, $h_v(x)$ and substitute Equation (2.1.45) in the QCD Lagrangian we get

$$\mathcal{L}_{QCD} \rightarrow \bar{h}_v(x)(i\not{D})h_v(x) = \bar{h}_v(x)(iv \cdot D)h_v(x) , \quad (2.1.48)$$

using that $P_- h_v(x) = 0$ and $P_+ \gamma_\mu P_+ = P_+ v_\mu P_+$.

As we can see the above Lagrangian has no dependence on the heavy quark mass, making it flavour symmetric. This gives rise to an $SU(N_h)$ symmetry where N_h is the number of heavy quark flavours. Furthermore, since the operator $v \cdot D$ does not include gamma matrices, interactions of the heavy quark with the gluons leave its spin unchanged. This is associated with an $SU(2)$ spin symmetry. Together for N_h heavy flavours we get an $SU(2N_h)$ flavour-spin symmetry, see e.g. [44]

Expanding the covariant derivative in Equation (2.1.48) we obtain

$$\mathcal{L}_{QCD} \rightarrow \bar{h}_v(x)(iv \cdot \partial + g_s T_\alpha v \cdot A^\alpha)h_v(x) , \quad (2.1.49)$$

from where we can obtain the same Feynman rules as earlier and can be seen in Figure 2.3. Considering the theory with only h_v we have no way of creating or annihilating antiquarks since $h_v(\bar{h}_v)$ annihilates (creates) a heavy quark Q . Thus, no pair production is possible in the infinite heavy quark mass limit.

To consider $1/m_Q$ corrections we substitute the full Equation (2.1.45) into the QCD Lagrangian and we obtain the effective one

$$\begin{aligned} \mathcal{L}_{QCD} &\rightarrow \bar{Q}(i\not{D} - m_Q)Q \rightarrow (\bar{h}_v + \bar{H}_v)(m_Q\not{v} + i\not{D} - m_Q)(h_v + H_v) \\ &= (\bar{h}_v + \bar{H}_v)(-2m_Q\not{v}H_v + i\not{D}h_v + i\not{D}H_v) \\ &= \bar{h}_v i\not{D}h_v + \bar{h}_v i\not{D}H_v + \bar{h}_v i\not{D}H_v + \bar{H}_v(i\not{D} - 2m_Q)H_v \\ &= \bar{h}_v(iv \cdot D)h_v - \bar{H}_v(iv \cdot D + 2m_Q)H_v + \bar{h}_v i\not{D}H_v + \bar{H}_v i\not{D}h_v , \end{aligned} \quad (2.1.50)$$

where in the first step we have used the right hand equality of Equation (2.1.47), in the second step the orthogonality of the two effective heavy quark fields and in the third step the left hand equality of Equation (2.1.47). To simplify the above Lagrangian it is convenient to define a parallel and an orthogonal part to the velocity vector v^μ of the covariant derivative. This reads

$$D_\perp^\mu = D^\mu - v^\mu(v \cdot D) . \quad (2.1.51)$$

Using this definition, the last two terms of Equation (2.1.50) are changed to

$$\bar{h}_v i \not{D}_\perp H_v + \bar{h}_v i \not{D}_\perp H_v . \quad (2.1.52)$$

This new effective Lagrangian has two separate quark fields (h_v, H_v) , where the first one describes a massless degree of freedom, while the second massive fluctuations with mass equal to twice the heavy quark mass m_Q . Finally, the last two terms of the effective Lagrangian mix the two fields and describe virtual processes. An example of such processes is the annihilation of a quark that moves forward in time to an antiquark moving backwards and then turns back to a quark moving forward again [55].

From Equation (2.1.50) above we can derive the equations of motion for $h_v(x)$ and $H_v(x)$

$$(iv \cdot D)h_v(x) = -i \not{D}_\perp H_v(x) \quad (2.1.53)$$

$$(iv \cdot D + 2m_Q)H_v(x) = i \not{D}_\perp h_v(x) . \quad (2.1.54)$$

Rearranging the second equation we can define $H_v(x)$ in terms of $h_v(x)$

$$H_v(x) = (iv \cdot D + 2m_Q - i\epsilon)^{-1} i \not{D}_\perp h_v(x) \quad (2.1.55)$$

With this redefinition we can derive the effective Lagrangian from Equation (2.1.50) as

$$\mathcal{L}_{eff} = \bar{h}_v (iv \cdot D) h_v + \bar{h}_v i \not{D}_\perp (iv \cdot D + m_Q - i\epsilon)^{-1} i \not{D}_\perp h_v . \quad (2.1.56)$$

This makes very clear that effects from H_v correspond to $1/m_Q$ corrections in the effective Lagrangian. The remaining two terms of Equation (2.1.50) cancel each other by using Equations (2.1.54) and (2.1.55). The effective Lagrangian is now expressed only in terms of the large component of the heavy quark field $h_v(x)$ while it includes the effects of the small component $H_v(x)$ in the second term clearly suppressed as an $1/m_Q$ correction.

From the initial expansion of the heavy quark field in Equation (2.1.45) the x -dependence of the field is weak and derivatives acting on $h_v(x)$ will return only the residual momentum k^μ which is of order Λ_{QCD} . We can take advantage of this and expand the second term of the Lagrangian in powers of $1/m_Q$. We then obtain

$$\mathcal{L}_{eff} = \bar{h}_v(i v \cdot D) h_v + \frac{1}{2m_Q} \bar{h}_v(i \not{D}_\perp)(i \not{D}_\perp) h_v + \mathcal{O}(1/m_Q^2) . \quad (2.1.57)$$

Next we can use the identity

$$P_+ i \not{D}_\perp i \not{D}_\perp P_+ = P_+ \left[(i D_\perp)^2 + \frac{g_s}{2} \sigma_{\mu\nu} G^{\mu\nu} \right] P_+ , \quad (2.1.58)$$

where we have used $[D_\mu, D_\nu] = i g_s G_{\mu\nu}$ and $\sigma_{\mu\nu} = i[\gamma_\mu, \gamma_\nu]/2$ to write it in the form

$$\mathcal{L}_{eff} = \bar{h}_v(i v \cdot D) h_v + \frac{1}{2m_Q} \bar{h}_v(i D_\perp)^2 h_v + \frac{g_s}{2m_Q} \bar{h}_v \frac{\sigma_{\mu\nu} G^{\mu\nu}}{2} h_v + \mathcal{O}(1/m_Q^2) . \quad (2.1.59)$$

Finally, we can remove the \perp subscript since the parallel component of the covariant derivative vanishes between the two fields i.e.

$$\bar{h}_v(x) v^\mu \sigma_{\mu\nu} h_v(x) = 0 , \quad (2.1.60)$$

which follows from Equation (2.1.47). With this rewriting we can identify two operators arising at order $1/m_Q$

$$\begin{aligned} \mathcal{O}_1 &= \bar{h}_v(x) (i D_\perp)^2 h_v(x) , \\ \mathcal{O}_2 &= \frac{g_s}{2} \bar{h}_v(x) \sigma_{\mu\nu} G^{\mu\nu} h_v(x) . \end{aligned} \quad (2.1.61)$$

The first operator describes the kinetic energy of the heavy quark arising from its off-shell motion inside the hadron state, while the second one describes the interaction of the spin operator of the heavy quark with the gluon field. We will call them kinetic and chromomagnetic operator respectively. Due to their nature, the kinetic operator breaks the heavy quark flavour symmetry due to its explicit dependence on m_Q , while the chromomagnetic operator breaks additionally the heavy quark symmetry and so on.

Before continuing, it is convenient to organise the Lagrangian differently. This will become clear in the calculation of matrix elements in HQET. In Equation (2.1.56), we consider the first term as the HQET Lagrangian, and the second term as power corrections expanded in $1/m_Q$

$$\begin{aligned}\mathcal{L}_{HQET} &= \bar{h}_v(iv \cdot D)h_v, \\ \mathcal{L}_{power} &= \bar{h}_v i \not{D}_\perp (iv \cdot D + m_Q - i\epsilon)^{-1} i \not{D}_\perp h_v \\ &= \frac{1}{2m_Q} \mathcal{L}_1 + \left(\frac{1}{2m_Q} \right)^2 \mathcal{L}_2 + \mathcal{O}((1/2m_Q)^3). \end{aligned} \quad (2.1.62)$$

In this case, the equation of motion for $h_v(x)$ reads

$$iv \cdot Dh_v(x) = 0. \quad (2.1.63)$$

Up to order $\mathcal{O}(1/m_Q^2)$, the effective Lagrangian becomes

$$\mathcal{L}_{eff} = \bar{h}_v(iv \cdot D)h_v + \frac{1}{2m_Q} \bar{h}_v (i \not{D}_\perp)^2 h_v + \mathcal{O}(1/m_Q^2). \quad (2.1.64)$$

A big advantage of expressing the effective Lagrangian as in Equation (2.1.62) is the calculation of matrix elements. To begin with, we will assume our Lagrangian takes the form of Equation (2.1.50) and using Equation (2.1.55) express the QCD quark field as

$$\begin{aligned}Q(x) &= e^{-im_Q v \cdot x} \left(1 + (iv \cdot D + 2m_Q - i\epsilon)^{-1} i \not{D}_\perp \right) h_v(x) \\ &= e^{-im_Q v \cdot x} \left(1 + \frac{i \not{D}_\perp}{2m_Q} + \mathcal{O}(1/m_Q^2) \right) h_v(x). \end{aligned} \quad (2.1.65)$$

If we consider the vector current involving a heavy quark and a light one i.e. $\mathcal{V}^\mu(x) = \bar{q}(x)\gamma^\mu Q(x)$ then this can be expressed as

$$\mathcal{V}^\mu(x) = e^{-im_Q v \cdot x} \bar{q}(x) \gamma_\mu \left(1 + \frac{i \not{D}_\perp}{2m_Q} + \mathcal{O}(1/m_Q^2) \right) h_v(x). \quad (2.1.66)$$

Taking the matrix element of this current between a heavy meson with velocity v , $\mathcal{M}(v)$ and the vacuum. The QCD matrix element can then be written as

$$\langle 0 | \mathcal{V}^\mu | \mathcal{M}(v) \rangle = \langle 0 | \bar{q} \gamma_\mu h_v | \mathcal{M}(v) \rangle + \frac{1}{2m_Q} \langle 0 | \bar{q} \gamma_\mu i \not{D}_\perp h_v | \mathcal{M}(v) \rangle + \mathcal{O}(1/m_Q^2). \quad (2.1.67)$$

However, even if we ignore the explicit dependence in m_Q in the prefactor, the second term in the RHS still depends on m_Q as the equation of motion for $h_v(x)$ includes such corrections. If we instead use the Lagrangian form of Equation (2.1.62), the equation of motion is independent on m_Q and the matrix element of \mathcal{V}^μ can be written as

$$\begin{aligned} \langle 0 | \mathcal{V}^\mu | \mathcal{M}(v) \rangle_{QCD} &= \langle 0 | \bar{q} \gamma_\mu h_v | \mathcal{M}(v) \rangle_{HQET} + \frac{1}{2m_Q} \langle 0 | \bar{q} \gamma_\mu i \not{D}_\perp h_v | \mathcal{M}(v) \rangle_{HQET} \\ &+ \frac{1}{2m_Q} \langle 0 | i \int dx T \{ \bar{q} \gamma^\mu h_v(0), \mathcal{L}_1(x) \} | \mathcal{M}(v) \rangle_{HQET} \\ &+ \mathcal{O}(1/m_Q^2), \end{aligned} \quad (2.1.68)$$

where T is the time ordered operator. Now all the mass dependence of the matrix element has been absorbed by the last term which is a power correction to the leading order matrix element of the current.

Finally, we will discuss hadron masses in the HQET framework. Splitting the quark field in two components we see that we have absorbed the heavy quark mass in the exponential factor outside the field. Because of that, we can express the hadron mass in HQET as

$$\bar{\Lambda} = M_H - m_Q + \mathcal{O}(1/m_Q), \quad (2.1.69)$$

As a consequence, all hadrons with a heavy quark Q have the same mass m_Q at order m_Q^1 . The parameter $\bar{\Lambda}$ which is of order m_Q^0 stems from the interactions of the

heavy quark with the light degrees of freedom inside the hadron and can be defined as

$$\bar{\Lambda} = \frac{1}{2} \langle H | \mathcal{H}_0 | H \rangle , \quad (2.1.70)$$

where \mathcal{H}_0 is the Hamiltonian derived from the $\mathcal{L}_{HQET} + \mathcal{L}_{light,gluons}$ and the Lagrangian for the light quarks and gluons is the same as in QCD. We have also used the normalisation of [56]. Similarly, the $1/m_Q$ correction to the hadron mass can be expressed as the expectation value of the Hamiltonian derived from the first power correction \mathcal{L}_1 .

2.2 Heavy Quark Expansion

The Heavy Quark Expansion (HQE) is a very powerful tool in the study of heavy hadron inclusive decays, e.g. their lifetimes or mixing-induced decay widths. As it was mentioned earlier, a heavy hadron system can be considered as the heavy quark approximating the hadron state at leading order, while the interactions with the lighter degrees of freedom are included as correction terms suppressed by some power of $1/m_Q$. In the limit of $m_Q \rightarrow \infty$, only the leading term survives and one can write $\Gamma(H_Q) = \Gamma_Q$ where H_Q is the heavy hadron. As a result, all hadrons with a Q quark should have the same lifetime. In the case $Q = b$ the correction to the experimental values are of the order of few percent, but in the charm system they are much larger. More specifically, the experimental values show that the biggest lifetime ratio among charmed hadrons can reach almost 7 ($\tau(D^+)/\tau(\Xi_c^0) \approx 6.8$) while in the B system it is $\tau(\Omega_b^-)/\tau(\Lambda_b^0) \approx 1.1$. It is clear that the infinite mass limit is not a good approximation for the charm system and in the remaining of this section we will develop the framework that will help us consider the corrections to the infinite mass limit systematically. It is instructive to mention the primary contributions to the development of the HQE for inclusive weak decays through the years and its early uses. Many terms of the HQE were published first in [57] while its first applications were focused both in semi-leptonic [58–60] and non-leptonic decays [61].

A very good review focusing on the main steps in the development of HQE is [62].

The decay rate of a particle H to an n -particle final state is given by

$$\Gamma(H) = \frac{1}{2M_H} \sum_n \int \prod_{i=1}^n \frac{d^3 p_i}{(2\pi)^3 2E_i} (2\pi)^4 \delta\left(p_H - \sum_{i=1}^n p_i\right) |\langle n | \mathcal{M} | H \rangle|^2. \quad (2.2.1)$$

We can also calculate the decay of the particle H in a different way though, using the optical theorem which connects the imaginary part of the forward scattering amplitude with the total cross section for the production of all possible final states. To see this we need to start from the definition of the scattering amplitude S_{fi} between an initial state i and a final state f

$$S_{fi} = \langle f | S | i \rangle = \delta_{fi} + iT_{fi}, \quad (2.2.2)$$

where

$$T_{fi} = (2\pi)^4 \delta(p_f - p_i) \mathcal{M}_{fi} \quad (2.2.3)$$

is ensuring the conservation of 4-momentum between initial and final state particles.

In the matrix element between a general initial and final state we can add a full set of states while integrating over the phase space and write using the unitarity of S

$$\sum_n \int \prod_{i=1}^n \frac{d^3 p_i}{(2\pi)^3 2E_i} \langle f | S | n \rangle \langle n | S^\dagger | i \rangle = \delta_{fi}, \quad (2.2.4)$$

where

$$\langle n | S^\dagger | i \rangle = \langle i | S | n \rangle^*. \quad (2.2.5)$$

Using that and Equation (2.2.2) we can rewrite Equation (2.2.4) in the case of forward scattering ($|f\rangle = |i\rangle$) as

$$\begin{aligned} \sum_n \int \prod_{i=1}^n \frac{d^3 p_i}{(2\pi)^3 2E_i} (\delta_{in} - iT_{in}^*) (\delta_{in} + iT_{in}^*) &= \delta_{ii} \implies \\ i(T_{ii} - T_{ii}^*) + \sum_n \int \prod_{i=1}^n \frac{d^3 p_i}{(2\pi)^3 2E_i} T_{in}^* T_{in} &= 0 \implies \\ 2\text{Im}T_{ii} = \sum_n \int \prod_{i=1}^n \frac{d^3 p_i}{(2\pi)^3 2E_i} |T_{in}|^2, & \quad (2.2.6) \end{aligned}$$

and after substituting Equation (2.2.3) one gets

$$2\text{Im}\mathcal{M}_{HH} = \sum_n \int \prod_{i=1}^n \frac{d^3 p_i}{(2\pi)^3 2E_i} (2\pi)^4 \delta\left(p_H - \sum_{i=1}^n p_i\right) |\mathcal{M}_{Hn}|^2 . \quad (2.2.7)$$

Finally, if we apply Equation (2.2.1) we obtain

$$\Gamma(H) = \frac{1}{m_H} \text{Im}\mathcal{M}_{HH} . \quad (2.2.8)$$

In the presence of an effective Hamiltonian (as in our EFT) we can write the transition matrix as

$$T_{HH} = \frac{1}{2} \langle H | \mathcal{S} | H \rangle , \quad (2.2.9)$$

where

$$\mathcal{S} = i \int d^4 x \int d^4 y T \left\{ \mathcal{H}_{eff}(x) \mathcal{H}_{eff}(y) \right\} \quad (2.2.10)$$

is the first non-vanishing term from the expansion of the scattering matrix

$$S = T e^{-i \int d^4 x \mathcal{H}_{eff}(x)} . \quad (2.2.11)$$

The notation T in the definition above indicates the time-ordering operator. After some algebraic manipulation we can get rid of the integration over y (without loss of generality one could eliminate x), and applying Equation (2.2.3), Equation (2.2.8) becomes

$$\Gamma(H) = \frac{1}{2m_H} \text{Im} \langle H | \mathcal{T} | H \rangle \quad (2.2.12)$$

where

$$\mathcal{T} = i \int d^4 x T \left\{ \mathcal{H}_{eff}(x) \mathcal{H}_{eff}(0) \right\} . \quad (2.2.13)$$

Taking H to be a heavy hadron with heavy quark Q and considering the soft interactions of Q with the background gluon field³ or the spectator quarks we expand Equation (2.2.12) in a series of local operators \mathcal{O}_d of increasing dimension d i.e.

$$\Gamma(H_Q) = \frac{1}{2M_{H_Q}} \sum_d c_d \frac{\langle \mathcal{O}_d \rangle}{m_Q^{d-3}} , \quad (2.2.14)$$

³For more details about the expansion of the quark propagator to the soft gluon background field we point you to the excellent reviews [63, 64]

where $\langle \mathcal{O}_d \rangle = \langle H_Q | \mathcal{O}_d | H_Q \rangle$ and c_d are their corresponding $\Delta Q = 0$ Wilson coefficients. Because of the double insertion of the \mathcal{H}_{eff} , in our calculations c_d will be quadratic functions of the $\Delta Q = 1$ Wilson coefficients. The operators can have any gauge-invariant form and should be bilinear in the heavy quark.

Since the heavy quark Q is interacting with the light degrees of freedom at scales of order Λ_{QCD} , much smaller than m_Q we can extract this large mechanical part from Q i.e.

$$Q(x) = e^{-im_Q v \cdot x} Q_v(x) , \quad (2.2.15)$$

where v is the hadron 4-velocity. Notice that Q_v is similar to h_v from HQET but in this case it is a rescaled full QCD four-component spinor and not a two-component static field as described in Section 2.1.2. In general, the HQET is an effective theory designed to systematically use the simplified QCD interactions at the heavy quark limit. The HQE on the other hand is a framework that lets us calculate inclusive decays of heavy hadrons without having to calculate all exclusive decay channels at hadronic level. Furthermore it is, an OPE that by definition is expressed in full QCD i.e. the fields entering Equation (2.2.14) are four-component full QCD fields. Of course it can be implemented with HQET fields as well (as is done in Chapter 4). More details about the difference between the HQET and the HQE can be found in [64].

Starting with the lowest order operator, $\bar{Q}Q$ we can express it at leading order as $\bar{Q}_v Q_v$ but we can also get higher order corrections. To do so we will need the following identities stemming directly from the expansion of Equation (2.2.15) and the equation of motion $(i\not{D} - m_Q)Q = 0$

$$P_- Q_v(x) = \frac{i\not{D}}{2m_Q} Q_v(x) , \quad (2.2.16)$$

and its conjugate form

$$\bar{Q}_v(x)P_- = \bar{Q}_v(x)\frac{\overleftarrow{i\not{D}}}{2m_Q}, \quad (2.2.17)$$

where P_- is the projection operator defined in Equation (2.1.44). Expanding $\bar{Q}Q$ we get

$$\begin{aligned} \bar{Q}Q &= \bar{Q}_v Q_v = \bar{Q}_v Q_v - \bar{Q}_v \not{\psi} Q_v + \bar{Q}_v \not{\psi} Q_v \\ &= \bar{Q}_v \not{\psi} Q_v + 2\bar{Q}_v P_- Q_v \\ &= \bar{Q}_v \not{\psi} Q_v + 2\bar{Q}_v P_- P_- Q_v \\ &= \bar{Q}_v \not{\psi} Q_v + 2\bar{Q}_v \frac{\overleftarrow{i\not{D}}}{2m_Q} \frac{i\not{D}}{2m_Q} Q_v \\ &= \bar{Q}_v \not{\psi} Q_v + \bar{Q}_v \frac{(i\not{D})^2}{2m_Q^2} Q_v + \text{total derivative}, \end{aligned} \quad (2.2.18)$$

where the total derivative does not contribute to the forward scattering since the matrix element of such an operator vanishes in zero momentum transfer [65]. Now we take the middle term and expand it splitting the Dirac structure into a symmetric and antisymmetric half.

$$\begin{aligned} \bar{Q}_v \frac{(i\not{D})^2}{2m_Q^2} Q_v &= \bar{Q}_v \left(\frac{[\gamma_\mu, \gamma_\nu](iD^\mu)(iD^\nu)}{4m_Q^2} \right) Q_v + \bar{Q}_v \left(\frac{\{\gamma_\mu, \gamma_\nu\}(iD^\mu)(iD^\nu)}{4m_Q^2} \right) Q_v \\ &= \frac{1}{2m_Q^2} \bar{Q}_v (iD^\mu)(iD^\nu)(-i\sigma_{\mu\nu}) Q_v + \frac{1}{2m_Q^2} \bar{Q}_v (iD_\mu)(iD^\mu) Q_v. \end{aligned} \quad (2.2.19)$$

So finally we can write (excluding the total derivative term)

$$\bar{Q}Q = \bar{Q}_v \not{\psi} Q_v + \frac{1}{m_Q^2} \bar{Q}_v (iD^\mu)(iD^\nu)(-i\sigma_{\mu\nu}) Q_v + \frac{1}{m_Q^2} \bar{Q}_v (iD_\mu)(iD^\mu) Q_v. \quad (2.2.20)$$

Following this expansion we can make some interesting observations:

- The first term arising in the expansion of $\bar{Q}Q$ is proportional to unity up to a normalisation factor as it corresponds to a conserved charge related to the heavy quark flavour [61].
- There is no correction proportional to $1/m_Q$. Such dimension-four operators

would have a single derivative and through equations of motion are reduced to dimension-five or higher. Also we can not include a dimension-four operator in Equation (2.2.14) either as it would have the form $\bar{Q}\not{D}Q$ and it would reduce to $\bar{Q}Q$ via equation of motion. This result is known as the CGG/BUV theorem [58, 61]. In HQET this result is known as Luke's Theorem [50].

From here on we will indicate the two operators at dimension-five as

$$\mathcal{O}_{kin} = \bar{Q}_v(iD_\mu)(iD^\mu)Q_v, \quad (2.2.21)$$

$$\mathcal{O}_{cmag} = \bar{Q}_v(iD^\mu)(iD^\nu)(-i\sigma_{\mu\nu})Q_v, \quad (2.2.22)$$

where both are the equivalent operators we derived in HQET. Further expansion gives us the $1/m_Q^3$ corrections [66]

$$\mathcal{O}_{\rho_D} = \bar{Q}_v(iD_\mu)(iv \cdot D)(iD^\mu)Q_v, \quad (2.2.23)$$

$$\mathcal{O}_{LS} = \bar{Q}_v(iD^\mu)(iv \cdot D)(iD^\nu)(-i\sigma_{\mu\nu})Q_v. \quad (2.2.24)$$

At dimension-six we are also getting four-quark operators of the form $\bar{Q}\Gamma q\bar{q}\Gamma Q$ where Γ refers to a Dirac structure and q is the spectator quark. For brevity we are not including the colour indices here but when necessary they will be made explicit.

In general we can expand Equation (2.2.14) for the decay of a hadron H_Q as

$$\Gamma(H_Q) = \Gamma_3 + \Gamma_5 \frac{\langle \mathcal{O}_5 \rangle}{m_Q^2} + \Gamma_6 \frac{\langle \mathcal{O}_6 \rangle}{m_Q^3} + \dots + 16\pi^2 \left(\tilde{\Gamma}_6 \frac{\langle \tilde{\mathcal{O}}_6 \rangle}{m_Q^3} + \tilde{\Gamma}_7 \frac{\langle \tilde{\mathcal{O}}_7 \rangle}{m_Q^4} + \dots \right), \quad (2.2.25)$$

where the tilde indicates the four-quark contributions. These terms at leading order in α_s arise from one-loop diagrams while the two-quark contributions come from two-loop diagrams. Therefore, the first ones are enhanced by a $16\pi^2$ phase space factor. The Γ_i coefficients can be calculated as a series in α_s i.e.

$$\Gamma_i = \Gamma_i^{(0)} + \frac{\alpha_s}{4\pi} \Gamma_i^{(1)} + \left(\frac{\alpha_s}{4\pi} \right)^2 \Gamma_i^{(2)} + \mathcal{O}(\alpha_s^3), \quad (2.2.26)$$

while in Equation (2.2.25) we also use the notation

$$\langle \mathcal{O}_i \rangle = \frac{\langle H_Q | \mathcal{O}_i | H_Q \rangle}{2M_{H_Q}} . \quad (2.2.27)$$

In terms of units, the $\frac{\Gamma_i}{m_Q^{i-3}}$ functions have units GeV^{4-i} while $\langle \mathcal{O}_i \rangle$ come with units GeV^{i-3} . Thus each term of Equation (2.2.25), and hence the total decay rate $\Gamma(H)$, has units GeV .

We still need a way to calculate the matrix elements of Equation (2.2.14). These encode low energy effects so we need to use non-perturbative methods to evaluate them such as Lattice QCD [67] or QCD Sum Rules [68]. In the HQET framework these matrix elements can be expanded in series in $1/m_Q$ and parametrised by non-perturbative parameters. Depending on the matrix element we are evaluating, various methods can be used, such as fitting to experimental data (see e.g. [69]) or spectroscopic relations (see e.g. [55]). The matrix element of $\bar{Q}Q$ can be expanded in this framework as

$$\langle H_Q | \bar{Q}Q | H_Q \rangle = 1 - \frac{\mu_\pi^2 - \mu_G^2}{2m_Q^2} + \mathcal{O}(1/m_Q^5) , \quad (2.2.28)$$

where μ_π^2, μ_G^2 parametrise the matrix elements of the kinetic and chromomagnetic operators respectively, i.e.

$$-\langle H_Q | \bar{Q}_v (iD_\mu) (iD^\mu) Q_v | H_Q \rangle = 2M_{H_Q} \mu_\pi^2 , \quad (2.2.29)$$

$$\langle H_Q | \bar{Q}_v (iD_\mu) (iD_\nu) (-i\sigma_{\mu\nu}) Q_v | H_Q \rangle = 2M_{H_Q} \mu_G^2 . \quad (2.2.30)$$

Identical to Equation (2.2.30) we can parametrise the matrix elements of \mathcal{O}_{ρ_D} and \mathcal{O}_{LS} just by replacing μ_G^2 with ρ_D^3 and ρ_{LS}^3 respectively.

For the four-quark operators, apart from the standard non-perturbative methods one can apply Vacuum Insertion Approximation (VIA) to estimate their matrix elements.

Using VIA we can write

$$\langle H_Q | \bar{Q} \Gamma q \bar{q} \Gamma Q | H_Q \rangle = \langle H_Q | \bar{Q} \Gamma q | 0 \rangle \langle 0 | \bar{q} \Gamma Q | H_Q \rangle . \quad (2.2.31)$$

The four-quark operators we will be mostly interested in will have the Dirac structure $V - A$ or $S - P$. To evaluate them one can start from the definition of the hadron decay constant

$$\langle 0 | \bar{q} \gamma_\mu \gamma_5 Q | H_Q \rangle = i f_{H_Q} p_\mu , \quad (2.2.32)$$

where p_μ is the hadron momentum. Also in the case of a pseudoscalar meson, parity conservation requires

$$\langle 0 | \bar{q} \gamma^\mu Q | H_Q \rangle = 0 , \quad (2.2.33)$$

$$\langle 0 | \bar{q} Q | H_Q \rangle = 0 , \quad (2.2.34)$$

and thus we can construct the $V - A$ and $S - P$ structures.

Chapter 3

D-Mixing

In this chapter we will introduce the basics of neutral meson mixing focusing on the case of D^0 mesons. We will derive the basic quantities that define a mixing system and see why the D^0 -mixing system has some peculiarities that make its theoretical description very difficult. To tackle them we show two different ways of choosing the renormalisation scale and present updated results that show better agreement with the experimental measurements even with large uncertainties. A great review of neutral meson mixing can be found in [70] while for a recent update in the D^0 -mixing we refer you to [71].

3.1 Introduction to Neutral Meson Mixing

Out of all the mesons, K, D^0, B_d and B_s are the only ones that mix with their antiparticles. These processes are driven by $\Delta F = 2$ transitions at the partonic level where $F = S, C, B$ (strangeness, charmness, bottomness). The Feynman diagrams for D-mixing can be seen in Figure 3.1. In order to develop the framework of neutral meson mixing systems we start with the time-dependent state $|D^0(t)\rangle$. We use the D meson as an example in this section but all this applies to all other mesons mentioned

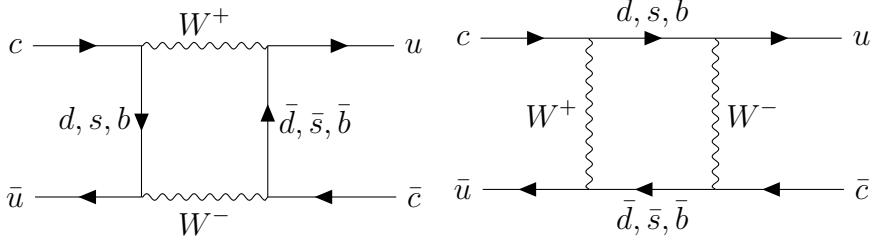


Figure 3.1: The box diagrams contributing to D-mixing.

above, unless specified otherwise. We can express the state as

$$|D^0(t)\rangle = A(t)|D^0\rangle + \bar{A}(t)|\bar{D}^0\rangle + \sum_i A_i(t)|f_i\rangle, \quad (3.1.1)$$

where the A coefficients carry the time dependence and correspond to the likelihood of the original state transitioning to the respective one in the RHS. Out of the terms above, for mixing we are only interested in the transition $|D^0\rangle \rightarrow |\bar{D}^0\rangle$, and vice versa. Using the Wigner-Weisskopf approximation [72] we write down a Schrödinger-like equation describing the $D^0 - \bar{D}^0$ system

$$i \frac{d}{dt} \begin{pmatrix} |D^0(t)\rangle \\ |\bar{D}^0(t)\rangle \end{pmatrix} = \hat{\mathcal{H}} \begin{pmatrix} |D^0\rangle \\ |\bar{D}^0\rangle \end{pmatrix}, \quad (3.1.2)$$

where

$$\hat{\mathcal{H}} = \left(\hat{M} - \frac{i}{2} \hat{\Gamma} \right). \quad (3.1.3)$$

The matrices $\hat{M}, \hat{\Gamma}$ are 2×2 complex and hermitian. The latter stems from the fact that you can decompose any matrix in a hermitian (\hat{M}) and an anti-hermitian ($\frac{i}{2}\hat{\Gamma}$) part. By considering the hermicity of these matrices as well as CPT invariance we can write \hat{M} and $\hat{\Gamma}$ as

$$\hat{\Gamma} = \begin{pmatrix} \Gamma_{11} & \Gamma_{12} \\ \Gamma_{12}^* & \Gamma_{11} \end{pmatrix}; \quad \hat{M} = \begin{pmatrix} M_{11} & M_{12} \\ M_{12}^* & M_{11} \end{pmatrix}. \quad (3.1.4)$$

The non-vanishing Γ_{12}, M_{12} are the quantities that drive the mixing dynamics. These are the absorptive and dispersive parts of \mathcal{H}_{12} . The first one corresponds to box diagrams with internal on-shell particles, while the latter includes only virtual contributions (including possible BSM particles). Because of their CKM structure these

quantities can be complex and so can be written as

$$\Gamma_{12} = |\Gamma_{12}|e^{i\phi_\Gamma} , \quad (3.1.5)$$

$$M_{12} = |M_{12}|e^{i\phi_M} . \quad (3.1.6)$$

In the case of no mixing, the non-diagonal elements would vanish, M_{11} would correspond to the mass of the meson and Γ_{11} would describe the total inclusive decay rate of the meson. In the case of mixing, in order to get the physical eigenstates of the mesons we need to diagonalise the matrices $\hat{M}, \hat{\Gamma}$. To do so we can write

$$\hat{U}^{-1} \left(\hat{M} - \frac{i}{2} \hat{\Gamma} \right) \hat{U} = \begin{pmatrix} M_L - \frac{i}{2} \Gamma_L & 0 \\ 0 & M_H - \frac{i}{2} \Gamma_H \end{pmatrix} , \quad (3.1.7)$$

where the matrix \hat{U} has the form

$$\hat{U} = \begin{pmatrix} p & p \\ q & -q \end{pmatrix} . \quad (3.1.8)$$

This form is possible because of the original structure of $\hat{\Gamma}$ and \hat{M} . The subscripts $\{L, H\}$ indicate the light and heavy meson eigenstate respectively. Once we substitute Equation (3.1.7) in Equation (3.1.2) and solve it we can write

$$\begin{pmatrix} |D^0(t)\rangle \\ |\bar{D}^0(t)\rangle \end{pmatrix} = \begin{pmatrix} g_+(t) & \frac{q}{p}g_-(t) \\ \frac{p}{q}g_-(t) & g_+(t) \end{pmatrix} \begin{pmatrix} |D^0\rangle \\ |\bar{D}^0\rangle \end{pmatrix} , \quad (3.1.9)$$

where

$$g_+(t) = e^{-imt} e^{-\frac{1}{2}\Gamma t} \left\{ \cosh \frac{\Delta\Gamma t}{4} \cos \frac{\Delta M t}{2} - i \sinh \frac{\Delta\Gamma t}{4} \sin \frac{\Delta M t}{2} \right\} , \quad (3.1.10)$$

$$g_-(t) = e^{-imt} e^{-\frac{1}{2}\Gamma t} \left\{ -\sinh \frac{\Delta\Gamma t}{4} \cos \frac{\Delta M t}{2} + i \cosh \frac{\Delta\Gamma t}{4} \sin \frac{\Delta M t}{2} \right\} \quad (3.1.11)$$

In the above expressions we have used the following notation:

$$m = \frac{M_H + M_L}{2} , \quad \Gamma = \frac{\Gamma_H + \Gamma_L}{2} , \quad (3.1.12)$$

$$\Delta M = M_H - M_L , \quad \Delta\Gamma = \Gamma_L - \Gamma_H . \quad (3.1.13)$$

It is easy to check that the $g_+(t), g_-(t)$ functions satisfy the obvious initial conditions $g_+(0) = 1, g_-(0) = 0$. Using Equations (3.1.10) and (3.1.11) we can now calculate the time-dependent decay rate of a meson (or an antimeson) to a final state f or \bar{f} . For the transitions $D \rightarrow f, \bar{D} \rightarrow f$ we define the amplitudes

$$A_f = \langle f|D\rangle, \quad \bar{A}_f = \langle f|\bar{D}\rangle, \quad (3.1.14)$$

and similarly for $D \rightarrow \bar{f}$ and $\bar{D} \rightarrow \bar{f}$

$$A_{\bar{f}} = \langle \bar{f}|D\rangle, \quad \bar{A}_{\bar{f}} = \langle \bar{f}|\bar{D}\rangle. \quad (3.1.15)$$

For this work we will only focus on flavour specific decays which have the following properties:

1. The decays $\bar{D} \rightarrow f$ and $D \rightarrow \bar{f}$ are forbidden and these transitions can only occur as $\bar{D} \rightarrow D \rightarrow f$ and $D \rightarrow \bar{D} \rightarrow \bar{f}$. This means $\bar{A}_f = A_{\bar{f}} = 0$.
2. No direct CP violation arises in such decays, which means $|A_f| = |\bar{A}_{\bar{f}}|$

An example of such a decay is $D^0 \rightarrow Xl^+\nu_l$.

In general, for the time dependent decay of a D meson to a state f we can write

$$\Gamma[D \rightarrow f](t) = N_f |\langle f|D(t)\rangle|^2, \quad (3.1.16)$$

where N_f is a normalisation constant and we take $N_f = N_{\bar{f}}$ since it depends only on the kinematics. Using Equation (3.1.9), the expressions for $g_+(t)$ and $g_-(t)$ and considering only flavour specific decays we get

$$\Gamma[D \rightarrow f](t) = \frac{N_f |A_f|^2}{2} e^{-\Gamma t} \left(\cosh \frac{\Delta\Gamma t}{2} + \cos \Delta M t \right). \quad (3.1.17)$$

Similarly for the other processes we get

$$\Gamma[\bar{D} \rightarrow f](t) = \frac{N_f |A_f|^2}{2} e^{-\Gamma t} \left| \frac{p}{q} \right|^2 \left(\cosh \frac{\Delta\Gamma t}{2} - \cos \Delta M t \right), \quad (3.1.18)$$

$$\Gamma[D \rightarrow \bar{f}](t) = \frac{N_f |\bar{A}_{\bar{f}}|^2}{2} e^{-\Gamma t} \left| \frac{q}{p} \right|^2 \left(\cosh \frac{\Delta\Gamma t}{2} - \cos \Delta M t \right), \quad (3.1.19)$$

$$\Gamma[\bar{D} \rightarrow \bar{f}](t) = \frac{N_f |\bar{A}_f|^2}{2} e^{-\Gamma t} \left(\cosh \frac{\Delta\Gamma t}{2} + \cos \Delta M t \right). \quad (3.1.20)$$

3.2 Mixing Observables

So far, we have introduced the time-evolution equation for the mixing system and built most of the notation we will need to define the quantities that describe this system. We start by considering the eigenvalues of $\hat{\mathcal{H}}$:

$$\lambda_{L,H} = M_{L,H} - \frac{i}{2} \Gamma_{L,H}, \quad (3.2.1)$$

which satisfy

$$(\lambda_L - \lambda_H)^2 = 4\mathcal{H}_{12}\mathcal{H}_{21}. \quad (3.2.2)$$

The LHS of the equation above can be expressed as

$$\begin{aligned} (\lambda_L - \lambda_H)^2 &= \left((M_H - M_L) + \frac{i}{2}(\Gamma_L - \Gamma_H) \right)^2 = \left(\Delta M + \frac{i}{2}\Delta\Gamma \right)^2 \\ &= \Delta M^2 - \frac{1}{4}\Delta\Gamma^2 + i\Delta M\Delta\Gamma, \end{aligned} \quad (3.2.3)$$

while for the RHS we get

$$\begin{aligned} 4\mathcal{H}_{12}\mathcal{H}_{21} &= 4\left(M_{12} - \frac{i}{2}\Gamma_{12}\right)\left(M_{21} - \frac{i}{2}\Gamma_{21}\right) \\ &= 4\left(M_{12}M_{21} - \frac{1}{4}\Gamma_{12}\Gamma_{21} - \frac{i}{2}(M_{12}\Gamma_{21} + M_{21}\Gamma_{12})\right) \\ &= 4|M_{12}|^2 - |\Gamma_{12}|^2 + 4i|M_{12}||\Gamma_{12}|\cos\phi_{12}, \end{aligned} \quad (3.2.4)$$

where in the last line we have used $M_{12} = M_{21}^*$ and $\Gamma_{12} = \Gamma_{21}^*$. Using additionally that the non-diagonal elements of the matrix $\hat{U}^{-1}\hat{\mathcal{H}}\hat{U}$ vanish we can write

$$\frac{q}{p} = -\frac{2M_{12}^* - i\Gamma_{12}^*}{\Delta M + \frac{i}{2}\Delta\Gamma} = -\frac{\Delta M + \frac{i}{2}\Delta\Gamma}{2M_{12} - i\Gamma_{12}}. \quad (3.2.5)$$

Equating the real and imaginary parts of Equations (3.2.3) and (3.2.4) we get

$$4|M_{12}|^2 - |\Gamma_{12}|^2 = \Delta M^2 - \frac{1}{4}\Delta\Gamma^2 \equiv a, \quad (3.2.6)$$

$$4|M_{12}||\Gamma_{12}|\cos\phi_{12} = \Delta M\Delta\Gamma \equiv b, \quad (3.2.7)$$

where $\phi_{12} = \arg\left(-\frac{M_{12}}{\Gamma_{12}}\right)$. In B-mixing one can simplify these equation by using $|\Gamma_{12}/M_{12}| \ll 1$. This is not valid in D-mixing and in order to calculate $\Delta\Gamma, \Delta M$ one needs to calculate both M_{12} and Γ_{12} .

Experimentally it is found that the CP -violating phase ϕ_{12} is small (HFLAV [73] states a $[-1.2^\circ, 2.42^\circ]$ range) and so we can use it to expand the mass and decay width in a Taylor series⁴ [71]. To do so we solve Equation (3.2.6) and Equation (3.2.7) for $\Delta\Gamma, \Delta M$ and write

$$\Delta M^2 = \frac{\sqrt{a^2 + b^2} + a}{2}, \quad (3.2.8)$$

$$\Delta\Gamma^2 = 2\left(\sqrt{a^2 + b^2} - a\right). \quad (3.2.9)$$

The quantities $\Delta M, \Delta\Gamma, a, b$ can also be rewritten in terms of the ratio

$$r_{12} = |\Gamma_{12}/M_{12}| \quad (3.2.10)$$

as

$$\Delta M = \pm \frac{\sqrt{2}}{2} |M_{12}| \sqrt{w + 4 - r_{12}}, \quad (3.2.11)$$

$$\Delta\Gamma = \pm \sqrt{2} |M_{12}| \sqrt{w + r_{12} - 4}, \quad (3.2.12)$$

$$a = |M_{12}|^2 (4 - r_{12}), \quad (3.2.13)$$

$$b = 4 |M_{12}|^2 \sqrt{r_{12}} \cos \phi_{12}, \quad (3.2.14)$$

where $w = \sqrt{(4 - r_{12})^2 + 16r_{12} \cos^2 \phi_{12}}$ and then we can write

$$\sqrt{a^2 + b^2} \pm a = |M_{12}|^2 \left(\sqrt{(4 - r_{12})^2 + 16r_{12} \cos^2 \phi_{12}} \pm (4 - r_{12}) \right). \quad (3.2.15)$$

If we expand this in small ϕ_{12} we get

$$\sqrt{a^2 + b^2} \pm a = |M_{12}|^2 (4 + r_{12}) \left(1 - \frac{16r_{12}}{(4 + r_{12})^2} \frac{\phi_{12}^2}{2} \right) \pm (4 - r_{12}) + \mathcal{O}(\phi_{12}^4). \quad (3.2.16)$$

⁴The expansion in ϕ_{12} that is included in this section and in Ref [71] has been independently cross-checked by us before its publication.

Now we can express $\Delta\Gamma, \Delta M$ in the small ϕ_{12} regime

$$\Delta\Gamma = \pm 2|\Gamma_{12}| \left(1 - \frac{4}{4+r_{12}} \frac{\phi_{12}^2}{2} + \mathcal{O}(\phi_{12}^4) \right), \quad (3.2.17)$$

$$\Delta M = \pm 2|M_{12}| \left(1 - \frac{r_{12}}{4+r_{12}} \frac{\phi_{12}^2}{2} + \mathcal{O}(\phi_{12}^4) \right). \quad (3.2.18)$$

We notice that the quantities $\frac{4}{4+r_{12}}, \frac{r_{12}}{4+r_{12}}$ can only vary between 0 and 1 and the first corrections to Equations (3.2.17) and (3.2.18) arise at order ϕ_{12}^2 . Using the range of values of ϕ_{12} stated above⁵, the correction to the leading term for both $\Delta\Gamma$ and ΔM is less than 0.1%. Finally, we can easily derive from Equations (3.2.17) and (3.2.18) the approximations

$$|\Delta\Gamma| \approx 2|\Gamma_{12}|, \quad |\Delta M| \approx 2|M_{12}|. \quad (3.2.19)$$

In the case of B^q -mixing we can also consider the approximation $|\Gamma_{12}^q| \ll |M_{12}^q|$ and express the ratio of $\Delta\Gamma^q/\Delta M^q$ and the semi-leptonic CP asymmetries very simply in terms of Γ_{12}^q and M_{12}^q . First by solving the system of Equations (3.2.6), (3.2.7) for $\Delta\Gamma^q$ and ΔM^q we can write

$$\Delta\Gamma^q = 2|\Gamma_{12}^q| \cos \phi_{12}^q + \mathcal{O}((|\Gamma_{12}^q|/|M_{12}^q|)^2), \quad (3.2.20)$$

$$\Delta M^q = 2|M_{12}^q| + \mathcal{O}((|\Gamma_{12}^q|/|M_{12}^q|)^2). \quad (3.2.21)$$

Then we can write

$$\frac{\Delta\Gamma^q}{\Delta M^q} = \left| \frac{\Gamma_{12}^q}{M_{12}^q} \right| \cos \phi_{12}^q = \text{Re} \left(-\frac{\Gamma_{12}^q}{M_{12}^q} \right). \quad (3.2.22)$$

Next we define the CP asymmetry in flavour specific decays a_{fs}^q as

$$a_{fs} = \frac{\Gamma[\bar{B}^q \rightarrow f](t) - \Gamma[B^q \rightarrow \bar{f}](t)}{\Gamma[\bar{B}^q \rightarrow f](t) + \Gamma[B^q \rightarrow \bar{f}](t)}, \quad (3.2.23)$$

where f is a flavour specific state. In the case of semi-leptonic decays the above quantity is also called semi-leptonic CP asymmetry, a_{sl}^q . Considering the semi-

⁵HFLAV defines $\phi_{12} = \arg\left(\frac{M_{12}}{\Gamma_{12}}\right)$ which is a π factor different from our definition. This however does not change the above results since the only dependence on ϕ_{12} comes from $\cos(\phi_{12})^2$ which is the same for both definitions.

leptonic case we insert Equations (3.1.18) and (3.1.19) in the above formula and write

$$\begin{aligned}
a_{sl}^q &= \frac{1 - \left|\frac{q}{p}\right|^4}{1 + \left|\frac{q}{p}\right|^4} \\
&= \frac{4|M_{12}^q||\Gamma_{12}^q| \sin \phi_{12}}{4|M_{12}^q| + |\Gamma_{12}^q|} \\
&= \left| \frac{\Gamma_{12}^q}{M_{12}^q} \right| \sin \phi_{12}^q + \mathcal{O}((|\Gamma_{12}^q|/|M_{12}^q|)^3) \\
&\approx \text{Im} \left(\frac{\Gamma_{12}^q}{M_{12}^q} \right) , \tag{3.2.24}
\end{aligned}$$

where in the second line we have used the two expressions of Equation (3.2.5). The result up to the second line is valid for all neutral meson mixing, however, in the third line we have used $|\Gamma_{12}^q| \ll |M_{12}^q|$ and it can be used only in B^q -mixing.

3.3 D-Mixing

All the definitions and formulas above are not valid only for the D^0 -mixing system but can be generalised to other mesons that mix with their antiparticles. From now on though we will focus specifically on the D-mixing system. The current theoretical understanding of charm physics needs to be improved so that we will be able to use the current and future huge amount of data obtained from experiments like LHCb [74], BESIII [75] and Belle II [76]. One of the latest big discoveries was the announcement of a non-vanishing measurement of ΔA_{CP} [77]

$$\Delta A_{CP} = A_{CP}(D^0 \rightarrow K^+K^-) - A_{CP}(D^0 \rightarrow \pi^+\pi^-) , \tag{3.3.1}$$

where

$$A_{CP}(t, f) = \frac{\Gamma(D^0(t) \rightarrow f) - \Gamma(\bar{D}^0(t) \rightarrow f)}{\Gamma(D^0(t) \rightarrow f) + \Gamma(\bar{D}^0(t) \rightarrow f)} . \tag{3.3.2}$$

In fact, the value measured was $\Delta A_{CP} = (-15.4 \pm 2.9) \times 10^{-4}$ and it is the first discovery of CP violation in the charm system. Possible explanations of this deviation from zero can be contributions from BSM physics (see e.g. [78, 79] partly

based on the calculation of [80]) or it could still also be explained within the SM (see e.g. [81–84]).

The quantitative description of D-mixing is still an unsolved puzzle in charm physics. Due to immense recent progress, D-mixing is by now experimentally very well established and precisely measured [73, 85]

$$x = \frac{\Delta M}{\Gamma_D} = 0.409^{+0.048}_{-0.049}\% , \quad y = \frac{\Delta\Gamma}{2\Gamma_D} = 0.615^{+0.056}_{-0.055}\% , \quad (3.3.3)$$

where Γ_D is the total decay of the D^0 meson. Using Equation (3.2.17) and Equation (3.2.18) we can rewrite the quantities x, y as

$$x \approx x_{12} = 2 \frac{|M_{12}|}{\Gamma_D} , \quad y \approx y_{12} = \frac{|\Gamma_{12}|}{\Gamma_D} \quad (3.3.4)$$

up to corrections of $\mathcal{O}(\phi_{12}^2)$. This way x and y depend on the non-diagonal elements of the mixing matrix. Different theory approaches for x, y can cover a huge range of values, differing by several orders of magnitude, see e.g. [86, 87]. Future measurements are expected to give even more precise values and also a stronger bound (or even a measurement) of the CP -violating phase ϕ_{12} . So is there a way to improve the theoretical values of these quantities?

3.4 HQE in D-Mixing

We start to investigate Γ_{12} within the framework of the HQE, as presented in Section 2.2. The study of M_{12} is beyond the scope of this work. Therefore we are not in a position to determine the value of $\phi_{12} = \pi - \phi_\Gamma - \phi_M$. Using HQE we can write

$$\Gamma_{12} = \left[\Gamma_6^{(0)} + \frac{\alpha_s}{4\pi} \Gamma_6^{(1)} + \mathcal{O}(\alpha_s^2) \right] \frac{\langle Q_6 \rangle}{m_c^3} + \left[\Gamma_7^{(0)} + \mathcal{O}(\alpha_s) \right] \frac{\langle Q_7 \rangle}{m_c^4} + \mathcal{O}(1/m_c^5) . \quad (3.4.1)$$

Unlike the full decay rate of the D meson the HQE for mixing starts from dimension-six with four-quark operator contributions. Diagrammatically one can see Equation (3.4.1) in Figure 3.2. The product of two $\Delta C = 1$ operators from the effective

Hamiltonian is matched into a series of local $\Delta C = 2$ operators (note in this case this is the “full” theory unlike in Section 2.1.1 where full theory was the SM). The operators arising at dimension-six are

$$Q = \bar{c}_i \gamma_\mu (1 - \gamma_5) u_i \bar{c}_j \gamma^\mu (1 - \gamma_5) u_j , \quad (3.4.2)$$

$$Q_S = \bar{c}_i (1 - \gamma_5) u_i \bar{c}_j (1 - \gamma_5) u_j , \quad (3.4.3)$$

$$\tilde{Q}_S = \bar{c}_i (1 - \gamma_5) u_j \bar{c}_j (1 - \gamma_5) u_i , \quad (3.4.4)$$

which are not independent from each other. In fact, a linear combination of them gives a $1/m_c$ suppressed operator [88, 89]

$$R_0 = Q_S + \alpha_1 \tilde{Q}_S + \frac{1}{2} \alpha_2 Q + \mathcal{O}(\bar{\Lambda}/m_c) , \quad (3.4.5)$$

where

$$\alpha_1 = 1 + \frac{\alpha_s}{4\pi} C_F \left(12 \log \frac{\mu_2}{m_c} + 6 \right) , \quad (3.4.6)$$

$$\alpha_2 = 1 + \frac{\alpha_s}{4\pi} C_F \left(6 \log \frac{\mu_2}{m_c} + \frac{13}{2} \right) . \quad (3.4.7)$$

The matrix elements of the above operators can be parametrised as (see e.g. [88])

$$\langle D^0 | Q | \bar{D}^0 \rangle = \frac{8}{3} M_D^2 f_D^2 B_1 , \quad (3.4.8)$$

$$\langle D^0 | Q_S | \bar{D}^0 \rangle = -\frac{5}{3} M_D^2 f_D^2 B'_2 , \quad (3.4.9)$$

$$\langle D^0 | \tilde{Q}_S | \bar{D}^0 \rangle = \frac{1}{3} M_D^2 f_D^2 B'_3 , \quad (3.4.10)$$

where

$$B'_2 = \frac{M_D^2}{m_c^2} B_2 , \quad (3.4.11)$$

$$B'_3 = \frac{M_D^2}{m_c^2} B_3 , \quad (3.4.12)$$

and the bag parameters B_1, B_2, B_3 are equal to 1 in VIA. Equation (3.4.15) is traditionally used to eliminate Q_s or \tilde{Q}_S from the calculation.

At subleading order $1/m_c$ we have four additional operators arising, along R_0

$$R_2 = \frac{1}{m_c} \bar{c}_i \overleftarrow{D}_\nu \gamma_\mu (1 - \gamma_5) D_\nu u_i \bar{c}_j \gamma^\mu (1 - \gamma_5) u_j, \quad (3.4.13)$$

$$R_3 = \frac{1}{m_c} \bar{c}_i \overleftarrow{D}_\nu (1 - \gamma_5) D_\nu u_i \bar{c}_j (1 - \gamma_5) u_j, \quad (3.4.14)$$

and the operators \tilde{R}_i which are obtained by switching the colour indices to get the colour rearranged operators. Note that the missing R_1 operator is not present in D-mixing since it is proportional to $m_u \approx 0$ (see e.g [88]). We just choose to follow the notation of most literature, e.g. [88–93]. Their matrix elements can be parametrised as

$$\langle D^0 | R_0 | \bar{D}^0 \rangle = -\frac{4}{3} \left(\frac{M_D^2}{(m_c^p)^2} - 1 \right) M_D^2 f_D^2 B_{R_0}, \quad (3.4.15)$$

$$\langle D^0 | R_2 | \bar{D}^0 \rangle = -\frac{2}{3} \left(\frac{M_D^2}{(m_c^p)^2} - 1 \right) M_D^2 f_D^2 B_{R_2}, \quad (3.4.16)$$

$$\langle D^0 | \tilde{R}_2 | \bar{D}^0 \rangle = \frac{2}{3} \left(\frac{M_D^2}{(m_c^p)^2} - 1 \right) M_D^2 f_D^2 B_{\tilde{R}_2}, \quad (3.4.17)$$

$$\langle D^0 | R_3 | \bar{D}^0 \rangle = \frac{7}{6} \left(\frac{M_D^2}{(m_c^p)^2} - 1 \right) M_D^2 f_D^2 B_{R_3}, \quad (3.4.18)$$

$$\langle D^0 | \tilde{R}_3 | \bar{D}^0 \rangle = \frac{5}{6} \left(\frac{M_D^2}{(m_c^p)^2} - 1 \right) M_D^2 f_D^2 B_{\tilde{R}_3}, \quad (3.4.19)$$

see e.g. [88]. The parameter m_c^p by definition is the pole charm quark mass. Normally, the pole mass is not a suitable parameter in HQE due to renormalon ambiguity that leads to bad convergence of the perturbation series. These can be avoided by using an alternative mass scheme (like the short-distance \overline{MS} mass scheme). However, we can not just replace the pole mass with another one. We need to use a conversion formula between them. Typically this conversion formula has the form

$$m_Q^{Pole} = m_Q^{alt} (1 + \mathcal{O}(\alpha_s)) \quad (3.4.20)$$

As we can see, at LO the pole mass can be taken equal to the new one and all their differences are included as QCD corrections. However since Γ_7 is only known to LO we can lose significant information by just using the LO result of the mass conversion. Therefore we choose to use the initial value of the pole mass. Additionally in the

case of B-mixing it was suggested in [93] to use a power correction mass for similar reasons and also to make sure the bracketed terms of the Equations (3.4.15) - (3.4.19) are of order $\Lambda_{QCD} \sim 0.2 \text{ GeV}$. Here we find that even when using the value of pole mass we can achieve that and hence we will use $m_c^p = 1.67 \text{ GeV}$. Ideally of course, with more orders of Γ_7 known, m_c^p can be replaced by a renormalon-free mass safely, using additional terms of the conversion formula.

To calculate $\Gamma_6^{(0)}$ and $\Gamma_6^{(1)}$ we need to evaluate the left and middle⁶ diagram of Figure 3.2. The results can be found in [88–93] after substituting $m_b \rightarrow m_c$, $m_c \rightarrow m_s$ and all other relevant parameters. The LO calculation can also be found in Appendix D. The expression for $\Gamma_7^{(0)}$ can be taken with similar switches from [88, 90, 93] and is included in Appendix D as well. The dimension-six matrix elements have been calculated in [4, 94]. Using the experimental value for y in Equation (3.3.3) we can

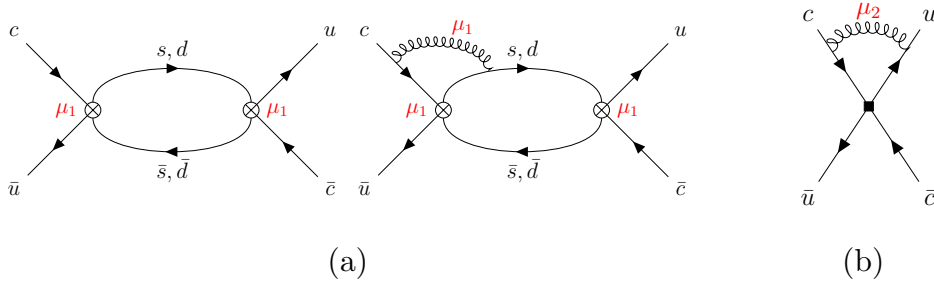


Figure 3.2: (a) Diagrams describing the mixing of neutral D mesons via intermediate $s\bar{s}$, $s\bar{d}$, $d\bar{s}$ and $d\bar{d}$ states in the “full” theory at LO-QCD (left) and NLO-QCD (right). The crossed circles denote the insertion of $\Delta C = 1$ operators of the effective Hamiltonian describing the charm-quark decay. The dependence on the renormalisation scale μ_1 in the Wilson coefficients cancels against the μ_1 dependence of the QCD corrections. (b) Diagram describing mixing of neutral D mesons at NLO-QCD in the HQE. The full dot indicates the insertion of $\Delta C = 2$ operators. The dependence on the renormalisation scale μ_2 cancels out between the QCD corrections to the diagram and the matrix elements of the corresponding $\Delta C = 2$ operators.

write

$$\Delta\Gamma^{Exp} \geq 0.027ps^{-1} , \quad (3.4.21)$$

⁶The middle diagram is only one of the diagrams contributing to $\Gamma_6^{(1)}$. See [89].

at one standard deviation.⁷ Based on that and using the approximation $|\Delta\Gamma| \approx 2|\Gamma_{12}|$ we define the following quantity

$$\Omega = \frac{2|\Gamma_{12}|^{\text{SM}}}{0.027 \text{ ps}^{-1}}. \quad (3.4.22)$$

A value of Ω smaller than 1 indicates that we are unable to describe D-mixing within 1σ . A naive application of HQE leads to $\Omega = 3.4 \times 10^{-5}$ at LO-QCD and $\Omega = 6.2 \times 10^{-5}$ at NLO-QCD. As we can see this prediction is around five orders of magnitude smaller than 1. We can split y into separate contributions based on the internal quark content

$$y = \underbrace{(y^{sd} + y^{ds})}_{\Delta S=1} - \underbrace{(y^{ss} + y^{dd})}_{\Delta S=0}. \quad (3.4.23)$$

It turns out that every bracket gives a value larger than the experimental measurement of y with an implicit uncertainty of at least 20%. By taking the numerical difference of $\Delta S = 1$ and $\Delta S = 0$ however, we end up with a result approximately in the range $[10^{-4}, 10^{-5}]$. Taking this result at its face value we are implicitly assuming a precision of $10^{-4} \dots 10^{-5}$ in the individual $\Delta S = 1$, $\Delta S = 0$ which of course is unrealistic. For the above calculation of Ω and the following ones we are using PDG [95] for all the masses and the strong coupling while for the CKM elements we are using input from [96]. For the non-perturbative matrix elements we have used [4] and the meson decay constant is from [97].

Using CKM unitarity we can further work out where this huge cancellation is originating from, expressing Γ_{12} as

$$\Gamma_{12} = - \left(\lambda_s^2 \Gamma_{12}^{ss} + 2 \lambda_s \lambda_d \Gamma_{12}^{sd} + \lambda_d^2 \Gamma_{12}^{dd} \right) \quad (3.4.24)$$

$$= - \lambda_s^2 \left(\Gamma_{12}^{ss} - 2\Gamma_{12}^{sd} + \Gamma_{12}^{dd} \right) + 2\lambda_s \lambda_b \left(\Gamma_{12}^{sd} - \Gamma_{12}^{dd} \right) - \lambda_b^2 \Gamma_{12}^{dd}, \quad (3.4.25)$$

⁷In [6] a value of 0.028 ps^{-1} was used since the latest measurement of y was not available. This difference does not have a significant numerical impact.

where $\lambda_q = V_{cq}V_{uq}^*$ and $\Gamma_{12}^{qq'}$ denotes the contribution from the diagrams with internal quark pair qq' . We have also used the CKM unitarity equation $\lambda_d + \lambda_s + \lambda_b = 0$. The peculiar feature of Equation (3.4.25) is that in terms of absolute size, the CKM dominant factor λ_s^2 multiplies the doubly GIM suppressed term, the CKM suppressed factor $\lambda_s\lambda_b$ multiplies the more lightly GIM suppressed term and the doubly CKM suppressed factor λ_b^2 multiplies a term with no GIM suppression. This results in all three terms of Equation (3.4.25) having similar size and all of them being heavily suppressed:

$$\begin{aligned}\Gamma_{12} &= (2.08 \cdot 10^{-7} - 1.34 \cdot 10^{-11} I) \text{ (1st term)} \\ &\quad - (3.74 \cdot 10^{-7} + 8.31 \cdot 10^{-7} I) \text{ (2nd term)} \\ &\quad + (2.22 \cdot 10^{-8} - 2.5 \cdot 10^{-8} I) \text{ (3rd term)} .\end{aligned}\tag{3.4.26}$$

This feature is very different from the case of B-mixing, where the CKM dominant term multiplies the term with no GIM suppression.

The suppression in Γ_{12} seems to be lifted by one order of $z = m_s^2/m_c^2$ if we go from LO-QCD to NLO-QCD [98]. More specifically, if one expands the Γ_{ij} combinations of Equation (3.4.25) in powers of z one finds

$$\Gamma_{12}^{ss} = \begin{cases} 1.62 - 2.34 z - 5.07 z^2 + \dots & \text{(LO),} \\ 1.42 - 4.30 z - 12.45 z^2 + \dots & \text{(NLO),} \end{cases}\tag{3.4.27}$$

$$\Gamma_{12}^{sd} - \Gamma_{12}^{dd} = \begin{cases} -1.17 z - 2.53 z^2 + \dots & \text{(LO),} \\ -2.15 z - 6.26 z^2 + \dots & \text{(NLO),} \end{cases}\tag{3.4.28}$$

$$\Gamma_{12}^{ss} - 2\Gamma_{12}^{sd} + \Gamma_{12}^{dd} = \begin{cases} -13.38 z^3 + \dots & \text{(LO),} \\ 0.07 z^2 - 29.72 z^3 + \dots & \text{(NLO).} \end{cases}\tag{3.4.29}$$

Several possible solutions have been proposed as an explanation for this big difference between HQE and experiment:

- Higher orders in HQE could be less affected by GIM suppression [99–101]. A

full determination of dimension-nine and twelve will be needed for that though (first estimates of dimension-nine can be found in [102]).

- Quark hadron duality could also explain it. In [103] it was shown that a duality violation of only 20% could be enough to match the experimental values. For a recent investigation see also [104].
- One might also argue that the HQE is simply not applicable in the charm sector because of the relatively small mass of the charm quark. In e.g. [105–107] different methods, such as summing over exclusive decay channels, have been investigated.
- It is also possible that contributions from BSM physics could enhance the theoretical predictions (see e.g. [108–110]).

3.5 Alternative scale setting

If we look at Figure 3.2 we will see that there are two renormalisation scales arising, μ_1 and μ_2 . The first one originates from the $\Delta C = 1$ Wilson coefficients and from the NLO-QCD correction diagrams. It is essentially the same scale we introduced in Section 2.1.1. The second scale comes from a different matching procedure and is included in the radiative corrections of the HQE diagrams (right diagram of Figure 3.1.7). This cancels exactly with the scale dependence of the matrix elements of the $\Delta C = 2$. Normally, in a calculation going from LO-QCD to NLO-QCD the dependence to the renormalisation scale is reduced, but that does not seem to be the case in D-mixing. In fact, if you look at Figure 3.3 it looks like the scale dependence gets worse in the case of $|\Gamma_{12}|$. However, if we look in a specific Γ_{12}^{ij} contribution in Figure 3.4, the scale dependence looks better at NLO-QCD. This weird scale dependence behaviour in $|\Gamma_{12}|$ can be understood then as another effect of the severe GIM cancellations. Since the cancellation of the μ_2 dependence is very pronounced we will only consider the μ_1 scale.

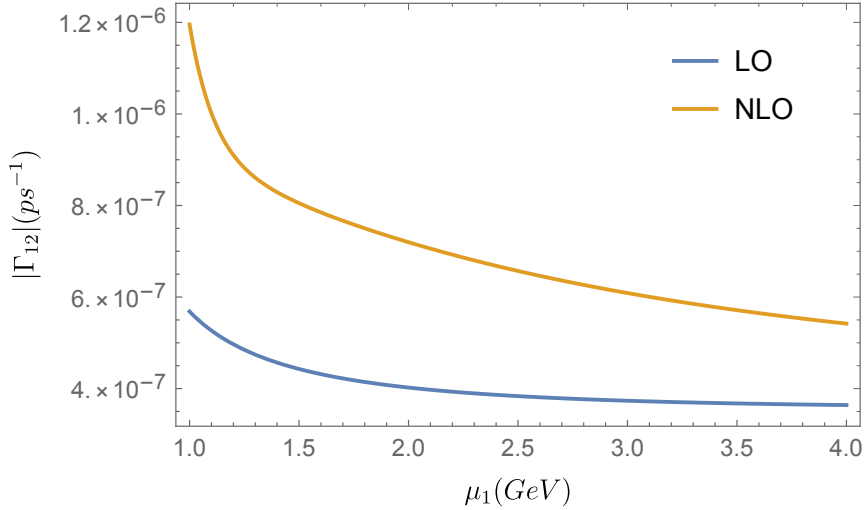


Figure 3.3: Scale dependence of $|\Gamma_{12}|$ at LO-QCD (blue) and NLO-QCD (orange)

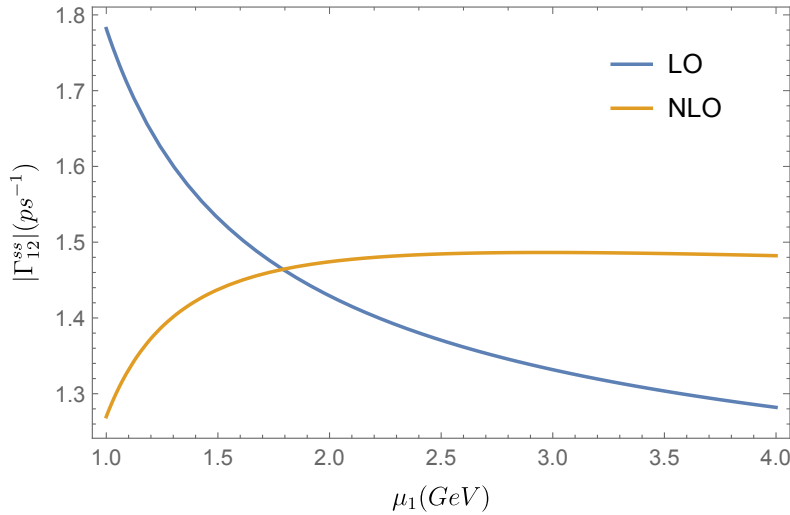


Figure 3.4: Scale dependence of $|\Gamma_{12}^{ss}|$ at LO-QCD (blue) and NLO-QCD (orange)

In the naive application of HQE that we mentioned earlier, we set $\mu_1 = m_c$ so that terms proportional to $\alpha_s(\mu_1) \log(\mu_1^2/m_c^2)$ are minimised. In order to estimate the scale uncertainties due to truncation of higher orders, we vary μ_1 from 1 GeV to $2m_c$. Normally in the B system we would vary between $m_b/2$ to $2m_b$, but for the charm mass that would lead us to very low energies where the perturbation theory is not valid anymore. Thus we set a bound at 1 GeV. Here we propose two alternative ways of treating the scale μ_1 . Both of them are based on the idea that different internal quark pairs contribute to different decay channels of the $D^0(\bar{D}^0)$

meson. More specifically, the $s\bar{s}$ pair corresponds to a K^+K^- final state, the $s\bar{d}(d\bar{s})$ to $K^-\pi^+(K^+\pi^-)$ and the $d\bar{d}$ pair to $\pi^+\pi^-$. For each of these observables we will introduce their specific μ_1 scale indicated as μ_1^{ij} , where i, j is the internal quark pair. While traditionally these scales were set equal $\mu_1^{ss} = \mu_1^{sd} = \mu_1^{dd} = m_c$, we introduce two alternative renormalisation scale setting schemes.

1. The central values of all three scales are set to m_c but they are varied independently from each other between 1 GeV and $2m_c$. Note that we set $\mu_1^{ss} = \mu_1^{dd}$ throughout this calculation while μ_1^{sd} is varied independently from the other two. The reason for this is because final states K^+K^- and $\pi^+\pi^-$ are not fully independent as can be connected through rescattering, but the $\Delta S = 1$ state is independent.
2. We introduce a new parameter ϵ which is related to the kinematics of the decay and set the scales according to the available phase space. For $s\bar{s}$ we will set $\mu_1^{ss} = m_c - 2\epsilon$, for $s\bar{d}$ (and $d\bar{s}$) we set $\mu_1^{sd} = m_c - \epsilon$ and for dd we keep $\mu_1^{dd} = m_c$.

By using the first method, we get a very extended range of values for Ω : $\Omega \in [4.5 \times 10^{-5}, 1.82]$. In fact, by scanning independently the two available scale parameters, 84 out of the 121 values give $\Omega > 0.1$, while only 11 yield $\Omega < 10^{-3}$. These 11 values correspond to $\mu_1^{ss} = \mu_1^{sd} = \mu_1^{dd}$. As we see, even a slight deviation from equal scale values starts lifting the GIM suppression. In this calculation we are using the \overline{MS} scheme, the $\{Q, \tilde{Q}_S\}$ operator basis for dimension-six and HQET Sum Rules results for the computation of the matrix elements. Using instead the Pole scheme, the $\{Q, Q_S\}$ operator basis or Lattice QCD results for the matrix elements, we find in general an increased range of values for Ω :

- Using the Pole scheme we get $\Omega \in [9.8 \times 10^{-6}, 9.07]$ with all choices of different scale parameters giving $\Omega > 0.1$.
- The choice of $\{Q, Q_S\}$ basis increases the maximum value of Ω to almost 7 for the \overline{MS} scheme and 23 for the Pole.

- Using the Lattice QCD values increases the result by 2-3 units in all cases, compared to the HQET Sum Rules.

Importantly, in all cases we can obtain values of $\Omega > 1$!

Using instead the ϵ method for setting the renormalisation scales, we can estimate the numerical value of the parameter ϵ as the strange quark mass, i.e $\epsilon \approx 0.1$ GeV, or we can compare the energy release of $D^0 \rightarrow K^+K^-$, $M_{D^0} - 2M_{K^+} = 0.88$ GeV, with that of $D^0 \rightarrow \pi^+\pi^-$, $M_{D^0} - 2M_{\pi^+} = 1.59$ GeV, leading to an expectation of $\epsilon \approx 0.35$ GeV. As we can see in the top right plot of Figure 3.5 we can match the experimental value of y for $\epsilon \approx 0.2$ GeV. Again, the above calculation is done in the \overline{MS} scheme, using the $\{Q, \tilde{Q}_S\}$ operators and HQET Sum Rules results for the matrix elements. In Figure 3.5 we can see the behaviour of Ω as we vary ϵ in all different scenarios (mass scheme, operator basis, non-perturbative input). In all of them we can see that we can achieve $\Omega = 1$ with a choice of $\epsilon \approx 0.2-0.3$ GeV.

Finally, we need to test this alternative renormalisation scale setting procedure with other HQE predictions and see how it affects them. In lifetime calculations (both in charm or bottom system) as well as in the decay rate difference in B^q -mixing there are no significant suppressions arising, thus our alternative scale setting (any of the two methods) would produce results already covered by the current range of theoretical uncertainties. However, there are (less pronounced) GIM cancellations in the calculation of semi-leptonic CP asymmetries in B^q -mixing. In the SM we get:

$$\text{Re} \left(\frac{\Gamma_{12}^q}{M_{12}^q} \right)^{\text{SM}} = -\frac{\Delta\Gamma_q}{\Delta M_q} = \begin{cases} -(49.9 \pm 6.7) \cdot 10^{-4} & q = s \\ -(49.7 \pm 6.8) \cdot 10^{-4} & q = d \end{cases}, \quad (3.5.1)$$

$$\text{Im} \left(\frac{\Gamma_{12}^q}{M_{12}^q} \right)^{\text{SM}} = a_{sl}^q = \begin{cases} (+2.2 \pm 0.2) \cdot 10^{-5} & q = s \\ (-5.0 \pm 0.4) \cdot 10^{-4} & q = d \end{cases}. \quad (3.5.2)$$

The results of applying the ϵ method in these observables can be found in Table 3.1. The blue entries in the table indicate values that lie within the theoretical

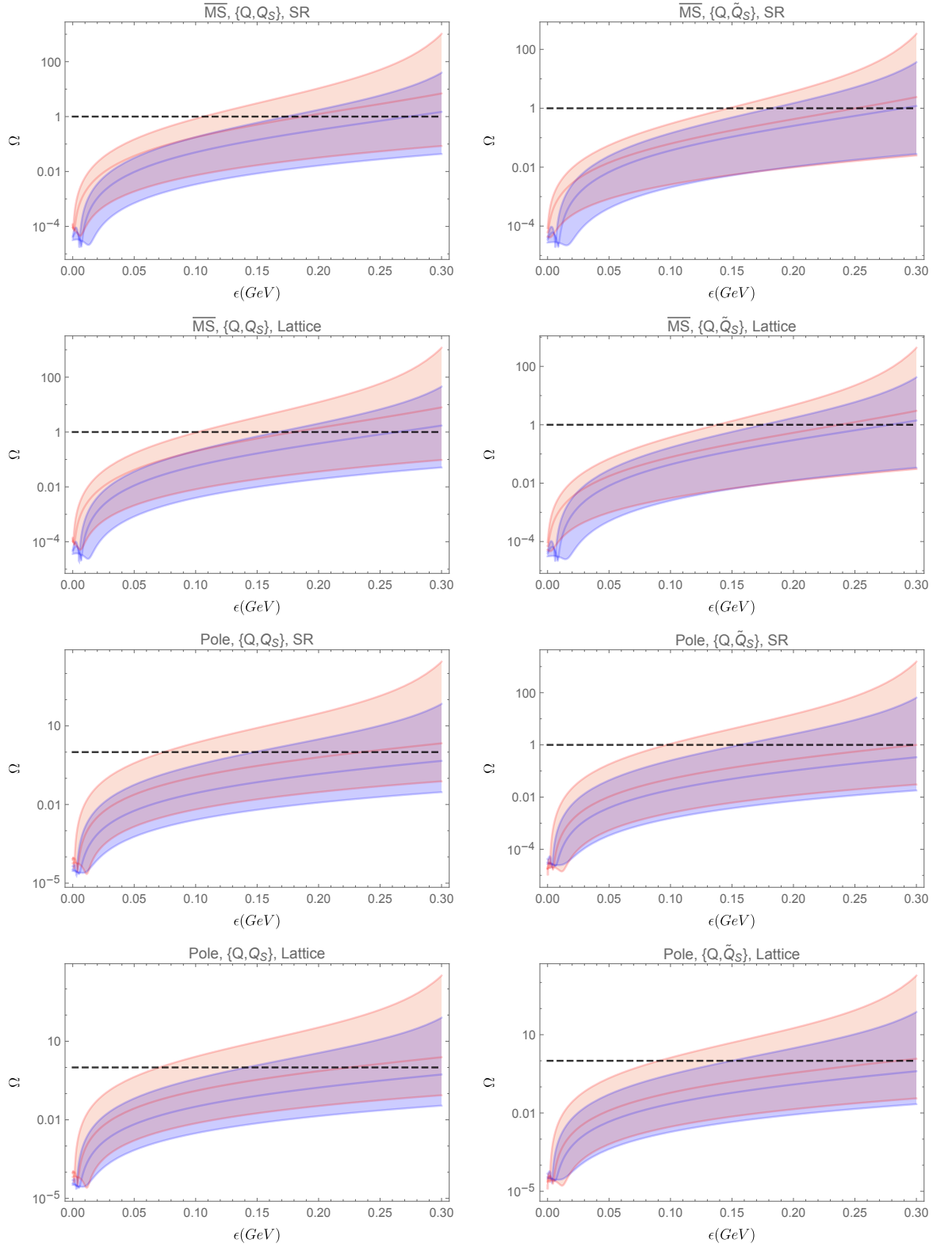


Figure 3.5: Comparison of the ϵ dependence of Ω at LO-QCD (blue) and NLO-QCD (pink) for different values of μ : the central lines corresponds to $\mu = m_c$ while the other lines to $\mu = 1 \text{ GeV}$ and $\mu = 2m_c$. In the label of each plot are stated the scheme used, the dimension-six operator basis and the values of the non-perturbative matrix elements.

ϵ (GeV)	Γ_{12}^s/M_{12}^s	Γ_{12}^d/M_{12}^d
0	-0.00499 + 0.000022 I	-0.00497 - 0.00050 I
0.2	-0.00494 + 0.000023 I	-0.00492 - 0.00053 I
0.5	-0.00484 + 0.000026 I	-0.00482 - 0.00059 I
1.0	-0.00447 + 0.000037 I	-0.00448 - 0.00084 I
1.5	-0.00287 + 0.000091 I	-0.00309 - 0.0021 I

Table 3.1: Numerical results of Γ_{12}/M_{12} for B_s and B_d meson mixing after applying the ϵ renormalisation scale setting.

uncertainties while the black ones are not covered by them. We can see that the real part of Γ_{12}^s/M_{12}^s remains within the uncertainties for values of ϵ up to 1 GeV, while the imaginary part can be increased by almost 100% for both B_s and B_d mesons. Note that we use values of ϵ up to 1.5 GeV since in the B system the heaviest internal quark would be the charm instead of the strange.

Chapter 4

Lifetimes of D Mesons

The lifetimes of charmed mesons are very precisely known experimentally [1, 111]. Unlike the B meson lifetimes though, they exhibit a much wider range of values, as mentioned in Section 2.2. Apart from the lifetimes, inclusive semi-leptonic branching fractions have been measured [1], including a very recent measurement for the D_s^+ meson by the BESIII Collaboration [2]. In this chapter we revisit the inclusive decays of D mesons. Including the recently evaluated Darwin operator contribution [8] and D_s^+ Bag parameters [5], we present an updated theory status of the D lifetimes. We start by summarising the results for the calculation of the perturbative HQE, followed by a listing of non-perturbative parameters for the $\Delta C = 0$ matrix elements. Finally, we show our numerical results for different quark mass definition schemes.

4.1 Introduction

The current status of lifetimes and semi-leptonic branching ratios for all three D mesons is shown in Table 4.1. To calculate such inclusive decays we will use the HQE framework. The decay of a D meson can be written then as in Equation (2.2.25) with the substitution of $m_Q \rightarrow m_c$. The $\Gamma_i, \langle \mathcal{O}_i \rangle$ follow the notation of Equations (2.2.25)-(2.2.27). We can see the expression for the decay of a D-meson is a series expansion in two parameters Λ/m_c and $\alpha_s(m_c)$ where $\Lambda \approx \Lambda_{QCD}$. While in the B

	D^0	D^+	D_s^+
τ [ps]	0.4101(15)	1.040(7)	0.504(4)
Γ [ps^{-1}]	2.44(1)	0.96(1)	1.98(2)
$\tau(D_q)/\tau(D^0)$	1	2.54(2)	1.20(1)
$\text{Br}(D_q \rightarrow X e^+ \nu_e)$ [%]	6.49(11)	16.07(30)	6.30(16)
$\frac{\Gamma(D_q \rightarrow X e^+ \nu_e)}{\Gamma(D^0 \rightarrow X e^+ \nu_e)}$	1	0.977(26)	0.790(26)

Table 4.1: Status of the experimental determinations of the lifetime and the semi-leptonic branching fractions of the lightest charmed mesons ($D^q \in \{D^0, D^+, D_s^+\}$). All values are taken from the PDG [1] apart from the semi-leptonic D_s^+ -meson decays which were recently measured by the BESIII Collaboration [2].

system these parameters are small enough to expand in them, for the charm one this is not very clear. As a starting point we will investigate whether these parameters can give a convergent series. The Particle Data Group [1] gives the following values for the pole and \overline{MS} mass of the charm quark

$$m_c^{pole} = 1.67 \pm 0.07 \text{ GeV} , \quad (4.1.1)$$

$$\overline{m}_c(\overline{m}_c) = 1.27 \pm 0.02 \text{ GeV} . \quad (4.1.2)$$

The choice of mass as well as the loop order of the calculation has a big effect on the value of the running coupling. In Table 4.2 we show the values of $\alpha_s(m_c)$ for three different values of m_c at 2-loop and 5-loop using the RunDec package [3]. Even

$\alpha_s(m_c)$	$m_c = 1.67 \text{ GeV}$	$m_c = 1.48 \text{ GeV}$	$m_c = 1.27 \text{ GeV}$
2-loop	0.322	0.346	0.373
5-loop	0.329	0.356	0.387

Table 4.2: Numerical values of the strong coupling α_s evaluated at different scales and different loop order, obtained using the RunDec package [3].

though the determination of the \overline{MS} mass is well founded, that of the pole mass seems to be affected by a potential breakdown of the perturbation theory. However, we can not just choose the \overline{MS} -mass a priori as the HQE is naturally defined via the pole mass. We can write the pole mass as a function of the \overline{MS} mass up to third

order of the running coupling [112–114]

$$\begin{aligned} m_c^{\text{Pole}} &= \bar{m}_c(\bar{m}_c) \left[1 + \frac{4}{3} \frac{\alpha_s(\bar{m}_c)}{\pi} + 10.43 \left(\frac{\alpha_s(\bar{m}_c)}{\pi} \right)^2 + 116.5 \left(\frac{\alpha_s(\bar{m}_c)}{\pi} \right)^3 \right] \\ &= \bar{m}_c(\bar{m}_c) [1 + 0.1642 + 0.1582 + 0.2176] , \end{aligned} \quad (4.1.3)$$

where we have used the 5-loop result for the running coupling. In Table 4.2 we have used a third value for m_c which corresponds to the pole mass at first order in α_s as calculated from Equation (4.1.3).

The leading term in the decay of a free charm quark (Γ_3) is proportional to m_c^5 so the way we treat these higher orders in the mass relation can potentially have big effects. If we truncate the series at first order in α_s then we can write

$$\left(m_c^{\text{Pole}} \right)^5 = \bar{m}_c(\bar{m}_c)^5 [1 + 0.1642]^5 = 2.14 \bar{m}_c(\bar{m}_c)^5 . \quad (4.1.4)$$

If we keep only the terms up to α_s , discarding higher orders, we obtain

$$\left(m_c^{\text{Pole}} \right)^5 \approx \bar{m}_c(\bar{m}_c)^5 [1 + 5 \cdot 0.1642] = 1.82 \bar{m}_c(\bar{m}_c)^5 , \quad (4.1.5)$$

which is almost 15% smaller than Equation (4.1.4). Finally, if we keep all the terms of Equation (4.1.3) we get

$$\left(m_c^{\text{Pole}} \right)^5 = \bar{m}_c(\bar{m}_c)^5 [1 + 0.1642 + 0.1582 + 0.2176]^5 = 8.66 \bar{m}_c(\bar{m}_c)^5 , \quad (4.1.6)$$

which is almost 4 times larger than the value of Equation (4.1.4). Since our results seem to have a strong dependence on the way we treat the charm mass we will consider the following possibilities.

1. Use Equation (4.1.3) to first order in α_s , since this is the order to which most of the Wilson coefficients are known. In this case we fix $m_c^{\text{Pole}} = 1.48$ GeV and $\alpha_s = 0.356$ and express everything in terms of the pole mass. A further possibility would be to consider the expansion in Equation (4.1.3) to be an asymptotic one, whose smallest correction appears at order α_s^2 , which is where we stop the expansion. In this case we get the pole mass value from

PDG, $m_c^{\text{Pole}} = 1.67$ GeV. We did a numerical test for this large value of the charm quark mass and the results for decay rates are roughly 30% larger than the values obtained in the $1S$ scheme discussed below. Since we expect this enhancement to be compensated by missing NNLO corrections to the non-leptonic decay rates, we will not separately present results for $m_c^{\text{Pole}} = 1.67$ GeV.

- Express the c -quark mass in terms of the $\overline{\text{MS}}$ mass [115],

$$m_c^{\text{Pole}} = \overline{m}_c(\overline{m}_c) \left[1 + \frac{4}{3} \frac{\alpha_s(\overline{m}_c)}{\pi} \right], \quad (4.1.7)$$

taking $\overline{m}_c(\overline{m}_c) = 1.27$ GeV [1], and expand consistently up to order α_s . Because of the dependence on the fifth power of the charm-quark mass, in this case Γ_3 is affected by a large correction $5 \times (4/3)(\alpha_s/\pi)$.

- Express the c -quark mass in terms of the kinetic mass [65, 116]. The kinetic scheme has been introduced in order to obtain a short distance definition of the heavy quark mass which allows a faster convergence of the perturbative series and is still valid at small scales $\mu \sim 1$ GeV. The relation between the kinetic scheme and the $\overline{\text{MS}}$ and Pole schemes can be found, up to N³LO corrections, in [117]. At order α_s one has

$$m_c^{\text{Pole}} = m_c^{\text{Kin}} \left[1 + \frac{4\alpha_s}{3\pi} \left(\frac{4}{3} \frac{\mu^{\text{cut}}}{m_c^{\text{Kin}}} + \frac{1}{2} \left(\frac{\mu^{\text{cut}}}{m_c^{\text{Kin}}} \right)^2 \right) \right], \quad (4.1.8)$$

where μ^{cut} is the Wilsonian cutoff separating the perturbative and non-perturbative regimes. Using $\overline{m}_c(\overline{m}_c)$ as an input, the authors of [117] obtain

$$m_c^{\text{Kin}}(1\text{GeV}) = 1.128 \text{ GeV} \quad (\text{N}^3\text{LO}), \quad (4.1.9)$$

$$m_c^{\text{Kin}}(1\text{GeV}) = 1.206 \text{ GeV} \quad (\text{NLO}). \quad (4.1.10)$$

Comparing with Equation (4.1.7) it follows that the kinetic scheme might be preferred to the $\overline{\text{MS}}$ scheme, if the coefficient of $\alpha_s/4\pi$ in Equation (4.1.8), would give a suppression factor. For $\mu^{\text{cut}} = 1$ GeV and $m_c^{\text{Kin}} = 1.2$ GeV, this

is not the case, while using lower values i.e. $\mu^{\text{cut}} < 1$ GeV, the convergence of the series could be improved, however this would bring in an additional uncertainty due to the closeness to the non-perturbative scale Λ_{QCD} . In our numerical analysis we will investigate the kinetic scheme with $\mu^{\text{cut}} = 0.5$ GeV. From [117] we take the following value

$$m_c^{\text{kin}}(0.5 \text{ GeV}) = 1.363 \text{ GeV} \quad (4.1.11)$$

obtained for consistency at NLO in α_s and using as an input $\overline{m}_c(\overline{m}_c)$.

4. In addition, we will consider the $1S$ -mass scheme defined as [118, 119]

$$m_c^{\text{Pole}} = m_c^{1S} \left(1 + \frac{(\alpha_s C_F)^2}{8} \right), \quad (4.1.12)$$

where $C_F = 4/3$, and the $1S$ mass $m_c^{1S} \approx 1.44$ GeV is obtained using the conversion from the \overline{MS} -scheme (implemented in the RunDec package [3]) at one loop level. Note that the correction within the $1S$ scheme in fact starts at order α_s^2 , which however is still considered to be a NLO (not NNLO) effect⁸ [118].

In the following study we are using updated results for both the $\Delta C = 0$ Wilson coefficients and for the non-perturbative parameters. Γ_3 is known at NLO-QCD [121–128] for non-leptonic decays. NNLO-QCD [129–138] and NNNLO-QCD [139, 140] corrections have been computed for semi-leptonic decays, while for non-leptonic decays NNLO corrections have been determined in the massless case and in full QCD (i.e. no effective Hamiltonian was used) in [141]. Γ_5 was determined at LO-QCD for both semi-leptonic and non-leptonic decays [61, 142–144]. For the semi-leptonic modes even NLO-QCD corrections are available [145–147]. In the b -system, Γ_6 was first computed at LO-QCD in [148] and recently the NLO-QCD corrections were determined in [149], both for the semi-leptonic case only. Very recently Γ_6 has been determined also for non-leptonic decays [150–152] and the coefficient was found to

⁸Similarly, another possibility would be to study the potential subtracted mass [120].

be large. For semi-leptonic D -meson decays, Γ_6 was determined in [153], see also the recent [154], while the corresponding results for the non-leptonic charm modes are presented for the first time in [8]. $\tilde{\Gamma}_6$ is known at NLO-QCD for lifetimes of B -meson [155, 156] and of D -meson [157], while $\tilde{\Gamma}_7$ and $\tilde{\Gamma}_8$ have been estimated in LO-QCD in [158, 159]. The calculation of $\tilde{\Gamma}_6$ and $\tilde{\Gamma}_7$ can also be found in Appendix D.

On the non-perturbative side, at dimension-five, the matrix element of the chromomagnetic operator can be determined from spectroscopy, while for the kinetic operator there exist several Heavy Quark Effective Theory (HQET) determinations with lattice simulations [160–164] and using sum rules [65, 165, 166]. The matrix elements of the four-quark operators $\langle \tilde{\mathcal{O}}_6 \rangle$ have been computed using HQET sum rules [4]. Violations of $SU(3)_F$ and so far undetermined eye-contractions could yield visible effects and a calculation of these corrections with HQET sum rules, following [167], has been performed in [5]. Corresponding lattice results for the matrix elements of the four-quark operators would be highly desirable.

4.2 Total Decay Rates

The effective Hamiltonian for inclusive charm decays can be decomposed in three parts

$$\mathcal{H}_{eff} = \mathcal{H}_{eff}^{NL} + \mathcal{H}_{eff}^{SL} + \mathcal{H}_{eff}^{rare}, \quad (4.2.1)$$

where the three terms correspond to non-leptonic decays of the charm quark ($c \rightarrow q_1 \bar{q}_2 u$, $q_i = u, d, s$), semi-leptonic decays of the charm quark ($c \rightarrow q \ell^+ \nu_\ell$, $\ell = e, \mu$ and $q = d, s$) and rare decays of the D meson like $D \rightarrow \pi \ell^+ \ell^-$. The branching fraction of such rare decays is much smaller than tree-level transitions, and hence we will not include them from now on (see e.g. [168, 169] for studies for New Physics in such decays) The other two terms can be written as

$$\mathcal{H}_{eff}^{NL} = \frac{G_F}{\sqrt{2}} \left[\sum_{q_{1,2}=d,s} \lambda_{q_1 q_2} [C_1 Q_1^{q_1 q_2} + C_2 Q_2^{q_1 q_2}] - \lambda_b \sum_{j=3}^6 C_j Q_j \right] + \text{h.c.}, \quad (4.2.2)$$

$$\mathcal{H}_{\text{eff}}^{\text{SL}} = \frac{G_F}{\sqrt{2}} \sum_{q=d,s} \sum_{\ell=e,\mu} V_{cq}^* Q^{q\ell} + \text{h.c.}, \quad (4.2.3)$$

where $\lambda_{q_1 q_2} = V_{cq_1}^* V_{uq_2}$ and $\lambda_b = V_{cb}^* V_{ub}$ are the CKM factors and $C_i(\mu_1)$ denote the Wilson coefficients evaluated at the renormalisation scale $\mu_1 \sim m_c$. The operators $Q_1^{q_1 q_2}, Q_2^{q_1 q_2}$ denote the tree-level $\Delta C = 1$ operators while $Q_i, i = 3 \dots 6$ are the penguin operators arising in the single Cabibbo suppressed decays $c \rightarrow s\bar{s}u$ and $c \rightarrow d\bar{d}u$, or in even further suppressed decays like $c \rightarrow u\bar{u}u$. The operator $Q^{q\ell}$ is the semi-leptonic operator arising at tree-level and its Wilson coefficient is equal to 1. The tree-level operators can be written as

$$Q_1^{q_1 q_2} = (\bar{q}_1^i \gamma_\mu (1 - \gamma_5) c^i) (\bar{u}^j \gamma^\mu (1 - \gamma_5) q_2^j), \quad (4.2.4)$$

$$Q_2^{q_1 q_2} = (\bar{q}_1^i \gamma_\mu (1 - \gamma_5) c^j) (\bar{u}^j \gamma^\mu (1 - \gamma_5) q_2^i), \quad (4.2.5)$$

$$Q^{q\ell} = (\bar{q} \gamma^\mu (1 - \gamma_5) c) (\bar{\nu}_\ell \gamma_\mu (1 - \gamma_5) \ell). \quad (4.2.6)$$

The values of the Wilson coefficient for the non-leptonic operators can be found in Table 4.3. We see that the Wilson coefficients of the penguin operators are very small

$\mu_1[\text{GeV}]$	1	1.27	1.36	1.44	1.48	3
$C_1(\mu_1)$	1.25 (1.34)	1.20 (1.27)	1.19 (1.26)	1.18 (1.25)	1.18 (1.24)	1.10 (1.15)
$C_2(\mu_1)$	-0.48 (-0.62)	-0.39 (-0.50)	-0.40 (-0.53)	-0.37 (-0.49)	-0.37 (-0.48)	-0.24 (-0.32)
$C_3(\mu_1)$	0.03 (0.02)	0.02 (0.01)	0.02 (0.01)	0.01 (0.01)	0.01 (0.01)	0.00 (0.00)
$C_4(\mu_1)$	-0.06 (-0.04)	-0.05 (-0.03)	-0.04 (-0.03)	-0.04 (-0.02)	-0.04 (-0.02)	-0.01 (-0.01)
$C_5(\mu_1)$	0.01 (0.01)	0.01 (0.01)	0.01 (0.01)	0.01 (0.01)	0.01 (0.01)	0.00 (0.00)
$C_6(\mu_1)$	-0.08 (-0.05)	-0.05 (-0.03)	-0.05 (-0.03)	-0.04 (-0.03)	-0.04 (-0.03)	-0.01 (-0.01)

Table 4.3: Comparison of the Wilson coefficients at NLO-QCD (LO-QCD) for different values of μ_1 .

and additionally their contributions are also strongly CKM suppressed by a factor $\lambda_b \ll \lambda_{q_1 q_2}$. Therefore in our analysis we will neglect their effect. The expansion in

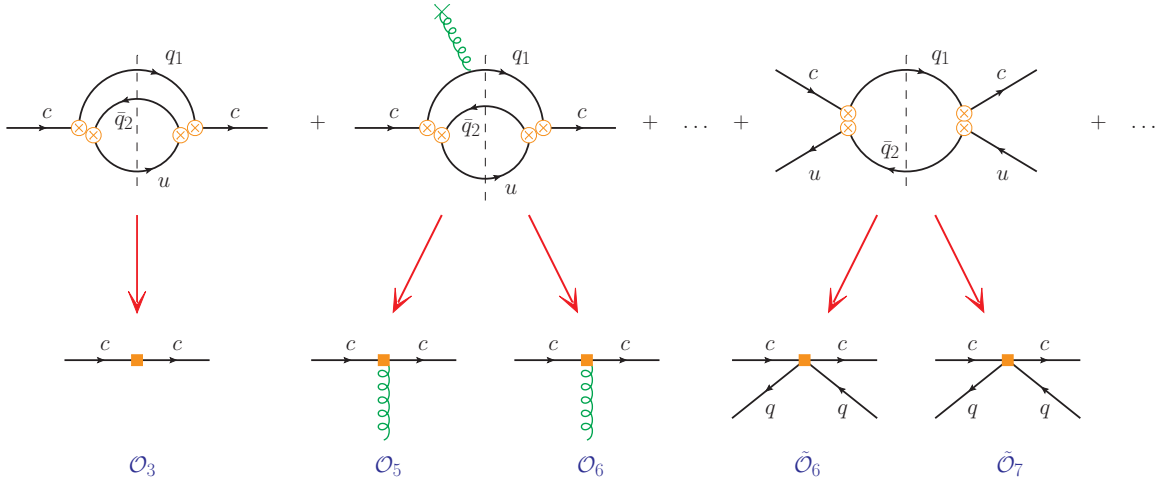


Figure 4.1: The diagrams describing contributions to the HQE in Equation (2.2.25). The crossed circles denote the $\Delta C = 1$ operators Q_i of the effective Hamiltonian while the squares denote the local $\Delta C = 0$ operators \mathcal{O}_i and $\tilde{\mathcal{O}}_i$. The two-loop and the phase space enhanced one-loop diagrams correspond respectively to the two-quark operators \mathcal{O}_i and to the four-quark operators $\tilde{\mathcal{O}}_i$ in the HQE.

these terms as in Equation (2.2.25) can be presented graphically as in Figure 4.1.

Starting from the lowest order in the HQE we obtain the free decay of the charm quark Γ_3 , which at LO can be written as

$$\Gamma_3^{(0)} = \Gamma_0 c_3 = \Gamma_0 \left[f(z_s, z_e, z_{\nu_e}) + f(z_s, z_\mu, z_{\nu_\mu}) + |V_{ud}|^2 \mathcal{N}_a f(z_s, z_u, z_d) + \dots \right], \quad (4.2.7)$$

where the following notation is introduced

$$\Gamma_0 = \frac{G_F^2 m_c^5}{192\pi^3} |V_{cs}|^2, \quad (4.2.8)$$

$$\mathcal{N}_a = 3C_1^2 + 2C_1C_2 + 3C_2^2, \quad (4.2.9)$$

and we introduce as well $z_q = m_q^2/m_c^2$. In the remaining of the thesis we assume the masses of the electron, neutrino and up and down quarks negligible, thus $z_e = z_\nu = z_u = z_d = 0$. The function $f(z_{q_1}, z_{q_2}, z_{q_3})$ denotes the phase space effect of the final state particles. In the approximations of one massive particle and two equally

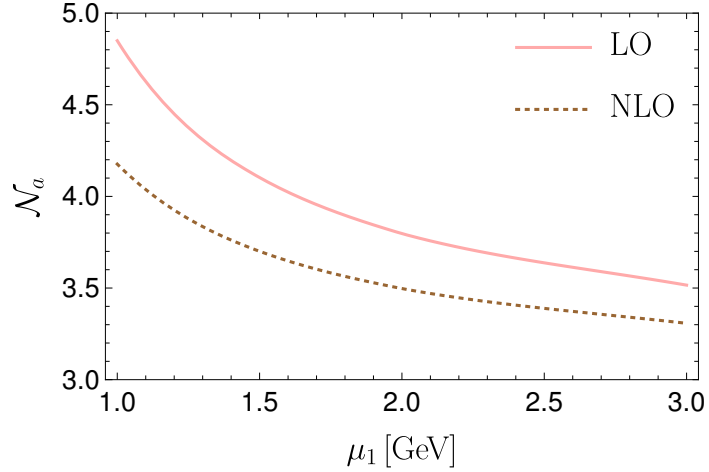


Figure 4.2: Scale dependence of the Wilson coefficient combination $\mathcal{N}_a = 3C_1^2 + 3C_2^2 + 2C_1C_2$.

massive particles it can be simplified to

$$f(z, 0, 0) = 1 - 8z + 8z^3 - z^4 - 12z^2 \log z, \quad (4.2.10)$$

$$f(z, z, 0) = \sqrt{1-4z}(1-14z-2z^2-12z^3) + 24z^2(1-z^2) \log \frac{1+\sqrt{1-4z}}{1-\sqrt{1-4z}}, \quad (4.2.11)$$

while the general expression can be found in e.g. [170]. In Equation (4.2.7) the first two terms correspond to the semi-leptonic decays $c \rightarrow se^+\nu_e$ and $c \rightarrow s\mu^+\nu_\mu$ while the third term to the CKM favoured $c \rightarrow \bar{s}du$. The ellipsis denote the CKM suppressed modes. The dependence on the scale μ_1 enters the calculation via the Wilson coefficient \mathcal{N}_a . Its dependence on μ_1 is depicted in Figure 4.2 indicating a shift from LO to NLO and a reduction of the the scale uncertainty at NLO. In order to calculate the full NLO result of Γ_3 we also need corrections coming from NLO diagrams. It is helpful to express the full result for Γ_3 as

$$\Gamma_3 = \Gamma_0 \left[3C_1^2 \mathcal{C}_{3,11} + 2C_1C_2 \mathcal{C}_{3,12} + 3C_2^2 \mathcal{C}_{3,22} + \mathcal{C}_{3,SL} \right], \quad (4.2.12)$$

where each $\mathcal{C}_{3,ij}$ includes contributions from all possible decay modes. The NLO parts of $\mathcal{C}_{3,11}$, $\mathcal{C}_{3,22}$ and $\mathcal{C}_{3,SL}$ were calculated at [121] while we have used [124, 128] for $\mathcal{C}_{3,12}$. The LO results are presented in Appendix B.

Mass scheme	Γ_3^{LO} [ps ⁻¹]	Γ_3^{NLO} [ps ⁻¹]
Pole ($m_c = 1.48$ GeV)	$1.45_{-0.14}^{+0.17}$	$1.52_{-0.16}^{+0.20}$
$\overline{\text{MS}}$ (Equation (4.1.7))	$0.69_{-0.09}^{+0.06}$	$1.32_{-0.03}^{+0.06}$
Kinetic (Equation. (4.1.8))	$0.97_{-0.11}^{+0.10}$	$1.47_{-0.30}^{+0.27}$
$1S$ (Equation (4.1.12))	$1.25_{-0.13}^{+0.14}$	$1.50_{-0.25}^{+0.31}$

Table 4.4: Numerical values of $\Gamma_3^{\text{LO}} = \Gamma_3^{(0)}$ and $\Gamma_3^{\text{NLO}} = \Gamma_3^{(0)} + \alpha_s(m_c)/(4\pi) \Gamma_3^{(1)}$ using different schemes for the c -quark mass. The uncertainties are obtained by varying the renormalisation scale μ_1 between 1 GeV and 3 GeV.

Numerical results for Γ_3 in different mass are presented in Table 4.4. We find that the NLO values are in good agreement with the experimental measurements of Table 4.1. Looking more closely at the NLO effect in Γ_3 we see some very interesting cancellations, more visible in the Pole scheme. In fact, for non-leptonic modes the corrections from the NLO diagrams and the NLO corrections to the Wilson coefficients come with different signs. Additionally, the total NLO correction from the non-leptonic modes and the one from the semi-leptonic ones have similar sizes but different signs, cancelling each other out up to a final small NLO contribution. In the $\overline{\text{MS}}$ scheme though the correction coming from the mass conversion formula in Equation (4.1.7) is very large (due to the m_c^5 factor) and breaks this cancellation

$$\Gamma_3^{\text{Pole}} = \Gamma_3^{\text{LO}} \left[1 + \left(\underbrace{1.84}_{\text{diag.}} - \underbrace{0.74}_{\text{WC}} - 0.67 \right) \frac{\alpha_s}{\pi} + \mathcal{O} \left(\frac{\alpha_s}{\pi} \right)^2 \right], \quad (4.2.13)$$

$$\Gamma_3^{\overline{\text{MS}}} = \Gamma_3^{\text{LO}} \left[1 + \left(\underbrace{2.10}_{\text{diag.}} - \underbrace{0.70}_{\text{WC}} - 0.71 + \underbrace{6.66}_{\text{conv.fac.}} \right) \frac{\alpha_s}{\pi} + \mathcal{O} \left(\frac{\alpha_s}{\pi} \right)^2 \right]. \quad (4.2.14)$$

Similar effects happen in the $1S$ and Kinetic schemes. To obtain a first indication of the convergence rate of the QCD perturbative series we look at higher orders of the series. More specifically, NNLO [137] and NNNLO [139] corrections are known for the semi-leptonic decays of the b quark, and preliminary NNLO [141] corrections are available for the non-leptonic decays of the b quark. We find that higher order corrections seem to be crucial for a reliable determination of Γ_3 . Note however that the results of [141] can not be used for phenomenological applications since they are

not complete.

The first corrections to the decay of the free charm quark arise at dimension-five and can be split in two operators as we have seen in Section 2.2, the kinetic and chromomagnetic operators. By considering all contributions at this order in the HQE we can write schematically

$$\Gamma_5 \frac{\langle \mathcal{O}_5 \rangle}{m_c^2} = \Gamma_0 \left[c_{\mu\pi} \frac{\mu_\pi^2}{m_c^2} + c_G \frac{\mu_G^2}{m_c^2} \right], \quad (4.2.15)$$

where the coefficient $c_{\mu\pi} = -c_3^{(0)}/2$ and the coefficient c_G can be expressed as

$$c_G = 3 C_1^2 \mathcal{C}_{G,11} + 2 C_1 C_2 \mathcal{C}_{G,12} + 3 C_2^2 \mathcal{C}_{G,22} + \mathcal{C}_{G,SL}. \quad (4.2.16)$$

The individual contributions to c_G can be found in Appendix B. In e.g. [150] they were calculated for the non-leptonic decays of the b quark, but since there are no IR-divergencies we can use them for the charm system with the appropriate replacements e.g. $m_b \rightarrow m_c, m_c \rightarrow m_s$. For the $c \rightarrow s\mu^+\nu$ mode we would need the expression for two different massive particles in the final state which can be found in [170]. However, since $m_s \approx m_\mu \approx 100$ MeV we can safely use the formula from the $c \rightarrow s\bar{s}u$ mode by setting $N_c = 1, C_1 = 1$ and $C_2 = 0$. By neglecting the final state masses and the CKM suppressed modes we can approximate c_G as

$$c_G \approx -|V_{ud}|^2 \left[\frac{9}{2} (C_1^2 + C_2^2) + 19 C_1 C_2 \right] - 3. \quad (4.2.17)$$

The coefficient in front of $C_1 C_2$ is very large and comes with a negative sign, causing cancellations in c_G . In Figure 4.3 the μ_1 behaviour is shown in LO and in partial NLO where only corrections to the Wilson coefficients have been included. Because of the previously mentioned cancellations we can see that depending on the scale at which we compute c_G , the sign is changing, leading to big uncertainties due to scale variation between 1 GeV and 3 GeV.

For details about the calculation of short-distance effects and expansion of the

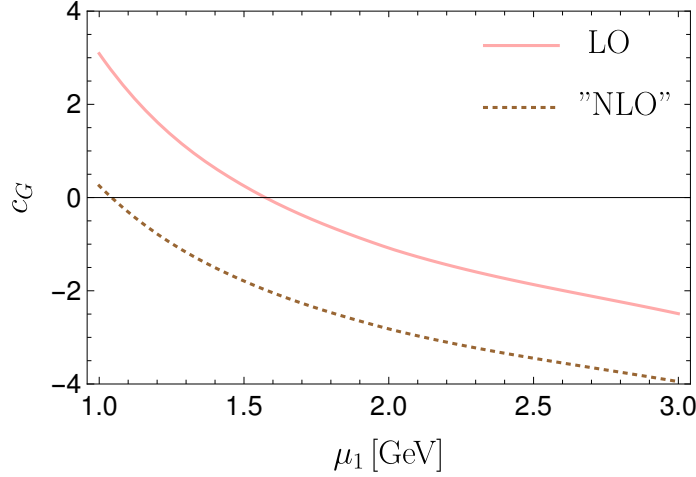


Figure 4.3: Scale dependence of the coefficient of the chromomagnetic operator.

dimension-three and five matrix elements one could refer to e.g. [142, 143, 150, 171] while a detailed calculation can be found in [172]. As before, we can write for Γ_6

$$\Gamma_6 \frac{\langle \mathcal{O}_6 \rangle}{m_c^3} = \Gamma_0 c_{\rho_D} \frac{\rho_D^3}{m_c^3}, \quad (4.2.18)$$

for the Darwin operator, where

$$c_{\rho_D} = 3 C_1^2 \mathcal{C}_{\rho_D,11} + 2 C_1 C_2 \mathcal{C}_{\rho_D,12} + 3 C_2^2 \mathcal{C}_{\rho_D,22} + \mathcal{C}_{\rho_D,SL}. \quad (4.2.19)$$

The non-leptonic coefficients have been computed in [150–152] for b quark decays but unlike c_G we can not simply change the masses and use the expressions for the charm quark. The expressions for the charm system can be found in Appendix B, after the authors of [150] modified them to include full dependence on the strange quark mass [8]. For the semi-leptonic modes we can simply use the expressions derived for the non-leptonic ones and substitute $N_C = 1, C_1 = 1, C_2 = 0$ and $m_s \rightarrow m_\mu$.

Neglecting the final state masses and the CKM suppressed modes we find

$$c_{\rho_D} \approx |V_{ud}|^2 \left(18 C_1^2 - \frac{68}{3} C_1 C_2 + 18 C_2^2 \right) + 12. \quad (4.2.20)$$

As we can see, no cancellation arises here since all coefficients have the same sign, and can potentially give a big contribution to the full decay rate of D mesons (based on the size of the coefficients). Of course there is still the non-perturbative

parameter ρ_D to be determined. We will discuss this in the next section. The μ_1 behaviour of Γ_6 can be seen in Figure 4.4 where again we compare the LO result with a partial NLO result, where only corrections from the Wilson coefficients are included.

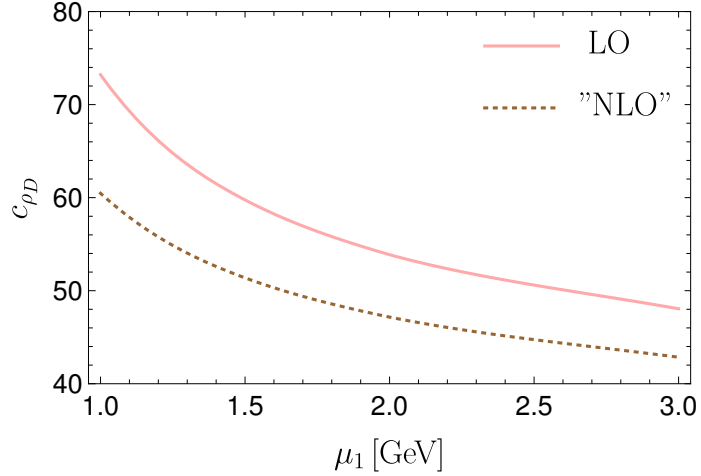


Figure 4.4: Scale dependence of the coefficient of the Darwin operator.

So far we have not discussed the spectator quark (the light quark of the meson), because all the previously mentioned contributions are the same for all charmed hadrons – the non-perturbative parameter can differ from hadron to hadron as we will see in the following section. Starting at order $1/m_c^3$, four-quark operators arise that involve the spectator quark. As mentioned in Section 2.2 we will denote these contributions with a tilde i.e. $\tilde{\Gamma}_6, \tilde{\Gamma}_7$ etc. There are three different topologies for these diagrams, shown in Figure 4.5, corresponding from left to right to Weak Exchange (WE), Pauli Interference (PI) and Weak Annihilation (WA) diagrams. Non-leptonic contributions enter through all three topologies; however, semi-leptonic

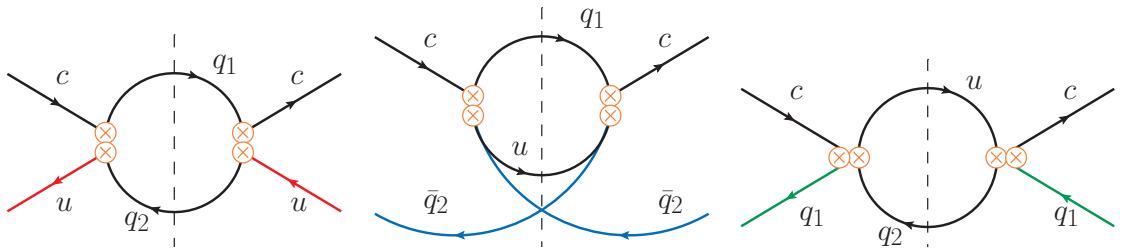


Figure 4.5: Spectator quark effects in the HQE expansion: WE (left), PI (middle) and WA (right).

modes can appear only through the WA diagram. The $\Delta C = 0$ operators appearing at dimension-six are

$$O_1^q = (\bar{c} \gamma_\mu (1 - \gamma_5) q) (\bar{q} \gamma^\mu (1 - \gamma_5) c), \quad (4.2.21)$$

$$O_2^q = (\bar{c} (1 - \gamma_5) q) (\bar{q} (1 + \gamma_5) c), \quad (4.2.22)$$

$$O_3^q = (\bar{c} \gamma_\mu (1 - \gamma_5) T^\alpha q) (\bar{q} \gamma^\mu (1 - \gamma_5) T^\alpha c), \quad (4.2.23)$$

$$O_4^q = (\bar{c} (1 - \gamma_5) T^\alpha q) (\bar{q} (1 + \gamma_5) T^\alpha c), \quad (4.2.24)$$

where q is the spectator quark and T^α are the colour matrices and summation over them is implied. Their matrix elements can be parametrised as

$$\langle D_q | O_i^q | D_q \rangle = f_{D_q}^2 A_i M_{D_q}^2 (B_i + \delta_i^{qq}), \quad (4.2.25)$$

$$\langle D_q | O_i^{q'} | D_q \rangle = f_{D_q}^2 A_i M_{D_q}^2 \delta_i^{qq'}, \quad q \neq q', \quad (4.2.26)$$

where $q, q' = u, d, s$, $A_{1,3} = 1$, $A_{2,4} = \frac{M_{D_q}^2}{(m_c + m_q)^2}$ and B_i are the Bag parameters⁹ in QCD. The $\delta_i^{qq'}$ parametrise the so-called eye-contractions, (see Figure 4.6) and describe subleading effects in the matrix elements. In VIA all δ 's vanish while $B_{1,2} = 1$ and $\epsilon_{1,2} = 0$. In the HQET framework one can also define a similar set of

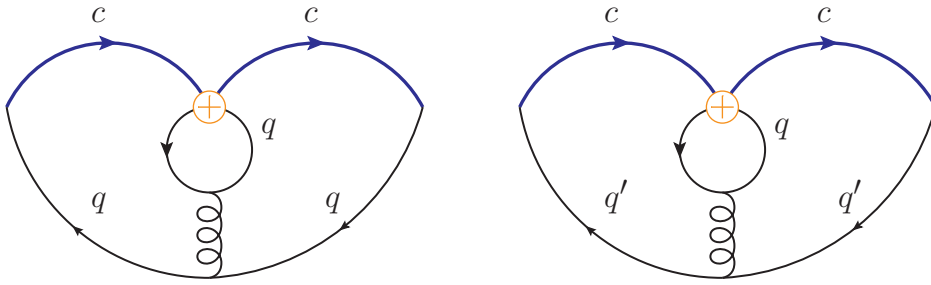


Figure 4.6: Diagrams describing the eye-contractions.

operators¹⁰

$$\tilde{O}_1^q = (\bar{h}_v \gamma_\mu (1 - \gamma_5) q) (\bar{q} \gamma^\mu (1 - \gamma_5) h_v), \quad (4.2.27)$$

⁹Note that in the remaining of the chapter we may refer to $B_{3,4}$ as $\epsilon_{1,2}$ as it is more standard in the literature.

¹⁰Note that all quantities defined in HQET will be defined with a tilde, comparing to the QCD ones.

$$\tilde{O}_2^q = (\bar{h}_v(1 - \gamma_5)q)(\bar{q}(1 + \gamma_5)h_v), \quad (4.2.28)$$

$$\tilde{O}_3^q = (\bar{h}_v \gamma_\mu(1 - \gamma_5)T^\alpha q)(\bar{q} \gamma^\mu(1 - \gamma_5)T^\alpha h_v), \quad (4.2.29)$$

$$\tilde{O}_4^q = (\bar{h}_v(1 - \gamma_5)T^\alpha q)(\bar{q}(1 + \gamma_5)T^\alpha h_v), \quad (4.2.30)$$

which are parametrised as

$$\langle D_q | \tilde{O}_i^q | D_q \rangle = F^2(m_c) M_{D_q} (\tilde{B}_i^q + \tilde{\delta}_i^{qq}), \quad (4.2.31)$$

$$\langle D_q | \tilde{O}_i^{q'} | D_q \rangle = F^2(m_c) M_{D_q} \tilde{\delta}_i^{q'q}, \quad q \neq q', \quad (4.2.32)$$

where $F(\mu)$ is the decay constant defined in the HQET as

$$\langle 0 | \bar{q} \gamma^\mu \gamma_5 h_v | D_q(v) \rangle = i F(\mu) \sqrt{M_{D_q}} v^\mu. \quad (4.2.33)$$

The relation between the QCD decay constant defined in Equation (2.2.32) and the HQET one up to α_s and $1/m_c$ corrections [55, 173] for $\mu = m_c$ is

$$f_{D_q} = \frac{F(m_c)}{\sqrt{M_{D_q}}} \left(1 - \frac{2}{3} \frac{\alpha_s(m_c)}{\pi} + \frac{G_1(m_c)}{m_c} + 6 \frac{G_2(m_c)}{m_c} - \frac{1}{2} \frac{\bar{\Lambda} - m_q}{m_c} \right), \quad (4.2.34)$$

where $\bar{\Lambda} = M_{D_q} - m_c$ and the parameters G_1, G_2 characterise the matrix elements of non-local operators of dimension-seven. Again in VIA $\tilde{B}_{1,2} = 1$ while $\tilde{B}_{3,4} = 0$. In this study we are assuming isospin symmetry i.e.

$$\overset{(\sim)}{B}_i^u = \overset{(\sim)}{B}_i^d, \quad \overset{(\sim)}{\delta}_i^{uq'} = \overset{(\sim)}{\delta}_i^{dq'}, \quad \overset{(\sim)}{\delta}_i^{qu} = \overset{(\sim)}{\delta}_i^{qd}. \quad (4.2.35)$$

Note that in order to work properly in HQET and calculate these contributions at NLO we need to take into account the extra corrections coming from Equation (4.2.34) instead of simply using f_{D_q} . There are also $1/m_c$ corrections in the same equation which will be included in the calculation of dimension-seven contributions.

By considering only the CKM dominant modes and neglecting for brevity the effect of eye contractions, we can write the LO-QCD expression of the dimension-six

contribution for D^0, D^+ and D_s^+ meson as

$$16\pi^2 \tilde{\Gamma}_6^{D^0} \frac{\langle \tilde{O}_6 \rangle^{D^0}}{m_c^3} = \Gamma_0 |V_{ud}^*|^2 16\pi^2 \frac{M_{D^0} f_{D^0}^2}{m_c^3} (1 - z_s)^2 \left\{ \left(\frac{1}{3} C_1^2 + 2 C_1 C_2 + 3 C_2^2 \right) \left[(\tilde{B}_2^u - \tilde{B}_1^u) + z_s \left(2\tilde{B}_2^u - \frac{\tilde{B}_1^u}{2} \right) \right] + 2 C_1^2 \left[(\tilde{\epsilon}_2^u - \tilde{\epsilon}_1^u) + z_s \left(2\tilde{\epsilon}_2^u - \frac{\tilde{\epsilon}_1^u}{2} \right) \right] \right\}, \quad (4.2.36)$$

$$16\pi^2 \tilde{\Gamma}_6^{D^+} \frac{\langle \tilde{O}_6 \rangle^{D^+}}{m_c^3} = \Gamma_0 |V_{ud}^*|^2 16\pi^2 \frac{M_{D^+} f_{D^+}^2}{m_c^3} (1 - z_s)^2 \left\{ (C_1^2 + 6 C_1 C_2 + C_2^2) \tilde{B}_1^d + 6 (C_1^2 + C_2^2) \tilde{\epsilon}_1^d \right\}, \quad (4.2.37)$$

$$16\pi^2 \tilde{\Gamma}_6^{D_s^+} \frac{\langle \tilde{O}_6 \rangle^{D_s^+}}{m_c^3} = \Gamma_0 |V_{ud}^*|^2 16\pi^2 \frac{M_{D_s^+} f_{D_s^+}^2}{m_c^3} \left\{ \left(3 C_1^2 + 2 C_1 C_2 + \frac{1}{3} C_2^2 + \frac{2}{|V_{ud}^*|^2} \right) (\tilde{B}_2^s - \tilde{B}_1^s) + 2 C_2^2 (\tilde{\epsilon}_2^s - \tilde{\epsilon}_1^s) \right\}, \quad (4.2.38)$$

where the equations correspond to the WE, PI and WA topologies respectively. Note that in the D_s^+ expression we are including two WA diagrams, one non-leptonic and one semi-leptonic as they are both CKM dominant. For the semi-leptonic expression we have neglected the muon mass for brevity but it will be included in the numerical evaluation. The above equations show some interesting numerical effects. First, in the charm system one expects that the spectator effects have a similar size to Γ_3 unless additional cancellations take place. Using $m_c^{pole} = 1.48$ and Lattice QCD value for the decay constants [97] we roughly get

$$16\pi^2 \frac{M_{D^0} f_{D^0}^2}{m_c^3} = 4.1 \approx \mathcal{O}(c_3), \quad 16\pi^2 \frac{M_{D_s^+} f_{D_s^+}^2}{m_c^3} = 6.0 \approx \mathcal{O}(c_3). \quad (4.2.39)$$

This result led the authors of [174] to suggest a different ordering of the HQE series for the charm system. Looking more closely to the Wilson coefficient combinations appearing in Equations (4.2.36) - (4.2.38) we find

$$C_{\text{WE}}^S = \frac{1}{3} C_1^2 + 2 C_1 C_2 + 3 C_2^2, \quad C_{\text{WE}}^O = 2 C_1^2, \quad (4.2.40)$$

$$C_{\text{PI}}^S = C_1^2 + 6 C_1 C_2 + C_2^2, \quad C_{\text{PI}}^O = 6 (C_1^2 + C_2^2), \quad (4.2.41)$$

$$C_{\text{WA}}^S = 3 C_1^2 + 2 C_1 C_2 + \frac{1}{3} C_2^2, \quad C_{\text{WA}}^O = 2 C_2^2, \quad (4.2.42)$$

where the superscripts S and O refer to the colour-singlet and colour-octet operator. In Table 4.5 we show the values for all six combinations at different values of the renormalisation scale μ_1 . As we can see, the coefficient C_{WE}^S is strongly suppressed

μ_1 [GeV]	1	1.27	1.36	1.44	1.48	3
$C_{\text{WE}}^S(\text{LO})$	0.09	0.03	0.02	0.02	0.01	0.01
$C_{\text{WE}}^S(\text{NLO})$	-0.03	-0.03	-0.03	-0.02	-0.02	0.04
$C_{\text{WE}}^O(\text{LO})$	3.57	3.24	3.16	3.11	3.08	2.63
$C_{\text{WE}}^O(\text{NLO})$	3.11	2.89	2.83	2.79	2.77	2.44
$C_{\text{PI}}^S(\text{LO})$	-2.80	-2.12	-1.96	-1.85	-1.79	-0.79
$C_{\text{PI}}^S(\text{NLO})$	-1.74	-1.28	-1.16	-1.08	-1.04	-0.27
$C_{\text{PI}}^O(\text{LO})$	13.0	11.4	11.0	10.7	10.6	8.50
$C_{\text{PI}}^O(\text{NLO})$	10.6	9.55	9.31	9.13	9.05	7.60
$C_{\text{WA}}^S(\text{LO})$	3.82	3.61	3.56	3.53	3.51	3.24
$C_{\text{WA}}^S(\text{NLO})$	3.57	3.42	3.38	3.36	3.35	3.16
$C_{\text{WA}}^O(\text{LO})$	0.77	0.55	0.51	0.47	0.46	0.21
$C_{\text{WA}}^O(\text{NLO})$	0.41	0.30	0.27	0.25	0.24	0.10

Table 4.5: Comparison of the combinations $C_{\text{WE,PI,WA}}^{S,O}$, respectively at LO- and NLO-QCD, for different values of the renormalisation scale μ_1 .

and it can even change sign within the considered range of μ_1 . On the other hand, the coefficient C_{WE}^O is much bigger. Additionally, the Bag parameters of the colour singlet operators cancel exactly in VIA in Equation (4.2.36). All this indicates that the octet and singlet terms might contribute similarly to the WE diagram. For PI the coefficients $C_{\text{PI}}^S, C_{\text{PI}}^O$ are significantly larger than the WE ones (again the octet coefficient is much larger than the singlet one) and we get large modifications compared to the case $C_1 = 1, C_2 = 0$, hinting that gluon radiative corrections can be very important. Finally, in WA we see that C_{WA} is the largest one, but the singlet Bag parameters cancel each other exactly in VIA, hence the octet term can not be neglected. Therefore, a determination of the non-perturbative parameters is crucial for the numerical calculation of the above expressions. If we include all CKM modes

and NLO corrections we can express the four-quark contribution at dimension-six as

$$16\pi^2 \tilde{\Gamma}_6^{D_q} \frac{\langle \tilde{\mathcal{O}}_6 \rangle^{D_q}}{m_c^3} = \frac{\Gamma_0}{|V_{cs}|^2} \sum_{i=1}^4 \left\{ \sum_{q_1, q_2=d,s} |\lambda_{q_1 q_2}|^2 \left[A_{i, q_1 q_2}^{\text{WE}} \frac{\langle D_q | \tilde{\mathcal{O}}_i^u | D_q \rangle}{m_c^3} + A_{i, q_1 q_2}^{\text{PI}} \frac{\langle D_q | \tilde{\mathcal{O}}_i^{q_2} | D_q \rangle}{m_c^3} + A_{i, q_1 q_2}^{\text{WA}} \frac{\langle D_q | \tilde{\mathcal{O}}_i^{q_1} | D_q \rangle}{m_c^3} \right] + \sum_{q_1=d,s} |V_{cq_1}|^2 \sum_{\ell=e,\mu} \left[A_{i, q_1 \ell}^{\text{WA}} \frac{\langle D_q | \tilde{\mathcal{O}}_i^{q_1} | D_q \rangle}{m_c^3} \right] \right\}, \quad (4.2.43)$$

where the matrix elements of the four-quark operators are given in Equations (4.2.31), (4.2.32), and the short-distance coefficients for the WE, PI and WA topologies, cf. Fig. 4.5 are denoted by $A_{i, q_1 q_2}^{\text{WE}}$, $A_{i, q_1 q_2}^{\text{PI}}$ and $A_{i, q_1 q_2}^{\text{WA}}$, $A_{i, q_1 \ell}^{\text{WA}}$, respectively. The LO calculation can be found in Appendix D. NLO corrections to $A_{i, q_1 q_2}^{\text{WE}}$ and $A_{i, q_1 q_2}^{\text{PI}}$ have been computed for HQET operators in [156]. The corresponding results for $A_{i, q_1 q_2}^{\text{WA}}$ can be obtained by Fierz transforming the $\Delta C = 1$ operators given in Equations (4.2.4), (4.2.5). Since the Fierz symmetry is respected also at one-loop level, the functions $A_{i, q_1 q_2}^{\text{WA}}$ are derived from $A_{i, q_1 q_2}^{\text{WE}}$ by replacing $C_1 \leftrightarrow C_2$. For the semi-leptonic modes, the coefficients $A_{i, q_1 \ell}^{\text{WA}}$ have been determined in [157]. Note that in our analysis we treat the contribution of the $\tilde{\delta}_i^{q'q}$ parameters as a subleading ‘‘NLO’’ effect, therefore their coefficients are included only at NLO-QCD. To demonstrate the importance of the NLO-QCD corrections to the spectator effects, we show in Table 4.6 the dimension-six contributions to the D -meson decay widths (see Equation (4.2.43)) splitting the LO and NLO parts, both in VIA and using HQET SR results for the Bag parameters (the values used will be discussed in the following section). NLO-QCD corrections turn out to have an essential numerical effect for the four-quark contributions. In the case of the D^0 and D_s^+ mesons these corrections lift the helicity suppression of weak exchange and weak annihilation in LO-QCD when using VIA. For the D_s^+ meson, in addition to the CKM dominant WA contribution, there is a correction due to the CKM suppressed but nevertheless large PI topology. In the case of the D^+ meson the overall contribution from Pauli interference turns out to be huge, of the order of -2.5 ps^{-1} . In addition, the NLO correction to Pauli interference also turns out to be very large, 50% – 100% of the LO term depending

on the mass scheme. Already in the B system this NLO-QCD corrections were found to be of the order of 30% for the ratio $\tau(B^+)/\tau(B_d)$, see e.g. [155] in the Pole scheme. Thus, neglecting these contributions for charm lifetime studies, as done in [175], is clearly not justified and a knowledge of NNLO-QCD corrections to the four-quark contributions would be highly desirable.

Mass scheme	D^0	D^+	D_s^+
VIA			
Pole	$\underbrace{-0.014}_{\text{NLO}} = \underbrace{0.000}_{\text{LO}} \underbrace{-0.014}_{\Delta\text{NLO}}$	$\underbrace{-2.64}_{\text{NLO}} = \underbrace{-1.68}_{\text{LO}} \underbrace{-0.97}_{\Delta\text{NLO}}$	$\underbrace{-0.20}_{\text{NLO}} = \underbrace{-0.12}_{\text{LO}} \underbrace{-0.08}_{\Delta\text{NLO}}$
$\overline{\text{MS}}$	$\underbrace{-0.010}_{\text{NLO}} = \underbrace{0.000}_{\text{LO}} \underbrace{-0.010}_{\Delta\text{NLO}}$	$\underbrace{-2.49}_{\text{NLO}} = \underbrace{-1.23}_{\text{LO}} \underbrace{-1.25}_{\Delta\text{NLO}}$	$\underbrace{-0.18}_{\text{NLO}} = \underbrace{-0.08}_{\text{LO}} \underbrace{-0.10}_{\Delta\text{NLO}}$
Kinetic	$\underbrace{-0.012}_{\text{NLO}} = \underbrace{0.000}_{\text{LO}} \underbrace{-0.012}_{\Delta\text{NLO}}$	$\underbrace{-2.53}_{\text{NLO}} = \underbrace{-1.42}_{\text{LO}} \underbrace{-1.11}_{\Delta\text{NLO}}$	$\underbrace{-0.19}_{\text{NLO}} = \underbrace{-0.10}_{\text{LO}} \underbrace{-0.09}_{\Delta\text{NLO}}$
$1S$	$\underbrace{-0.013}_{\text{NLO}} = \underbrace{0.000}_{\text{LO}} \underbrace{-0.013}_{\Delta\text{NLO}}$	$\underbrace{-2.60}_{\text{NLO}} = \underbrace{-1.58}_{\text{LO}} \underbrace{-1.02}_{\Delta\text{NLO}}$	$\underbrace{-0.19}_{\text{NLO}} = \underbrace{-0.11}_{\text{LO}} \underbrace{-0.08}_{\Delta\text{NLO}}$
HQET SR			
Pole	$\underbrace{0.007}_{\text{NLO}} = \underbrace{0.019}_{\text{LO}} \underbrace{-0.012}_{\Delta\text{NLO}}$	$\underbrace{-2.89}_{\text{NLO}} = \underbrace{-1.87}_{\text{LO}} \underbrace{-1.02}_{\Delta\text{NLO}}$	$\underbrace{-0.21}_{\text{NLO}} = \underbrace{-0.16}_{\text{LO}} \underbrace{-0.05}_{\Delta\text{NLO}}$
$\overline{\text{MS}}$	$\underbrace{0.020}_{\text{NLO}} = \underbrace{0.014}_{\text{LO}} \underbrace{+0.006}_{\Delta\text{NLO}}$	$\underbrace{-2.72}_{\text{NLO}} = \underbrace{-1.37}_{\text{LO}} \underbrace{-1.35}_{\Delta\text{NLO}}$	$\underbrace{-0.20}_{\text{NLO}} = \underbrace{-0.12}_{\text{LO}} \underbrace{-0.08}_{\Delta\text{NLO}}$
Kinetic	$\underbrace{0.014}_{\text{NLO}} = \underbrace{0.016}_{\text{LO}} \underbrace{-0.002}_{\Delta\text{NLO}}$	$\underbrace{-2.76}_{\text{NLO}} = \underbrace{-1.58}_{\text{LO}} \underbrace{-1.18}_{\Delta\text{NLO}}$	$\underbrace{-0.20}_{\text{NLO}} = \underbrace{-0.13}_{\text{LO}} \underbrace{-0.07}_{\Delta\text{NLO}}$
$1S$	$\underbrace{0.009}_{\text{NLO}} = \underbrace{0.018}_{\text{LO}} \underbrace{-0.008}_{\Delta\text{NLO}}$	$\underbrace{-2.84}_{\text{NLO}} = \underbrace{-1.76}_{\text{LO}} \underbrace{-1.08}_{\Delta\text{NLO}}$	$\underbrace{-0.21}_{\text{NLO}} = \underbrace{-0.15}_{\text{LO}} \underbrace{-0.06}_{\Delta\text{NLO}}$

Table 4.6: Dimension-six contributions to D -meson decay widths (see Equation (4.2.43)) (in ps^{-1}) and split up into LO-QCD and NLO-QCD corrections within different mass schemes and both in VIA and using the HQET SR for Bag parameters.

The $1/m_c^3$ contribution is obtained by ignoring the effects of the light quark in the incoming momentum expression $p^\mu = p_c^\mu + p_q^\mu$. If we include linear correction terms proportional to p_q/m_c we will get the $1/m_c^4$ contributions which can be

described by a basis of dimension-seven operators¹¹

$$P_1^q = m_q (\bar{c}(1 - \gamma_5)q)(\bar{q}(1 - \gamma_5)c), \quad (4.2.44)$$

$$P_2^q = \frac{1}{m_c} (\bar{c} \overleftarrow{D}_\nu \gamma_\mu (1 - \gamma_5) D^\nu q)(\bar{q} \gamma^\mu (1 - \gamma_5) c), \quad (4.2.45)$$

$$P_3^q = \frac{1}{m_c} (\bar{c} \overleftarrow{D}_\nu (1 - \gamma_5) D^\nu q)(\bar{q}(1 + \gamma_5)c), \quad (4.2.46)$$

together with the corresponding colour-octet operators S_1^q, S_2^q, S_3^q . Due to the presence of a covariant derivative acting on the charm field in the operators P_2^q, P_3^q (and the colour-octet ones) which scales as m_c at this order there is no immediate power counting for these operators cf. the HQET operators in Equations (4.2.48), (4.2.49). To evaluate the matrix elements of these operators in the HQET framework we need to expand the charm quark momentum i.e. $p^\mu = m_c v^\mu + k^\mu + p_q^\mu$ and also include $1/m_c$ corrections to the effective heavy quark field and to the HQET Lagrangian as shown in Section 2.2. Thus we get the following basis of dimension-seven operators

$$\tilde{P}_1^q = m_q (\bar{h}_v(1 - \gamma_5)q)(\bar{q}(1 - \gamma_5)h_v), \quad (4.2.47)$$

$$\tilde{P}_2^q = (\bar{h}_v \gamma_\mu (1 - \gamma_5) (i v \cdot D) q)(\bar{q} \gamma^\mu (1 - \gamma_5) h_v), \quad (4.2.48)$$

$$\tilde{P}_3^q = (\bar{h}_v(1 - \gamma_5) (i v \cdot D) q)(\bar{q}(1 + \gamma_5) h_v), \quad (4.2.49)$$

and

$$\tilde{R}_1^q = (\bar{h}_v \gamma_\mu (1 - \gamma_5) q)(\bar{q} \gamma^\mu (1 - \gamma_5) (i \not{D}) h_v), \quad (4.2.50)$$

$$\tilde{R}_2^q = (\bar{h}_v(1 - \gamma_5) q)(\bar{q}(1 + \gamma_5) (i \not{D}) h_v), \quad (4.2.51)$$

supplemented by the corresponding colour-octet operators $\tilde{S}_{1,2,3}^q$ and $\tilde{U}_{1,2}^q$, and the non-local operators

$$\tilde{M}_{1,\pi}^q = i \int d^4 y T [\tilde{O}_1^q(0), (\bar{h}_v (i D)^2 h_v)(y)], \quad (4.2.52)$$

¹¹Note that usually in literature a redundant basis is used in which the operator denoted by P_2^q is the hermitian conjugate of P_1^q , namely $P_2^q = m_q (\bar{c}(1 + \gamma_5)q)(\bar{q}(1 + \gamma_5)c)$. These two operators lead to the same matrix element so we only include P_1^q in our analysis.

$$\tilde{M}_{2,\pi}^q = i \int d^4 y T \left[\tilde{O}_2^q(0), (\bar{h}_v(iD)^2 h_v)(y) \right], \quad (4.2.53)$$

$$\tilde{M}_{1,G}^q = i \int d^4 y T \left[\tilde{O}_1^q(0), \frac{1}{2} g_s (\bar{h}_v \sigma_{\alpha\beta} G^{\alpha\beta} h_v)(y) \right], \quad (4.2.54)$$

$$\tilde{M}_{2,G}^q = i \int d^4 y T \left[\tilde{O}_2^q(0), \frac{1}{2} g_s (\bar{h}_v \sigma_{\alpha\beta} G^{\alpha\beta} h_v)(y) \right], \quad (4.2.55)$$

also supplemented by the corresponding colour-octet operators. The operators $\tilde{P}_1^q, \tilde{P}_2^q, \tilde{P}_3^q$ originate from taking into account light quark momentum, $\tilde{R}_1^q, \tilde{R}_2^q$ come from the expansion of the effective field h_v as in Equation (2.1.65), and $M_{1,\pi}^q, M_{2,\pi}^q, M_{1,G}^q, M_{2,G}^q$ stem from corrections to the HQET Lagrangian as shown in Equation (2.1.68). The parametrisation of these matrix elements is shown in Appendix C. At LO-QCD these matrix elements can be parametrised by the non-perturbative parameters $F(\mu), G_1(\mu), G_2(\mu)$ and $\bar{\Lambda}$. Because they are only determined in large uncertainties, we will be using instead the QCD decay constant as input which is computed very precisely using Lattice QCD [97]. In VIA and at the matching scale $\mu = m_c$ the matrix elements of the local operators $\tilde{R}_{1,2}^q$ as well as the that of the non-local ones can be absorbed in the QCD decay constant using Equation (4.2.34). To make this point clearer, consider the contribution to the PI diagram at LO-QCD including $1/m_c^4$ effects,

$$\begin{aligned} \text{Im } \mathcal{T}^{\text{PI}} = \Gamma_0 |V_{ud}^*|^2 \frac{32\pi^2}{m_c^3} (1 - z_s)^2 & \left[C_{\text{PI}}^S \left(\tilde{O}_1^d + \frac{\tilde{R}_1^d}{m_c} + \frac{\tilde{M}_{1,\pi}^d}{m_c} + \frac{\tilde{M}_{1,G}^d}{m_c} + 2 \frac{1 + z_s}{1 - z_s} \frac{\tilde{P}_3^q}{m_c} \right) \right. \\ & \left. + (\text{colour-octet part}) \right]. \end{aligned} \quad (4.2.56)$$

Evaluating this in VIA, the colour-octet contribution vanishes and using the parametrisation stated in Appendix C and in Equation (4.2.31) we get

$$\begin{aligned} \left\langle \tilde{O}_1^d + \frac{\tilde{R}_1^d}{m_c} + \frac{\tilde{M}_{1,\pi}^d}{m_c} + \frac{\tilde{M}_{1,G}^d}{m_c} \right\rangle_{\text{HQET}} & = F^2 M_{D^+} \left[1 - \frac{\bar{\Lambda}}{m_c} + \frac{2 G_1}{m_c} + \frac{12 G_2}{m_c} \right] \\ & = f_D^2 M_{D^+}^2 = \langle O_1^d \rangle_{\text{QCD}}, \end{aligned} \quad (4.2.57)$$

where the matrix elements are taken between the same D meson states and the parameters F, G_1, G_2 are calculated at $\mu = m_c$. The same arguments can be made for the WE and WA topologies. We should mention that in VIA, and neglecting the

strange quark mass, the contributions to WE, WA vanish due to helicity suppression. This is lifted once we include gluon corrections or strange mass effects, but again the contributions of \tilde{R}_i^q , $\tilde{\mathcal{M}}_{i,\pi}^q$ and $\tilde{\mathcal{M}}_{i,G}^q$ in HQET can be completely absorbed in f_D by evaluating the matrix elements in VIA. For O_2^q the only difference is that \tilde{R}_2^q is absorbed by the combination $(M_D f_D/m_c)^2 \approx (1 + 2\bar{\Lambda}/m_c) f_D^2$. A detailed analysis of $1/m_c^4$ contributions has been made in [173] for the case of B-mixing. It was found that in VIA, subleading effects of non-local operators can be absorbed in the QCD decay constant. Further corrections stemming from the running of local dimension-seven operators down to $\mu \approx 1$ GeV are small, and in fact neglecting them one can absorb all $1/m_c$ effects in f_D .

Similarly to the $1/m_c^3$ contributions, by summing over all CKM modes the $1/m_c^4$ effects can be written at LO-QCD as

$$\begin{aligned}
16\pi^2 \tilde{\Gamma}_7^{D_q} \frac{\langle \tilde{\mathcal{O}}_7 \rangle^{D_q}}{m_c^4} &= \frac{\Gamma_0}{|V_{cs}|^2} \sum_{i=1}^3 \left\{ \sum_{q_1, q_2=d,s} |\lambda_{q_1 q_2}|^2 \left[G_{i, q_1 q_2}^{\text{WE}} \frac{\langle D_q | \tilde{P}_i^u | D_q \rangle}{m_c^4} + G_{i, q_1 q_2}^{\text{PI}} \frac{\langle D_q | \tilde{P}_i^{q_2} | D_q \rangle}{m_c^4} \right. \right. \\
&\quad \left. \left. + G_{i, q_1 q_2}^{\text{WA}} \frac{\langle D_q | \tilde{P}_i^{q_1} | D_q \rangle}{m_c^4} \right] + \sum_{q_1=d,s} |V_{cq_1}|^2 \sum_{\ell=e,\mu} \left[G_{i, q_1 \ell}^{\text{WA}} \frac{\langle D_q | \tilde{P}_i^{q_1} | D_q \rangle}{m_c^4} \right] \right\} \\
&\quad + (\text{colour-octet part}) . \tag{4.2.58}
\end{aligned}$$

The results for the short-distance coefficients $G_{i, q_1 q_2}^{\text{WE}}$, $G_{i, q_1 q_2}^{\text{PI}}$ and $G_{i, q_1 q_2}^{\text{WA}}$, $G_{i, q_1 \ell}^{\text{WA}}$ are presented in [157] and the full calculation is included in Appendix D. Note that, due to the current accuracy of the analysis, at dimension-seven we include only the contribution of the valence-quark, therefore e.g. $\langle D^0 | P_i^s | D^0 \rangle = 0$. In Table 4.7 we show the central values for dimension-seven using the kinetic mass scheme. As we

	D^0	D^+	D_s^+
$16\pi^2 \tilde{\Gamma}_7^{D_q} \frac{\langle \tilde{\mathcal{O}}_7 \rangle^{D_q}}{m_c^4} [\text{ps}^{-1}]$	4.6×10^{-7}	1.05	0.10

Table 4.7: Dimension-seven contributions to D -meson decay widths (see Equation (4.2.58)) in ps^{-1} within VIA in the kinetic mass scheme.

can see, $1/m_c$ corrections can vary from almost negligible in the D^0 case to almost as big as Γ_3 for D^+ . It is therefore important to get a more precise measurement of this contribution.

4.3 Determination of Non-perturbative Parameters

In the previous section we discussed how to calculate several perturbative terms in the HQE. However, we also need to have a way to determine the non-perturbative parameters that couple them in order to get a reliable result. Starting with the kinetic operator at dimension-five, there is no precise determination available for the charm system. There are several predictions for the B system covering a wide range of values. These can be found in Table 4.8. Assuming heavy quark symmetry, we

Source	LQCD [176]	LQCD [161]	Exp. fit [69]	QCD SR [166]	QCD SR [165]
$\mu_\pi^2[\text{GeV}^2]$	0.05(22)	0.314(15)	0.477(56)	0.10(5)	0.6(1)

Table 4.8: Different determinations of $\mu_\pi^2(B)$ available in the literature.

can use the recently obtained value from [69] and get the estimate for the D meson

$$\mu_\pi^2(D) = (0.48 \pm 0.2) \text{ GeV}^2, \quad (4.3.1)$$

where we have added an uncertainty of 40% to account for heavy quark symmetry breaking. This value still fulfills the theoretical bound $\mu_\pi^2 \geq \mu_G^2$, see e.g. [54]. With this value we expect corrections of order -10% (based on Equation (4.2.15)). Due to isospin symmetry we can use this value of μ_π^2 for D^0 and D^+ mesons. For the D_s^+ meson we can use the $SU(3)_F$ breaking which has been estimated in [157, 177]

$$\mu_\pi^2(D_s^+) - \mu_\pi^2(D^0) \approx 0.09 \text{ GeV}^2, \quad (4.3.2)$$

leading to

$$\mu_\pi^2(D_s^+) = (0.57 \pm 0.23) \text{ GeV}^2. \quad (4.3.3)$$

Of course a more precise experimental determination from fits to semi-leptonic decays of D mesons (like it has happened for the B mesons) would be very desirable.

Moving to the chromomagnetic operator, the value of μ_G^2 has been determined for B decays by fitting to experimental data in semi-leptonic decays [69]

$$\mu_G^2(B) = (0.306 \pm 0.050) \text{ GeV}^2. \quad (4.3.4)$$

Again by assuming heavy quark symmetry we can expect a similar size for the charm system. However we can also use spectroscopy to estimate this parameter [178]

$$\mu_G^2(D_{(s)}) = \frac{3}{2} m_c (M_{D_{(s)}^*} - M_{D_{(s)}}), \quad (4.3.5)$$

up to power corrections. Using meson masses taken from PDG [1] and setting $m_c = 1.27$ one gets

$$\mu_G^2(D) = (0.268 \pm 0.107) \text{ GeV}^2, \quad \mu_G^2(D_s) = (0.274 \pm 0.110) \text{ GeV}^2, \quad (4.3.6)$$

where again we have added a 40% uncertainty. These values are roughly 19% smaller than the ones for the B system, while there is only a tiny amount of $SU(3)_F$ -symmetry breaking of $\approx 2\%$ which can be enhanced by power corrections. Alternatively, there is another relation widely used in the literature independent of the choice of m_c , see e.g. [179]

$$\mu_G^2(D_{(s)}) = \frac{3}{4} (M_{D_{(s)}^*}^2 - M_{D_{(s)}}^2), \quad (4.3.7)$$

that yields

$$\mu_G^2(D) = 0.41 \text{ GeV}^2, \quad \mu_G^2(D_s^+) = 0.44 \text{ GeV}^2, \quad (4.3.8)$$

which are roughly 23% higher than the value for the B mesons. In our analysis we will take the average of Equations (4.3.6) and (4.3.8) that gives

$$\mu_G^2(D) = (0.34 \pm 0.10) \text{ GeV}^2, \quad \mu_G^2(D_s^+) = (0.36 \pm 0.10) \text{ GeV}^2, \quad (4.3.9)$$

which agrees well with Equation (4.3.4). Again from Equation (4.2.15) the effect of the chromomagnetic operator lies between -6% and $+8\%$ compared to Γ_3 . We see again the issue with the coefficient c_G and the cancellations it exhibits. A full NLO-QCD determination of c_G would give us a better idea of the size of this term. For semi-leptonic decay rates the contribution of the chromomagnetic operator can reach up to 20% as we can see in the following section.

For the Darwin operator there is only a determination for the B system from fitting to semi-leptonic decays data [69]

$$\rho_D^3(B) = (0.185 \pm 0.031) \text{ GeV}^3. \quad (4.3.10)$$

Again using heavy quark symmetry and adding a 40% uncertainty we could write a first estimate for the charm system

$$\rho_D^3(D)^I = (0.185 \pm 0.08) \text{ GeV}^3. \quad (4.3.11)$$

Alternatively, the ρ_D^3 parameter can be expressed in terms of the Bag parameters of the dimension-six four quark operators by expanding the equation of motion for the gluon field [172]. At leading order $1/m_Q$ we have

$$\rho_D^3(H) = \frac{g_s^2}{18} f_H^2 M_H \left[2 \tilde{B}_2^{q'} - \tilde{B}_1^{q'} + \frac{3}{4} \tilde{\epsilon}_1^{q'} - \frac{3}{2} \tilde{\epsilon}_2^{q'} + \sum_{q=u,d,s} \left(2 \tilde{\delta}_2^{q'q} - \tilde{\delta}_1^{q'q} + \frac{3}{4} \tilde{\delta}_3^{q'q} - \frac{3}{2} \tilde{\delta}_4^{q'q} \right) \right], \quad (4.3.12)$$

where H is a heavy hadron with mass M_H and decay constant f_H , $q' = u, d, s$ is the light valence quark in the H -hadron, and the Bag parameters $\tilde{B}_1^q, \tilde{B}_2^q, \tilde{\epsilon}_1^q, \tilde{\epsilon}_2^q, \tilde{\delta}_1^{q'q}, \tilde{\delta}_2^{q'q}, \tilde{\delta}_3^{q'q}$ and $\tilde{\delta}_4^{q'q}$ were introduced in Section 4.2. The numerical values for all these parameters can be found in Appendix A. For the strong coupling g_s , [180] suggests setting $\alpha_s = 1$. Using Equation (4.3.12) we present in Table 4.9 the values for ρ_D^3 for B and D mesons for three different values of α_s . As we can see when setting $\alpha_s = 1$ we get values closest to Equation (4.3.10) indicating corrections at $1/m_c$ of

$\rho_D^3[\text{GeV}^3]$	$\mu = 1.5 \text{ GeV}$		$\mu = 1.0 \text{ GeV}$		$\alpha_s = 1$	
	VIA	HQET	VIA	HQET	VIA	HQET
B^+, B_d	0.048	0.047	0.066	0.064	0.133	0.129
B_s	0.072	0.070	0.098	0.095	0.199	0.193
D^+, D^0	0.021	0.020	0.027	0.026	0.059	0.056
D_s^+	0.030	0.029	0.040	0.038	0.086	0.082

Table 4.9: Values of $\rho_D^3(H)$ for B and D mesons in VIA and using HQET SR for Bag parameters for three different choices of α_s in Equation (4.3.12).

about 30%. Moreover, we find that VIA gives in Equation (4.3.12) values which are very close to the HQET sum rule ones. We emphasise that due to the sizeable $SU(3)_F$ breaking in the decay constants, Equation (4.3.12) leads also to a sizable $SU(3)_F$ breaking for the non-perturbative parameters $\rho_D^3(D)$, $\rho_D^3(D_s^+)$. Taking the values corresponding to $\alpha_s = 1$ and using HQET SR we get a second estimate for the Darwin parameter

$$\rho_D^3(D)^{II} = (0.056 \pm 0.022) \text{ GeV}^3, \quad \rho_D^3(D_s^+)^{II} = (0.82 \pm 0.033) \text{ GeV}^3, \quad (4.3.13)$$

where once more an uncertainty of 40% has been added. Equation (4.3.12) in VIA becomes

$$\rho_D^3(H) \approx \frac{g_s^2}{18} f_H^2 M_H. \quad (4.3.14)$$

If we assume the Darwin parameter has similar size in B and D mesons then we can write

$$\rho_D^3(D) \approx \frac{f_D^2 m_D}{f_B^2 m_B} \rho_D^3(B), \quad \rho_D^3(D_s) \approx \frac{f_{D_s}^2 m_{D_s}}{f_B^2 m_B} \rho_D^3(B). \quad (4.3.15)$$

These expressions lead us to a third estimate

$$\rho_D^3(D)^{III} = (0.082 \pm 0.035) \text{ GeV}^3, \quad \rho_D^3(D_s)^{III} = (0.119 \pm 0.052) \text{ GeV}^3, \quad (4.3.16)$$

where again 40% uncertainty has been added. These values are consistent with the last column of Table 4.9 and as we can see there is a much bigger $SU(3)_F$ -symmetry breaking stemming from the ratio $f_{D_s^+}/f_{D^0}$ (and a similar observation can be made

for the B mesons). In our numerical analysis we will use the values of Equation (4.3.16). Of course a more precise determination of ρ_D^3 would be very desirable.

The dimension-six Bag parameters of the D^+ and D^0 mesons have been determined using HQET Sum Rules [4]; strange quark mass corrections, relevant for the Bag parameter of the D_s^+ meson, as well as eye-contractions have been computed for the first time in [5]. The numerical values can be found in Appendix A and the HQET sum rules suggest values for the Bag parameter that are very close to VIA.

For the dimension-seven Bag parameters (defined in HQET), we apply VIA. As one can see from Appendix C, the matrix elements of dimension-seven operators in HQET depend also on the parameters $\bar{\Lambda}_{(s)} = m_{D_{(s)}} - m_c$, for which we use the following ranges [5].

$$\bar{\Lambda} = (0.5 \pm 0.1) \text{ GeV}, \quad (4.3.17)$$

$$\bar{\Lambda}_s = (0.6 \pm 0.1) \text{ GeV}. \quad (4.3.18)$$

Notice that we use only Equation (2.1.69) ignoring further $1/m_c$ corrections as they contribute to higher orders of the calculation.

4.4 Numerical Results

Moving to the numerical analysis we will be looking at total decay rates, semi-leptonic decay rates and their ratios. We investigate several quark mass schemes (with the kinetic scheme as default) and compare results using both VIA and HQET SR values for the Bag parameters. All input values for these calculations can be found in Appendix A. For the renormalisation scales, we fix the central values at $\mu_0 = \mu_1 = 1.5 \text{ GeV}$ and vary them independently between 1 and 3 GeV. For the μ_0 dependence of the Bag parameters we have used the anomalous dimension matrix from [4]. Moreover we add an estimated uncertainty due to missing higher order corrections.

VIA					
Observable	Pole	$\overline{\text{MS}}$	Kinetic	1 <i>S</i>	Exp. value
$\Gamma(D^0)[\text{ps}^{-1}]$	1.71	1.49	1.58	1.66	2.44
$\Gamma(D^+)[\text{ps}^{-1}]$	0.22	-0.01	0.11	0.18	0.96
$\bar{\Gamma}(D_s^+)[\text{ps}^{-1}]$	1.76	1.51	1.61	1.71	1.88
$\tau(D^+)/\tau(D^0)$	2.55	2.56	2.53	2.54	2.54
$\bar{\tau}(D_s^+)/\tau(D^0)$	0.97	0.99	0.98	0.98	1.30
$B_{sl}^{D^0} [\%]$	5.43	6.55	6.14	5.75	6.49
$B_{sl}^{D^+} [\%]$	13.8	16.6	15.6	14.6	16.07
$B_{sl}^{D_s^+} [\%]$	7.12	8.42	7.95	7.50	6.30
$\Gamma_{sl}^{D^+} / \Gamma_{sl}^{D^0}$	1.00	1.00	1.00	1.00	0.985
$\Gamma_{sl}^{D_s^+} / \Gamma_{sl}^{D^0}$	1.06	1.05	1.05	1.05	0.790

Table 4.10: Central values of the charm observables in different quark mass schemes using VIA for the matrix elements of the 4-quark operators compared to the corresponding experimental values (last column).

Starting with the total decay rates, we are expecting them to have big theoretical uncertainties due to the dependence of the free quark decay on m_c^5 and due to large perturbative and power corrections. In Tables 4.10, 4.11 we can see the central values of all observables for various mass schemes using VIA and HQET SR results respectively. In Table 4.12 we summarise the results for the kinetic scheme, using HQET SR values and including full uncertainties (parametric, μ_0 - and μ_1 -dependence). The estimated uncertainty due to missing higher orders is included in the parametric value. The values of the total decay rates can be found in the first three rows of these tables. These contents can also be visualised in the top graph of Figure 4.7.

In all tables the last column corresponds to most recent experimental measurements.

HQET SR					
Observable	Pole	$\overline{\text{MS}}$	Kinetic	1S	Exp. value
$\Gamma(D^0)[\text{ps}^{-1}]$	1.73	1.52	1.61	1.68	2.44
$\Gamma(D^+)[\text{ps}^{-1}]$	-0.03	-0.24	-0.12	-0.06	0.96
$\bar{\Gamma}(D_s^+)[\text{ps}^{-1}]$	1.75	1.50	1.60	1.69	1.88
$\tau(D^+)/\tau(D^0)$	2.83	2.83	2.80	2.82	2.54
$\bar{\tau}(D_s^+)/\tau(D^0)$	0.99	1.01	1.00	1.00	1.30
$B_{sl}^{D^0} [\%]$	5.26	6.42	6.00	5.59	6.49
$B_{sl}^{D^+} [\%]$	13.4	16.3	15.2	14.2	16.07
$B_{sl}^{D_s^+} [\%]$	7.10	8.36	7.91	7.48	6.30
$\Gamma_{sl}^{D^+}/\Gamma_{sl}^{D^0}$	1.002	1.001	1.001	1.002	0.985
$\Gamma_{sl}^{D_s^+}/\Gamma_{sl}^{D^0}$	1.08	1.06	1.07	1.08	0.790

Table 4.11: Central values of the charm observables in different quark mass schemes using HQET sum rule results [4, 5] for the matrix elements of the 4-quark operators compared to the corresponding experimental values (last column).

There is a small subtlety regarding $\tau_{D_s^+}$; the experimental result includes the semi-leptonic mode $D_s^+ \rightarrow \tau^+ \nu_\tau$ which is not included in the HQE as the tau lepton is heavier than the charm quark. Taking into account this we can define a reduced decay rate for D_s^+

$$\bar{\Gamma}(D_s^+) \equiv \Gamma(D_s^+) - \Gamma(D_s^+ \rightarrow \tau^+ \nu_\tau) = (1.88 \pm 0.02) \text{ps}^{-1}, \quad (4.4.1)$$

using [1]

$$\text{Br}(D_s^+ \rightarrow \tau^+ \nu_\tau) = (5.48 \pm 0.23)\%. \quad (4.4.2)$$

This also leads us to a reduced lifetime ratio

$$\frac{\bar{\tau}(D_s^+)}{\tau(D^0)} = 1.30 \pm 0.01. \quad (4.4.3)$$

Observable	HQE prediction	Exp. value
$\Gamma(D^0)[\text{ps}^{-1}]$	$1.61 \pm 0.37^{+0.46+0.01}_{-0.37-0.01}$	2.44 ± 0.01
$\Gamma(D^+)[\text{ps}^{-1}]$	$-0.12 \pm 0.77^{+0.59+0.25}_{-0.28-0.10}$	0.96 ± 0.01
$\bar{\Gamma}(D_s^+)[\text{ps}^{-1}]$	$1.60 \pm 0.44^{+0.52+0.02}_{-0.41-0.01}$	1.88 ± 0.02
$\tau(D^+)/\tau(D^0)$	$2.80 \pm 0.85^{+0.01+0.11}_{-0.14-0.26}$	2.54 ± 0.02
$\bar{\tau}(D_s^+)/\tau(D^0)$	$1.00 \pm 0.16^{+0.02+0.01}_{-0.03-0.01}$	1.30 ± 0.01
$B_{sl}^{D^0} [\%]$	$6.00 \pm 1.57^{+0.33}_{-0.28}$	6.49 ± 0.11
$B_{sl}^{D^+} [\%]$	$15.23 \pm 4.07^{+0.83}_{-0.72}$	16.07 ± 0.30
$B_{sl}^{D_s^+} [\%]$	$7.91 \pm 2.64^{+0.43}_{-0.38}$	6.30 ± 0.16
$\Gamma_{sl}^{D^+} / \Gamma_{sl}^{D^0}$	$1.001 \pm 0.008 \pm 0.001$	0.985 ± 0.028
$\Gamma_{sl}^{D_s^+} / \Gamma_{sl}^{D^0}$	$1.07 \pm 0.24 \pm 0.01$	0.790 ± 0.026

Table 4.12: HQE predictions for all the ten observables in the kinetic scheme (second column), using HQET SR results for the Bag parameters. The first uncertainty is parametric, the second and third uncertainties are due to μ_1 - and μ_0 -scales variation, respectively. The results are compared with the corresponding experimental measurements (third column).

The main result we can draw from Table 4.12 and Figure 4.7 is that the HQE can reproduce the experimental values of $\Gamma(D^0)$, $\Gamma(D^+)$ and $\bar{\Gamma}(D_s^+)$ within big uncertainties. The decay rate of D_s^+ is in good agreement with the experimental value while $\Gamma(D^0)$ and $\Gamma(D^+)$ are underestimated. A potential reason for that could be the missing NNLO-QCD corrections to the free charm quark decay. It is also expected that while the various mass schemes yield similar results, further higher order corrections will reduce these differences. We observe that the results on Table 4.10 and Table 4.11 do not differ much as the HQET SR values for the Bag parameters are very close to VIA. Of course we could not ignore the negative result we get for the D^+ meson; this is an effect of the large negative value of the PI diagram which is dominant for D^+ . This gets even worse if we consider NLO-QCD corrections but it is partly compensated by dimension-seven corrections. An independent confirmation of the HQET SR results with lattice QCD, as well as higher order QCD corrections

to the spectator effects might give some more insights.

To analyse further the result for the total decay rates we can express them in terms of the non-perturbative parameters. Using the kinetic scheme we can write for the D^0 meson¹²

$$\begin{aligned}
\Gamma(D^0) = & 6.15 \Gamma_0 \left[\underbrace{1}_{c_3^{\text{LO}}} + \underbrace{0.48}_{\Delta c_3^{\text{NLO}}} - 0.13 \frac{\mu_\pi^2(D)}{0.48 \text{ GeV}^2} + 0.01 \frac{\mu_G^2(D)}{0.34 \text{ GeV}^2} + 0.31 \frac{\rho_D^3(D)}{0.082 \text{ GeV}^3} \right. \\
& - \underbrace{0.01}_{\text{dim-6, VIA}} - 0.005 \frac{\delta \tilde{B}_1^q}{0.02} + 0.005 \frac{\delta \tilde{B}_2^q}{0.02} + 0.137 \frac{\tilde{\epsilon}_1^q}{-0.04} - 0.125 \frac{\tilde{\epsilon}_2^q}{-0.04} \\
& + \underbrace{0.00}_{\text{dim-7, VIA}} - 0.0045 r_1^{qq} - 0.0004 r_2^{qq} - 0.0035 r_3^{qq} + 0.0000 r_4^{qq} \\
& \left. - 0.0109 r_1^{sq} - 0.0079 r_2^{sq} - 0.0000 r_3^{sq} + 0.0001 r_4^{sq} \right], \quad (4.4.4)
\end{aligned}$$

where we have normalised the parameters μ_π^2 , μ_G^2 and ρ_D^3 to their central values and we have introduced the following notation as a measure of deviation from VIA for the colour singlet Bag parameters

$$\tilde{B}_i^q = 1 + \delta \tilde{B}_i^q \quad i = 1, 2. \quad (4.4.5)$$

The parameters $\delta \tilde{B}_i^q$ are normalised conservatively to 0.02 while ϵ_1, ϵ_2 are normalised to 0.04. Finally, we use the notation $r_i^{qq'} \equiv \tilde{\delta}_i^{qq'} / \langle \tilde{\delta}_i^{qq'} \rangle$, with $\langle \tilde{\delta}_i^{qq'} \rangle$ being the central values (shown in Appendix A). The contributions of the eye-contractions do not seem to be very important while, due to selecting $\mu_1 = 1.5 \text{ GeV}$, we get a very small value for the coefficient of μ_G^2 . By varying the scale between 1 and 3 GeV though we can get an effect of 5 – 10%. The series for the D^0 meson looks convergent with the biggest correction coming from the Darwin term and the NLO-QCD corrections to Γ_3 , making further QCD corrections to Γ_3 and a more profound determination of ρ_D^3 very important. Due to helicity suppression, the four-quark contributions are very small (especially since the HQET SR values are very close to VIA).

¹²From here on we will be using the same label q in the Bag parameters for both u and d quarks due to isospin symmetry.

For the D^+ meson we can write in the same way

$$\begin{aligned}
\Gamma(D^+) = & 6.15 \Gamma_0 \left[\underbrace{1}_{c_3^{\text{LO}}} + \underbrace{0.48}_{\Delta c_3^{\text{NLO}}} - 0.13 \frac{\mu_\pi^2(D)}{0.48 \text{ GeV}^2} + 0.01 \frac{\mu_G^2(D)}{0.34 \text{ GeV}^2} + 0.31 \frac{\rho_D^3(D)}{0.082 \text{ GeV}^3} \right. \\
& - \underbrace{2.66}_{\text{dim-6,VIA}} - 0.055 \frac{\delta \tilde{B}_1^q}{0.02} + 0.002 \frac{\delta \tilde{B}_2^q}{0.02} - 0.546 \frac{\tilde{\epsilon}_1^q}{-0.04} + 0.009 \frac{\tilde{\epsilon}_2^q}{-0.04} \\
& + \underbrace{1.10}_{\text{dim-7,VIA}} - 0.0000 r_1^{qq} - 0.0000 r_2^{qq} - 0.0011 r_3^{qq} + 0.0008 r_4^{qq} \\
& \left. - 0.0109 r_1^{sq} - 0.0080 r_2^{sq} - 0.0000 r_3^{sq} + 0.0001 r_4^{sq} \right], \quad (4.4.6)
\end{aligned}$$

where we encounter huge negative corrections due to Pauli Interference diagrams. Here we can see some very interesting cancellations between the three dominant terms $\Gamma_3^{(0)}$ and $16\pi^2 \left[(\tilde{\Gamma}_6^{(0)} + \alpha_s/\pi \tilde{\Gamma}_6^{(1)}) \langle \tilde{\mathcal{O}}_6 \rangle^{\text{VIA}}/m_c^3 + \tilde{\Gamma}_7^{(0)} \langle \tilde{\mathcal{O}}_7 \rangle^{\text{VIA}}/m_c^4 \right]$ that make the result sensitive to sub-dominant terms, e.g. higher order QCD corrections to $\tilde{\Gamma}_6$, $\tilde{\Gamma}_7$, Γ_3 , Γ_5 , Γ_6 , and to deviations of the Bag parameter from VIA. It would be interesting to study higher orders of the HQE, see e.g. [158, 159].

For D_s^+ we obtain

$$\begin{aligned}
\Gamma(D_s^+) = & 6.15 \Gamma_0 \left[\underbrace{1}_{c_3^{\text{LO}}} + \underbrace{0.48}_{\Delta c_3^{\text{NLO}}} - 0.15 \frac{\mu_\pi^2(D_s)}{0.57 \text{ GeV}^2} + 0.01 \frac{\mu_G^2(D_s)}{0.36 \text{ GeV}^2} + 0.46 \frac{\rho_D^3(D_s)}{0.119 \text{ GeV}^3} \right. \\
& - \underbrace{0.20}_{\text{dim-6,VIA}} - 0.161 \frac{\delta \tilde{B}_1^s}{0.02} + 0.157 \frac{\tilde{B}_2^s}{0.02} + 0.089 \frac{\tilde{\epsilon}_1^q}{-0.04} + 0.122 \frac{\tilde{\epsilon}_2^q}{0.04} \\
& \left. + \underbrace{0.10}_{\text{dim-7,VIA}} - 0.0064 r_1^{qs} - 0.0007 r_2^{qs} - 0.0036 r_3^{qs} + 0.0012 r_4^{qs} \right]. \quad (4.4.7)
\end{aligned}$$

Again here the series convergence looks nice and, similar to the D^0 case, the dominant correction comes from the Darwin operator and the NLO-QCD corrections to the free quark decay. There is still a cancellation between dimension-six and dimension-seven but it is less pronounced than D^0 because of the CKM suppressed PI diagrams.

Moving to lifetime ratios, we can define them as

$$\frac{\tau(D_{(s)}^+)}{\tau(D^0)} = 1 + [\Gamma^{\text{HQE}}(D^0) - \Gamma^{\text{HQE}}(D_{(s)}^+)] \tau^{\text{exp}}(D_{(s)}^+). \quad (4.4.8)$$

This way we can eliminate the contribution of the free-quark decay and also reduce the dependence on isolated non-perturbative parameters. The expressions for $\Gamma^{\text{HQE}}(D^0)$, $\Gamma^{\text{HQE}}(D^+)$ and $\Gamma^{\text{HQE}}(D_s^+)$ can be found in the kinetic scheme in Equations (4.4.4), (4.4.6) and (4.4.7) respectively, while their central values for several mass schemes both in VIA and HQET SR can be found in the fourth and fifth rows of Table 4.10, Table 4.11, Table 4.12 as well as in the second graph of Figure 4.7. As we can see, the ratio $\tau(D^+)/\tau(D^0)$ is well reproduced in all schemes while $\tau(D_s^+)/\tau(D^0)$, which is dominated by the $SU(3)_F$ -symmetry breaking differences of μ_π^2 , μ_G^2 and ρ_D^3 , is calculated to be closer to 1 than to the experimental value.

The large lifetime ratio $\tau(D^+)/\tau(D^0)$ can be written as

$$\begin{aligned} \frac{\tau(D^+)}{\tau(D^0)} &= 1 \underbrace{+ 2.62}_{\text{dim-6,VIA}} \underbrace{- 1.09}_{\text{dim-7,VIA}} \\ &+ 0.049 \frac{\delta \tilde{B}_1^q}{0.02} + 0.003 \frac{\delta \tilde{B}_2^q}{0.02} + 0.676 \frac{\tilde{\epsilon}_1^q}{-0.04} - 0.132 \frac{\tilde{\epsilon}_2^q}{-0.04} \\ &- 0.004 r_1^{qq} - 0.000 r_2^{qq} - 0.005 r_3^{qq} - 0.001 r_4^{qq}. \end{aligned} \quad (4.4.9)$$

Note that due to isospin symmetry there are no terms depending on μ_π^2 , μ_G^2 , ρ_D^3 or on any of the eye contractions. Again we find a big cancellation between dimension-six and dimension-seven, hinting that a more precise determination of the colour-octet Bag parameters, as well as a calculation of higher order QCD corrections to spectator effects can be very important.

Expanding the $\tau(D_s^+)/\tau(D^0)$ ratio we get

$$\begin{aligned} \frac{\tau(D_s^+)}{\tau(D^0)} &= 1 + 0.012 \frac{\mu_\pi^2(D_s) - \mu_\pi^2(D)}{0.09 \text{ GeV}^2} - 0.0002 \frac{\mu_G^2(D_s) - \mu_G^2(D)}{0.02 \text{ GeV}^2} \\ &- 0.071 \frac{\rho_D^3(D_s) - \rho_D^3(D)}{0.037 \text{ GeV}^3} \underbrace{+ 0.10}_{\text{dim-6,VIA}} \underbrace{- 0.05}_{\text{dim-7,VIA}} \end{aligned}$$

$$\begin{aligned}
& -0.003 \frac{\delta \tilde{B}_1^q}{0.02} + 0.003 \frac{\delta \tilde{B}_2^q}{0.02} + 0.081 \frac{\delta \tilde{B}_1^s}{0.02} - 0.079 \frac{\delta \tilde{B}_2^s}{0.02} \\
& + 0.069 \frac{\tilde{c}_1^q}{-0.04} - 0.063 \frac{\tilde{c}_2^q}{-0.04} - 0.045 \frac{\tilde{c}_1^s}{-0.04} - 0.062 \frac{\tilde{c}_2^s}{0.04} \\
& - 0.0033 r_1^{qq} - 0.0002 r_2^{qq} - 0.0018 r_3^{qq} + 0.0000 r_4^{qq} \\
& - 0.0055 r_1^{qs} - 0.0040 r_2^{qs} - 0.0000 r_3^{qs} + 0.0001 r_4^{qs} \\
& + 0.0032 r_1^{sq} + 0.0003 r_2^{sq} + 0.0018 r_3^{sq} - 0.0006 r_4^{sq}. \quad (4.4.10)
\end{aligned}$$

As we can see, the biggest $SU(3)_F$ -breaking effect comes from the Darwin term ($\approx -7\%$) while the four quark contributions are limited to only $+5\%$ using VIA.

Moving to the semi-leptonic decays we introduce the notation $\Gamma_{sl}^D \equiv \Gamma(D \rightarrow X e^+ \nu_e)$ and $B_{sl}^D \equiv \text{Br}(D \rightarrow X e^+ \nu_e)$ and determine the theoretical values of the semi-leptonic branching ratios as

$$B_{sl}^{D,\text{HQE}} = \Gamma_{sl}^{D,\text{HQE}} \cdot \tau(D)^{\text{Exp.}}. \quad (4.4.11)$$

The central values for the HQE predictions in various mass schemes, both in VIA and HQET SR, can be found in the sixth, seventh and eighth row of Table 4.10, Table 4.11 and Table 4.12 as well as in the third graph of Figure 4.7. We can write the semi-leptonic decay rate of D^0 in the kinetic scheme

$$\begin{aligned}
\Gamma_{sl}^{D^0} = & 1.02 \Gamma_0 \left[\underbrace{1}_{c_3^{\text{LO}}} - \underbrace{0.16}_{\Delta c_3^{\text{NLO}}} - 0.13 \frac{\mu_\pi^2(D)}{0.48 \text{ GeV}^2} - 0.28 \frac{\mu_G^2(D)}{0.34 \text{ GeV}^2} + 0.2 \frac{\rho_D^3(D)}{0.082 \text{ GeV}^3} \right. \\
& \left. - 0.0007 r_1^{qq} - 0.0005 r_2^{qq} - 0.0118 r_1^{sq} - 0.0087 r_2^{sq} \right], \quad (4.4.12)
\end{aligned}$$

where the biggest correction comes from the chromomagnetic operator. Notice that due to D^0 having only WE contributions in dimension-six, the only terms arising here come from eye contractions.

For the D^+ meson we similarly write

$$\Gamma_{sl}^{D^+} = 1.02 \Gamma_0 \left[\underbrace{1}_{c_3^{\text{LO}}} - \underbrace{0.16}_{\Delta c_3^{\text{NLO}}} - 0.13 \frac{\mu_\pi^2(D)}{0.48 \text{ GeV}^2} - 0.28 \frac{\mu_G^2(D)}{0.34 \text{ GeV}^2} + 0.20 \frac{\rho_D^3(D)}{0.082 \text{ GeV}^3} \right]$$

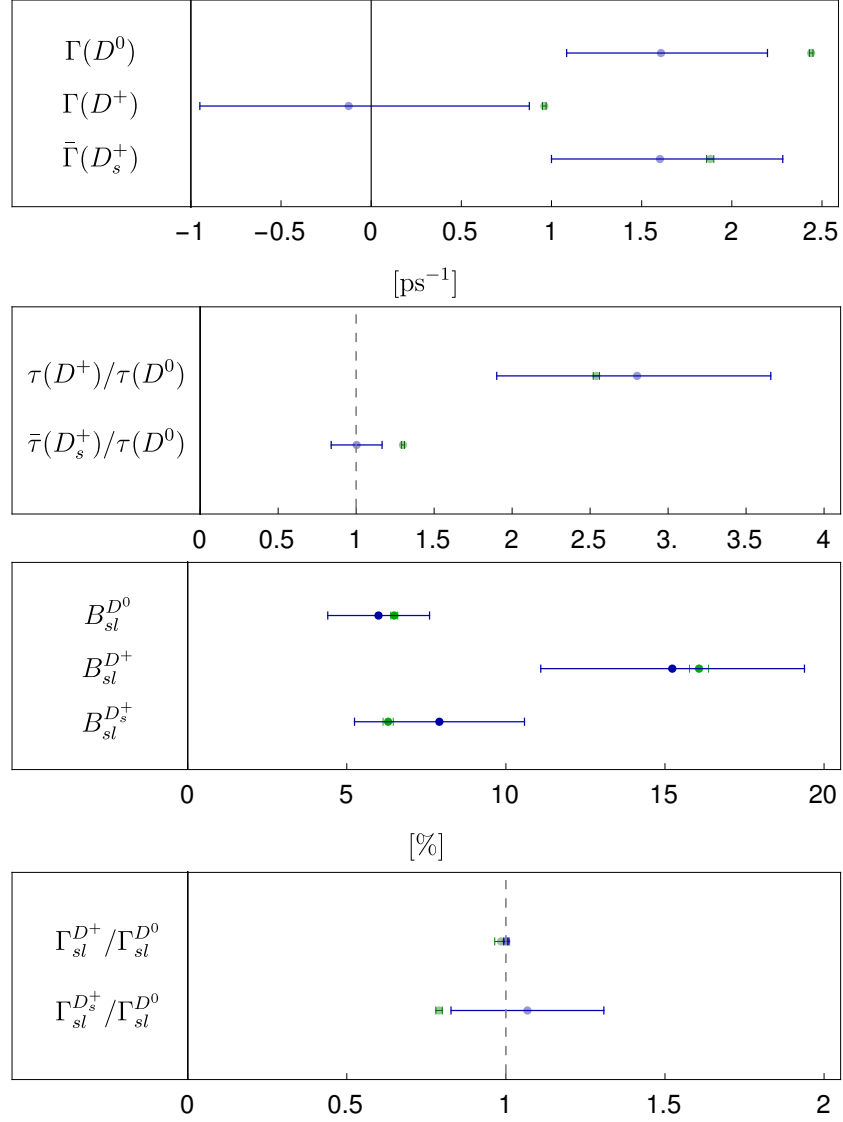


Figure 4.7: A comparison of the HQE prediction for the charm observables in the kinetic scheme (blue) with the corresponding experimental data (green).

$$\begin{aligned}
& - \underbrace{0.00}_{\text{dim-6, VIA}} - 0.005 \frac{\delta \tilde{B}_1^q}{0.02} + 0.005 \frac{\delta \tilde{B}_2^q}{0.02} + 0.004 \frac{\tilde{\epsilon}_1^q}{-0.04} - 0.004 \frac{\tilde{\epsilon}_2^q}{-0.04} \\
& - \left[- 0.0118 r_1^{sq} - 0.0088 r_2^{sq} \right] \tag{4.4.13}
\end{aligned}$$

which is the same series as D^0 up to two-quark contributions, supplemented by CKM suppressed WA terms that vanish at VIA. The deviations from VIA give only minor corrections.

Finally for the D_s^+ meson we obtain

$$\begin{aligned} \Gamma_{sl}^{D_s^+} = & 1.02 \Gamma_0 \left[\underbrace{1}_{c_3^{\text{LO}}} - \underbrace{0.16}_{\Delta c_3^{\text{NLO}}} - 0.15 \frac{\mu_\pi^2(D_s)}{0.57 \text{ GeV}^2} - 0.30 \frac{\mu_G^2(D_s)}{0.36 \text{ GeV}^2} + 0.29 \frac{\rho_D^3(D_s)}{0.119 \text{ GeV}^3} \right. \\ & - \underbrace{0.00}_{\text{dim-6, VIA}} - 0.15 \frac{\delta \tilde{B}_1^s}{0.02} + 0.15 \frac{\delta \tilde{B}_2^s}{0.02} + 0.10 \frac{\tilde{c}_1^s}{-0.04} + 0.09 \frac{\tilde{c}_2^s}{0.04} \\ & \left. - 0.0010 r_1^{qs} - 0.0007 r_2^{qs} \right], \end{aligned} \quad (4.4.14)$$

where we see higher two-quark contributions due to $SU(3)_F$ -breaking effects and we also have CKM dominant WA contributions to dimension-six and dimension-seven. Again due to helicity suppression they vanish in VIA but the terms deviating from it are much bigger than in D^+ .

Using the experimental value for $\tau(D^0)$ we can define the semi-leptonic ratios as

$$\frac{\Gamma_{sl}^{D^+}}{\Gamma_{sl}^{D^0}} = 1 + \left[\Gamma_{sl}^{D^+} - \Gamma_{sl}^{D^0} \right]^{\text{HQE}} \left[\frac{\tau(D^0)}{B_{sl}^{D^0}} \right]^{\text{exp}}, \quad (4.4.15)$$

$$\frac{\Gamma_{sl}^{D_s^+}}{\Gamma_{sl}^{D^0}} = 1 + \left[\Gamma_{sl}^{D_s^+} - \Gamma_{sl}^{D^0} \right]^{\text{HQE}} \left[\frac{\tau(D^0)}{B_{sl}^{D^0}} \right]^{\text{exp}}, \quad (4.4.16)$$

where $\left[\Gamma_{sl}^{D^0} \right]^{\text{HQE}}$, $\left[\Gamma_{sl}^{D^+} \right]^{\text{HQE}}$ and $\left[\Gamma_{sl}^{D_s^+} \right]^{\text{HQE}}$ are given in Eqs. (4.4.12), (4.4.13) and (4.4.14), respectively. The HQE predictions of these ratios can be found in the last two rows of of Table 4.10, Table 4.11 and Table 4.12 as well as in the last graph of Figure 4.7. For both ratios, HQE give values very close to 1, the first one agreeing with experimental data while the second one being higher than the experimental value. Expanding $\Gamma_{sl}^{D^+} / \Gamma_{sl}^{D^0}$

$$\frac{\Gamma_{sl}^{D^+}}{\Gamma_{sl}^{D^0}} = 1 - 0.005 \frac{\delta \tilde{B}_1^q}{0.02} + 0.005 \frac{\delta \tilde{B}_2^q}{0.02} + 0.004 \frac{\tilde{c}_1^q}{-0.04} - 0.003 \frac{\tilde{c}_2^q}{-0.04}, \quad (4.4.17)$$

we see that due to isospin symmetry all contributions at the two-quark level vanish and only deviations from VIA can move this ratio from 1. Finally, for $\Gamma_{sl}^{D_s^+} / \Gamma_{sl}^{D^0}$ we

obtain

$$\begin{aligned}
\frac{\Gamma_{sl}^{D_s^+}}{\Gamma_{sl}^{D^0}} = & 1 - 0.024 \frac{\mu_\pi^2(D_s) - \mu_\pi^2(D)}{0.09 \text{ GeV}^2} - 0.016 \frac{\mu_G^2(D_s) - \mu_G^2(D)}{0.02 \text{ GeV}^2} + 0.09 \frac{\rho_D^3(D_s) - \rho_D^3(D)}{0.037 \text{ GeV}^2} \\
& \underbrace{+ 0.00}_{\text{dim-6,7,VIA}} - 0.15 \frac{\delta \tilde{B}_1^s}{0.02} + 0.15 \frac{\delta \tilde{B}_2^s}{0.02} + 0.10 \frac{\tilde{\epsilon}_1^s}{-0.04} + 0.09 \frac{\tilde{\epsilon}_2^s}{0.04} \\
& + 0.0007 r_1^{qq} + 0.0005 r_2^{qq} + 0.0118 r_1^{sq} + 0.0087 r_2^{sq} \\
& - 0.0001 r_1^{qs} - 0.0007 r_2^{qs}, \tag{4.4.18}
\end{aligned}$$

which is clearly dominated by the $SU(3)_F$ -breaking effects as well as deviations from VIA. As we can see, the negative effect of the kinetic and chromomagnetic operators is more than compensated by the Darwin term, while even some of the eye contraction terms could have a visible effect, making their determination necessary.

Chapter 5

Conclusion

While experimental results become more and more precise, we need to improve our theoretical predictions in order to get a better understanding of the fundamental laws of physics. The Heavy Quark Expansion (HQE) has been proven a very effective tool in the b system, however its applicability in charm decays has been argued over. In this thesis we are testing this by considering the mixing of the D^0 meson and the inclusive decays of the D^0 , D^+ and D_s^+ mesons.

This study consists of two parts. We began with Chapter 1, introducing the Standard Model and flavour physics while also discussed briefly the role of the charm quark in it. We continued in Chapter 2, by introducing some of the fundamental tools needed in the study of heavy hadrons. More specifically, we presented the notion of an effective theory and discussed two examples that are necessary for the calculations following, the Weak Effective Theory (WET) and the Heavy Quark Effective Theory (HQET). These let us simplify our calculations significantly by decoupling heavy degrees of freedom from our theory. Moreover, we presented the HQE framework which we then used for the inclusive decays calculation.

In the second part of the thesis, we focused on the phenomenology of the charm system. More specifically, in Chapter 3 we presented the notation and framework

to understand the mixing of neutral mesons and focused on the decay width difference of the D^0 meson. This is a quantity well determined experimentally, but theoretical predictions within HQE failed to come close. This has been one of the main arguments against using HQE in the charm system. Finding that the reason behind this are pronounced Glashow-Iliopoulos-Maiani (GIM) cancellations appearing in the expression of $\Delta\Gamma_D$, we considered an alternative renormalisation scheme. We proposed two different versions for the alternative scale setting, finding in both of them that the GIM suppression is lifted. Moreover, considering different mass schemes, operator bases, and values of non-perturbative parameters we were able to reproduce the experimental value within large uncertainties. We also checked how the new renormalisation scale setting affects B_q -mixing, apart from the semi-leptonic CP asymmetries which exhibit weak GIM suppression, all other observables remain inside current theoretical uncertainties.

In Chapter 4, we studied the total and semi-leptonic decay rates of the D^0 , D^+ and D_s^+ mesons. We conducted a comprehensive study of the HQE for the decay rates of D mesons including the recently evaluated contribution of the Darwin operator and D_s^+ Bag parameters. We also presented a more consistent way of calculating the dimension-seven spectator effects both in QCD and in HQET. We explored various mass schemes and calculated the total and semi-leptonic decay rates and their ratios. All of them seem to agree or being close to agreeing with the experimental values, in some cases with large theoretical uncertainties. More specifically, we get good agreement with the ratio $\tau(D^+)/\tau(D^0)$, the decay rate of D_s^+ and all semi-leptonic results.

To conclude, our results, even coming with large uncertainties, do not support the claim that HQE breaks down in the charm system. Calculation of higher orders both in QCD and HQE, as well as theoretical determination of many non-perturbative parameters, are crucial to reducing these uncertainties and getting more precise results. For the study of D-mixing there is still no theoretical calculation of the

non-diagonal mass matrix element M_{12} . This could be done in the future, using dispersion relations, see e.g. [106, 181, 182]. Such a calculation would be highly desirable since it would enable us to calculate the CP -violating phase ϕ_{12} . Of course, to further test our solution to the D-mixing puzzle, higher orders in QCD and HQE would also be very important.

Appendix A

Numerical Input to Chapter 4

Parameter	Value	Source
$\alpha_s(M_Z)$	0.1179 ± 0.0010	PDG [1]
$ V_{us} $	$0.224834^{+0.000252}_{-0.000059}$	CKMfitter [96]
$ V_{cb} $	$0.04162^{+0.00026}_{-0.00080}$	CKMfitter [96]
$ V_{ub} / V_{cb} $	$0.088496^{+0.002244}_{-0.001885}$	CKMfitter [96]
δ	$(65.80^{+0.94}_{-1.29})^\circ$	CKMfitter [96]
$\bar{m}_c(\bar{m}_c)$ [GeV]	1.27 ± 0.02	PDG [1]
$m_c^{\text{kin}}(0.5\text{GeV})$ [GeV]	1.363	PDG [117]
m_s [MeV]	93^{+11}_{-5}	PDG [1]
M_{D^0} [GeV]	1.86493	PDG [1]
M_{D^+} [GeV]	1.86965	PDG [1]
$M_{D_s^+}$ [GeV]	1.968343	PDG [1]
f_D [GeV]	0.2120 ± 0.0007	Lattice QCD [97]
$f_{D_s^+}$ [GeV]	0.2499 ± 0.0005	Lattice QCD [97]

Table A.1: Numerical input used in our analysis.

HQET	\tilde{B}_1	\tilde{B}_2	$\tilde{\epsilon}_1$	$\tilde{\epsilon}_2$
$D^{+,0}$	$1.0026^{+0.0198}_{-0.0106}$	$0.9982^{+0.0052}_{-0.0066}$	$-0.0165^{+0.0209}_{-0.0346}$	$-0.0004^{+0.0200}_{-0.0326}$
D_s^+	$1.0022^{+0.0185}_{-0.0099}$	$0.9983^{+0.0052}_{-0.0067}$	$-0.0104^{+0.0202}_{-0.0330}$	$-0.0001^{+0.0199}_{-0.0324}$
HQET	$\tilde{\delta}_1$	$\tilde{\delta}_2$	$\tilde{\delta}_3$	$\tilde{\delta}_4$
$\langle D_q \tilde{O}^q D_q \rangle$	$0.0026^{+0.0142}_{-0.0092}$	$-0.0018^{+0.0047}_{-0.0072}$	$-0.0004^{+0.0015}_{-0.0024}$	$0.0003^{+0.0012}_{-0.0008}$
$\langle D_s \tilde{O}^q D_s \rangle$	$0.0025^{+0.0144}_{-0.0093}$	$-0.0018^{+0.0047}_{-0.0072}$	$-0.0004^{+0.0015}_{-0.0024}$	$0.0003^{+0.0012}_{-0.0008}$
$\langle D_q \tilde{O}^s D_q \rangle$	$0.0023^{+0.0140}_{-0.0091}$	$-0.0017^{+0.0046}_{-0.0070}$	$-0.0004^{+0.0015}_{-0.0023}$	$0.0003^{+0.0012}_{-0.0008}$

Table A.2: Numerical values of the HQET Bag parameters [4, 5] evaluated through a traditional HQET sum rule at $\mu_0 = 1.5$ GeV. The B_i^q and ϵ_i^q include the corresponding δ_i^{qq} and the column with δ_i^{ss} has been removed because it only exists in the sum with the valence parts, whereas δ_i^{qq} are present because we have $\delta_i^{ud/du}$.

Appendix B

LO Analytic Expressions for $\mathcal{C}_3^{(q_1\bar{q}_2)}$, $\mathcal{C}_G^{(q_1\bar{q}_2)}$ and $\mathcal{C}_{\rho D}^{(q_1\bar{q}_2)}$

Here we present the LO results for dimension-three, five and six in two-quark contributions as they have been used in [8] and Chapter 4 of this thesis. A detailed calculation can be found in [172].

The coefficients $\mathcal{C}_3^{q_1\bar{q}_2}$ for the decay $c \rightarrow q_1\bar{q}_2u$ that satisfy

$$\Gamma_3^{q_1\bar{q}_2} = \frac{G_F^2 m_c^5}{192\pi^3} |V_{cq_1}|^2 |V_{uq_2}|^2 \mathcal{N}_a \mathcal{C}_3^{q_1\bar{q}_2} ,$$

read for $\rho = m_s^2/m_c^2$, see e.g. [183]:

$$\mathcal{C}_3^{(d\bar{d})} = 1 , \tag{B.0.1}$$

$$\mathcal{C}_3^{(d\bar{s})} = 1 - 8\rho + 8\rho^3 - \rho^4 - 12\rho^2 \log(\rho) = \mathcal{C}_3^{(s\bar{d})} \tag{B.0.2}$$

$$\begin{aligned} \mathcal{C}_3^{(s\bar{s})} &= \sqrt{1-4\rho}(1-14\rho-2\rho^2-12\rho^3) \\ &+ 24\rho^2(1-\rho^2) \log\left(\frac{1+\sqrt{1-4\rho}}{1-\sqrt{1-4\rho}}\right) . \end{aligned} \tag{B.0.3}$$

The coefficients $\mathcal{C}_G^{q_1\bar{q}_2,ij}$ for the decay $c \rightarrow q_1\bar{q}_2u$ where $ij = 11, 12, 22$ read:

$$\mathcal{C}_{G,11}^{(d\bar{d})} = -\frac{3}{2} = \mathcal{C}_{G,22}^{(d\bar{d})} , \tag{B.0.4}$$

$$\mathcal{C}_{G,12}^{(d\bar{d})} = -\frac{19}{2}, \quad (\text{B.0.5})$$

$$\begin{aligned} \mathcal{C}_{G,11}^{(d\bar{s})} &= -\frac{1}{2} \left(3 - 8\rho + 24\rho^2 - 24\rho^3 + 5\rho^4 + 12\rho^2 \log(\rho) \right) \\ &= \mathcal{C}_{G,22}^{(d\bar{s})} = \mathcal{C}_{G,11}^{(s\bar{d})} = \mathcal{C}_{G,22}^{(s\bar{d})}, \end{aligned} \quad (\text{B.0.6})$$

$$\mathcal{C}_{G,12}^{(d\bar{s})} = -\frac{1}{2} \left(19 - 56\rho + 72\rho^2 - 40\rho^3 + 5\rho^4 + 12\rho^2 \log(\rho) \right) = \mathcal{C}_{G,12}^{(s\bar{d})} \quad (\text{B.0.7})$$

$$\begin{aligned} \mathcal{C}_{G,11}^{(s\bar{s})} &= -\frac{1}{2} \left(\sqrt{1-4\rho} (3 - 10\rho + 10\rho^2 + 60\rho^3) \right. \\ &\quad \left. - 24\rho^2 (1 - 5\rho^2) \log \left(\frac{1 + \sqrt{1-4\rho}}{1 - \sqrt{1-4\rho}} \right) \right) = \mathcal{C}_{G,22}^{(s\bar{s})}, \end{aligned} \quad (\text{B.0.8})$$

$$\begin{aligned} \mathcal{C}_{G,12}^{s\bar{s}} &= -\frac{1}{2} \left(\sqrt{1-4\rho} (19 - 2\rho + 58\rho^2 + 60\rho^3) \right. \\ &\quad \left. - 24\rho (2 + \rho - 4\rho^2 - 5\rho^3) \log \left(\frac{1 + \sqrt{1-4\rho}}{1 - \sqrt{1-4\rho}} \right) \right). \end{aligned} \quad (\text{B.0.9})$$

The coefficients $\mathcal{C}_{\rho_D, mn}^{(q_1\bar{q}_2)}(\rho, \mu_0)$ including full $\rho = m_s^2/m_c^2$ dependence are given by the expressions:

$$\mathcal{C}_{\rho_D,11}^{(d\bar{d})} = 6 + 8 \log \left(\frac{\mu_0^2}{m_c^2} \right), \quad (\text{B.0.10})$$

$$\mathcal{C}_{\rho_D,12}^{(d\bar{d})} = -\frac{34}{3}, \quad (\text{B.0.11})$$

$$\mathcal{C}_{\rho_D,22}^{(d\bar{d})} = 6 + 8 \log \left(\frac{\mu_0^2}{m_c^2} \right), \quad (\text{B.0.12})$$

$$\begin{aligned} \mathcal{C}_{\rho_D,11}^{(d\bar{s})} &= \frac{2}{3} (1 - \rho) \left[9 + 11\rho - 12\rho^2 \log(\rho) - 24 (1 - \rho^2) \log(1 - \rho) - 25\rho^2 + 5\rho^3 \right] \\ &\quad + 8 (1 - \rho) (1 - \rho^2) \log \left(\frac{\mu_0^2}{m_c^2} \right), \end{aligned} \quad (\text{B.0.13})$$

$$\begin{aligned} \mathcal{C}_{\rho_D,12}^{(d\bar{s})} &= -\frac{2}{3} \left[17 + 12\rho (5 + 2\rho - 2\rho^2) \log(\rho) + 48 (1 - \rho) (1 - \rho^2) \log(1 - \rho) \right. \\ &\quad \left. - 26\rho + 18\rho^2 - 38\rho^3 + 5\rho^4 + 24\rho (1 + \rho - \rho^2) \log \left(\frac{\mu_0^2}{m_c^2} \right) \right], \end{aligned} \quad (\text{B.0.14})$$

$$\begin{aligned} \mathcal{C}_{\rho_D,22}^{(d\bar{s})} &= \frac{2}{3} (1 - \rho) \left[9 + 11\rho - 12\rho^2 \log(\rho) - 24 (1 - \rho^2) \log(1 - \rho) - 25\rho^2 + 5\rho^3 \right] \\ &\quad + 8 (1 - \rho) (1 - \rho^2) \log \left(\frac{\mu_0^2}{m_c^2} \right), \end{aligned} \quad (\text{B.0.15})$$

$$\mathcal{C}_{\rho_D,11}^{(s\bar{d})} = \frac{2}{3} \left[9 - 16\rho - 12\rho^2 + 16\rho^3 - 5\rho^4 + 12 \log \left(\frac{\mu_0^2}{m_c^2} \right) \right], \quad (\text{B.0.16})$$

$$\begin{aligned} \mathcal{C}_{\rho_D,12}^{(s\bar{d})} &= -\frac{2}{3} \left[17 + 12\rho^2(3-\rho)\log(\rho) - 24(1-\rho)^3\log(1-\rho) \right. \\ &\quad \left. - 50\rho + 90\rho^2 - 54\rho^3 + 5\rho^4 - 12\rho(3-3\rho+\rho^2)\log\left(\frac{\mu_0^2}{m_c^2}\right) \right], \end{aligned} \quad (\text{B.0.17})$$

$$\begin{aligned} \mathcal{C}_{\rho_D,22}^{(s\bar{d})} &= \frac{2}{3}(1-\rho) \left[9 + 11\rho - 12\rho^2\log(\rho) - 24(1-\rho^2)\log(1-\rho) \right. \\ &\quad \left. - 25\rho^2 + 5\rho^3 + 12(1-\rho^2)\log\left(\frac{\mu_0^2}{m_c^2}\right) \right], \end{aligned} \quad (\text{B.0.18})$$

$$\begin{aligned} \mathcal{C}_{\rho_D,11}^{(s\bar{s})} &= \frac{2}{3} \left[\sqrt{1-4\rho}(17+8\rho-22\rho^2-60\rho^3) - 4(2-3\rho+\rho^3) + \right. \\ &\quad \left. - 12(1-\rho-2\rho^2+2\rho^3+10\rho^4)\log\left(\frac{1+\sqrt{1-4\rho}}{1-\sqrt{1-4\rho}}\right) \right. \\ &\quad \left. - 12(1-\rho)(1-\rho^2)\left(\log(\rho) - \log\left(\frac{\mu_0^2}{m_c^2}\right)\right) \right], \end{aligned} \quad (\text{B.0.19})$$

$$\begin{aligned} \mathcal{C}_{\rho_D,12}^{(s\bar{s})} &= \frac{2}{3} \left[\sqrt{1-4\rho}(-33+24\log(\rho) - 24\log(1-4\rho) + 46\rho - 106\rho^2 - 60\rho^3) \right. \\ &\quad \left. + 12(3-2\rho+4\rho^2-16\rho^3-10\rho^4)\log\left(\frac{1+\sqrt{1-4\rho}}{1-\sqrt{1-4\rho}}\right) \right. \\ &\quad \left. + 4(1-\rho)^2(4+3(1-\rho)\log(\rho) - \rho) \right. \\ &\quad \left. - 12(1-\sqrt{1-4\rho}-3\rho+3\rho^2-\rho^3)\log\left(\frac{\mu_0^2}{m_c^2}\right) \right], \end{aligned} \quad (\text{B.0.20})$$

$$\begin{aligned} \mathcal{C}_{\rho_D,22}^{(s\bar{s})} &= \frac{2}{3} \left[\sqrt{1-4\rho}(9+24\log(\rho) - 24\log(1-4\rho) + 22\rho - 34\rho^2 - 60\rho^3) \right. \\ &\quad \left. + 24(1-2\rho-\rho^2-2\rho^3-5\rho^4)\log\left(\frac{1+\sqrt{1-4\rho}}{1-\sqrt{1-4\rho}}\right) \right. \\ &\quad \left. + 12\sqrt{1-4\rho}\log\left(\frac{\mu_0^2}{m_c^2}\right) \right]. \end{aligned} \quad (\text{B.0.21})$$

Appendix C

Derivation of $\Delta C = 0$ matrix elements in HQET

Here we derive the expressions for the $\Delta C = 0$ matrix elements in HQET using VIA.

As a starting point we will use from e.g. [55]

$$\langle 0 | \bar{q} \Gamma h_v | \mathcal{M}(v) \rangle = \frac{i}{2} F(\mu_0) \text{Tr}(\Gamma \mathcal{M}(v)) , \quad (\text{C.0.1})$$

$$\langle 0 | \partial_\mu (\bar{q} \Gamma h_v) | \mathcal{M}(v) \rangle = \frac{i}{2} \bar{\Lambda} F(\mu_0) \text{Tr}(v_\mu \Gamma \mathcal{M}(v)) , \quad (\text{C.0.2})$$

$$\langle 0 | \bar{q} \Gamma (i D_\mu) h_v | \mathcal{M}(v) \rangle = \frac{i}{2} \text{Tr} \left\{ (F_1(\mu_0) v_\mu + F_2(\mu_0) \gamma_\mu) \Gamma \mathcal{M}(v) \right\} , \quad (\text{C.0.3})$$

where $\mathcal{M}(v)$ is the meson state with velocity v , Γ is a generic Dirac structure and $\bar{\Lambda} = M_D - m_c$. In order to calculate $F_1(\mu_0)$ and $F_2(\mu_0)$ we can contract Equation (C.0.3) with v^μ . Using $v^2 = 1$, $(iv \cdot D)h_v = 0$ and

$$\mathcal{M}(v) = -\frac{1 + \not{v}}{2} \gamma_5 \sqrt{M_D} , \quad (\text{C.0.4})$$

for the pseudo-scalar meson \mathcal{M} we get $F_1(\mu_0) = F_2(\mu_0)$. Next by taking the matrix elements on both sides of Equation (C.0.3), contracting with γ^μ , and using

$$i \partial_\mu (\bar{q} \Gamma h_v) = \bar{q} \Gamma i D_\mu h_v + \bar{q} (i \overleftarrow{D}_\mu) \Gamma h_v , \quad (\text{C.0.5})$$

as well as $\bar{q}(-i\overleftarrow{D}) = m_q \bar{q}$ we get

$$F_1(\mu_0) = F_2(\mu_0) = -\frac{1}{3}F_{\mu_0}(\bar{\Lambda} - m_q)\text{Tr}(\Gamma\mathcal{M}(v)) . \quad (\text{C.0.6})$$

Thus

$$\langle 0|\bar{q}\Gamma(iD_\mu)h_v|\mathcal{M}(v)\rangle = -\frac{i}{6}F(\mu_0)(\bar{\Lambda} - m_q)\text{Tr}\left\{\left(v_\mu + \gamma_\mu\right)\Gamma\mathcal{M}(v)\right\} . \quad (\text{C.0.7})$$

If we evaluate the matrix element of Equation (C.0.5) we can write

$$\langle 0|\bar{q}(-i\overleftarrow{D}_\mu)\Gamma h_v|\mathcal{M}(v)\rangle = -\frac{i}{6}F(\mu_0)\left\{\left(4\bar{\Lambda} - m_q\right)v_\mu\text{Tr}(\Gamma\mathcal{M}(v)) + \left(\bar{\Lambda} - m_q\right)\text{Tr}\left(\gamma_\mu\Gamma\mathcal{M}(v)\right)\right\} . \quad (\text{C.0.8})$$

Now we can calculate the building blocks of the local HQET operators matrix elements. Using the results in Equations (C.0.1), (C.0.7) and (C.0.8) we can find

$$\langle 0|\bar{q}\gamma^\mu(1 - \gamma_5)h_v|D_q\rangle = -i\sqrt{M_D}F(\mu_0)v^\mu , \quad (\text{C.0.9})$$

$$\langle 0|\bar{q}(1 \pm \gamma_5)h_v|D_q\rangle = \mp i\sqrt{M_D}F(\mu_0) , \quad (\text{C.0.10})$$

$$\langle 0|\bar{q}(-i\overleftarrow{D}^\nu)\gamma^\mu(1 - \gamma_5)h_v|D_q\rangle = i\bar{\Lambda}\sqrt{M_D}F(\mu_0)v^\mu v^\nu , \quad (\text{C.0.11})$$

$$\langle 0|\bar{q}(-i\overleftarrow{D}^\mu)(1 - \gamma_5)h_v|D_q\rangle = i\bar{\Lambda}\sqrt{M_D}F(\mu_0)v^\mu , \quad (\text{C.0.12})$$

$$\langle 0|\bar{q}\gamma^\mu(1 - \gamma_5)(i\overleftarrow{D})h_v|D_q\rangle = i(\bar{\Lambda} - m_q)\sqrt{M_D}F(\mu_0)v^\mu , \quad (\text{C.0.13})$$

$$\langle 0|\bar{q}(1 + \gamma_5)(i\overleftarrow{D})h_v|D_q\rangle = -i(\bar{\Lambda} - m_q)\sqrt{M_D}F(\mu_0) . \quad (\text{C.0.14})$$

The matrix elements of the $\Delta C = 0$ operators can be calculated in VIA based on Equation (2.2.31) as the product of two matrix elements of the above form. Starting with dimension-six we have

$$\begin{aligned} \langle D_q|\tilde{O}_1^q|D_q\rangle &= \langle D_q|\bar{h}_v\gamma_\mu(1 - \gamma_5)q|0\rangle\langle 0|\bar{q}\gamma^\mu(1 - \gamma_5)h_v|D_q\rangle \\ &= \left(\langle 0|\bar{q}\gamma_\mu(1 - \gamma_5)h_v|D_q\rangle\right)^\dagger \langle 0|\bar{q}\gamma^\mu(1 - \gamma_5)h_v|D_q\rangle \\ &= \left(-i\sqrt{M_D}F(\mu_0)v^\mu\right)^\dagger \left(-i\sqrt{M_D}F(\mu_0)v^\mu\right) \\ &= M_DF^2(\mu_0) , \end{aligned} \quad (\text{C.0.15})$$

Similarly for \tilde{O}_2

$$\begin{aligned}
\langle D_q | \tilde{O}_2^q | D_q \rangle &= \langle D_q | \bar{h}_v (1 - \gamma_5) q | 0 \rangle \langle 0 | \bar{q} (1 + \gamma_5) h_v D_q \rangle \\
&= \left(\langle 0 | \bar{q} (1 + \gamma_5) h_v | D_q \rangle \right)^\dagger \langle 0 | \bar{q} (1 + \gamma_5) h_v D_q \rangle \\
&= \left(-i \sqrt{M_D} F(\mu_0) \right)^\dagger \left(-i \sqrt{M_D} F(\mu_0) \right) \\
&= M_D F^2(\mu_0) .
\end{aligned} \tag{C.0.16}$$

Moving to dimension-seven operators, we use

$$\langle D_q | \bar{h}_v (1 - \gamma_5) q | 0 \rangle = \left(\langle 0 | \bar{q} (1 + \gamma_5) h_v | D_q \rangle \right)^\dagger , \tag{C.0.17}$$

$$\langle D_q | \bar{h}_v \gamma^\mu (1 - \gamma_5) (i v \cdot D) q | 0 \rangle = v_\nu \left(\langle 0 | \bar{q} (-i \overleftarrow{D}^\nu) \gamma^\mu (1 - \gamma_5) h_v | D_q \rangle \right)^\dagger \tag{C.0.18}$$

$$\langle D_q | \bar{h}_v (1 - \gamma_5) (i v \cdot D) q | 0 \rangle = v_\nu \left(\langle 0 | \bar{q} (-i \overleftarrow{D}^\nu) (1 + \gamma_5) h_v | D_q \rangle \right)^\dagger , \tag{C.0.19}$$

and now we have all pieces to calculate the matrix elements of \tilde{P}_i and \tilde{R}_i operators getting the following results

$$\langle D_q | \tilde{P}_1 | D_q \rangle = -m_q M_D F^2(\mu_0) , \tag{C.0.20}$$

$$\langle D_q | \tilde{P}_2 | D_q \rangle = -M_D F^2(\mu_0) \bar{\Lambda} , \tag{C.0.21}$$

$$\langle D_q | \tilde{P}_3 | D_q \rangle = -M_D F^2(\mu_0) \bar{\Lambda} , \tag{C.0.22}$$

$$\langle D_q | \tilde{R}_1 | D_q \rangle = -M_D F^2(\mu_0) (\bar{\Lambda} - m_q) , \tag{C.0.23}$$

$$\langle D_q | \tilde{P}_2 | D_q \rangle = M_D F^2(\mu_0) (\bar{\Lambda} - m_q) . \tag{C.0.24}$$

For the non-local operators $\tilde{M}_{(1,2),(\pi,G)}$ we use [55, 173] and define

$$\langle 0 | i \int d^4 x T [(\bar{q} \Gamma h_v)(0), \mathcal{O}_1(x)] | \mathcal{M}(v) \rangle = F(\mu_0) G_1(\mu_0) \text{Tr}[\Gamma \mathcal{M}(v)] , \tag{C.0.25}$$

$$\langle 0 | i \int d^4 x T [(\bar{q} \Gamma h_v)(0), \mathcal{O}_2(x)] | \mathcal{M}(v) \rangle = 6 F(\mu_0) G_2(\mu_0) \text{Tr}[\Gamma \mathcal{M}(v)] \tag{C.0.26}$$

Next we can write

$$\langle D_q | i \int d^4 x T [(\bar{q} \Gamma h_v)(0), \mathcal{O}_1(x)] | D_q \rangle$$

$$= \langle D_q | \bar{q} \Gamma h_v | 0 \rangle \langle 0 | i \int d^4x T [(\bar{q} \Gamma h_v)(0), \mathcal{O}_1(x)] | D_q \rangle \quad (\text{C.0.27})$$

and similarly for the \mathcal{O}_{cmaq} operator. Evaluating these for the specific Dirac structures appearing we find

$$\langle D_q | \tilde{M}_{1,\pi}^q | D_q \rangle = 2 M_D F^2(\mu_0) G_1(\mu_0), \quad (\text{C.0.28})$$

$$\langle D_q | \tilde{M}_{2,\pi}^q | D_q \rangle = 2 M_D F^2(\mu_0) G_1(\mu_0), \quad (\text{C.0.29})$$

$$\langle D_q | \tilde{M}_{1,G}^q | D_q \rangle = 12 M_D F^2(\mu_0) G_2(\mu_0), \quad (\text{C.0.30})$$

$$\langle D_q | \tilde{M}_{2,G}^q | D_q \rangle = 12 M_D F^2(\mu_0) G_2(\mu_0). \quad (\text{C.0.31})$$

Since we are doing this calculation in VIA all matrix elements of colour rearranged operators vanish. As a correction factor from VIA we insert in each result a bag parameter which measures the deviation from VIA. For the colour rearranged operators we are using the same parametrisation as their colour singlet counterparts but their bag parameters at VIA vanish.

Since at dimension-seven we are limited to LO-QCD we can substitute the HQET decay constant $F(\mu_0)$ with the full QCD, using $F(\mu_0) = f_D \sqrt{M_D}$.

Appendix D

Calculation of Spectator Effects for Γ_{12} and $\Gamma(D)$

Here we present the spectator effect calculation for both Γ_{12} and the total decay rate of D mesons. We start from the effective Hamiltonian for a general $c \rightarrow q_1 \bar{q}_2 u$.

$$\mathcal{H}_{eff} = \frac{G_F}{\sqrt{2}} \{C_1 Q_1 + C_2 Q_2\} + h.c. \quad (\text{D.0.1})$$

where $Q_1 = (c^i q_1^i)_{V-A} (q_2^j u^j)_{V-A}$, $Q_2 = (c^i q_1^j)_{V-A} (q_2^j u^i)_{V-A}$ are the $\Delta C = 1$ operators and $q_1, q_2 = s, d$. By considering the time-ordered product $T [\mathcal{H}_{eff}(x) \mathcal{H}_{eff}(0)]$ and contracting two pairs of light quarks¹³ and using the Wick theorem we get four different contributions

1. Decay width difference for the D^0 meson

$$T [\mathcal{H}_{eff}(x) \mathcal{H}_{eff}(0)] \Big|_{mix} =$$

$$: \bar{c}(x) \Gamma_\mu q_1(x) \bar{q}_2(x) \Gamma^\mu u(x) \bar{c}(0) \Gamma_\nu q_1(0) \bar{q}_2(0) \Gamma^\nu u(0) : . \quad (\text{D.0.2})$$

2. Dominant contribution to $\tilde{\Gamma}_6$ for $\Gamma(D^0)$ from Weak Exchange diagram (WE)

$$T [\mathcal{H}_{eff}(x) \mathcal{H}_{eff}(0)] \Big|_{WE} =$$

¹³Contracting all three pairs of light quarks corresponds to the Γ_3 contribution for the free charm quark decay.

$$: \bar{c}(x) \Gamma_\mu \overbrace{q_1(x) \bar{q}_2(x) \Gamma^\mu u(x) \bar{q}_1(0) \Gamma_\nu c(0) \bar{u}(0) \Gamma^\nu q_2(0)} : . \quad (\text{D.0.3})$$

3. Dominant contribution to $\tilde{\Gamma}_6$ for $\Gamma(D^+)$ from Pauli Interference diagram (PI)

$$T \left[\mathcal{H}_{eff}(x) \mathcal{H}_{eff}(0) \right] \Big|_{PI} =$$

$$: \bar{c}(x) \Gamma_\mu \overbrace{q_1(x) \bar{q}_2(x) \Gamma^\mu u(x) \bar{q}_1(0) \Gamma_\nu c(0) \bar{u}(0) \Gamma^\nu q_2(0)} : . \quad (\text{D.0.4})$$

4. Dominant contribution to $\tilde{\Gamma}_6$ for $\Gamma(D_s^+)$ from Weak Annihilation diagram (WA)

$$T \left[\mathcal{H}_{eff}(x) \mathcal{H}_{eff}(0) \right] \Big|_{WA} =$$

$$: \bar{c}(x) \Gamma_\mu \overbrace{q_1(x) \bar{q}_2(x) \Gamma^\mu u(x) q_1(0) \Gamma_\nu c(0) \bar{u}(0) \Gamma^\nu q_2(0)} : . \quad (\text{D.0.5})$$

In the above expressions we have used the notation $\Gamma_\mu = \gamma_\mu(1 - \gamma_5)$. For most of the calculation of these diagrams we will work with general colour structures of $\Delta C = 1$ operators and only in the end we will evaluate the specific operator insertions. We will also ignore the factor $\frac{G_F^2}{2} V_{CKM}$ where $V_{CKM} = (V_{cq_1}^* V_{uq_2})^2$ for mixing and $V_{CKM} = |V_{cq_1}^* V_{uq_2}|^2$ for brevity and we will add it in the end. The quantities $\Gamma_{12}^{q_1 q_2}$ and $\Gamma_A^{qq'}$ where $A = \text{WE, PI, WA}$ and qq' is the internal quark pair read

$$\Gamma_{12}^{q_1 q_2} = \frac{1}{2M_D} \langle \bar{D} | \mathcal{T}_{mix} | D \rangle , \quad (\text{D.0.6})$$

$$\Gamma_A^{qq'} = \frac{1}{2M_D} \langle D | \mathcal{T}_A | D \rangle , \quad (\text{D.0.7})$$

where

$$\mathcal{T}_{mix} = \text{Im} \left\{ i \int d^4x \text{T} \left[\mathcal{H}_{eff}(x) \mathcal{H}_{eff}(0) \right] \Big|_{mix} \right\} = \sum_{i,j} C_i C_j \mathcal{T}_{mix}^{ij} , \quad (\text{D.0.8})$$

$$\mathcal{T}_A = \text{Im} \left\{ i \int d^4x \text{T} \left[\mathcal{H}_{eff}(x) \mathcal{H}_{eff}(0) \right] \Big|_A \right\} = \sum_{i,j} C_i C_j \mathcal{T}_A^{ij} . \quad (\text{D.0.9})$$

Starting with the D-mixing expression we use the Wick theorem to write for the time ordered product:

$$T \left[\mathcal{H}_{eff}(x) \mathcal{H}_{eff}(0) \right] \Big|_{mix} =$$

$$\begin{aligned}
& : \bar{c}^i(x) \Gamma_\mu \overbrace{q_1^j(x) \bar{q}_2^k(x)} \Gamma^\mu u^l(x) \overbrace{\bar{c}^m(0) \Gamma_\nu q_1^n(0) \bar{q}_2^p(x)} \Gamma^\nu u^q(0) : \\
& = \bar{c}^i(x) \gamma_\mu (1 - \gamma_5) \overbrace{q_1^j(x) \bar{q}_1^p(0)} \gamma^\nu (1 - \gamma_5) u^q(0) \\
& \quad \bar{c}^m(0) \gamma_\nu (1 - \gamma_5) \overbrace{q_2^n(x) \bar{q}_2^k(x)} \gamma^\mu (1 - \gamma_5) u^l(x) \\
& = \bar{c}^i \gamma_\mu (1 - \gamma_5) \int \frac{d^4 k}{(2\pi)^4} \frac{i(\not{k} + m_1)}{k^2 - m_1^2 + i\epsilon} \gamma^\nu (1 - \gamma_5) u^k \\
& \quad \bar{c}^m \gamma_\nu (1 - \gamma_5) \int \frac{d^4 l}{(2\pi)^4} \frac{i(\not{l} + m_2)}{l^2 - m_2^2 + i\epsilon} \gamma^\mu (1 - \gamma_5) u^l \\
& \quad e^{i(p_c + p_u - k + l)} \delta^{jp} \delta^{nk} , \tag{D.0.10}
\end{aligned}$$

where the latin indices indicate the colour structure and the greek indices represent the components of four-vectors. We have also used

$$\psi(x) = \psi e^{ipx} \text{ (outgoing (anti)fermion with momentum } p), \tag{D.0.11}$$

$$\psi(x) = \psi e^{-ipx} \text{ (incoming (anti)fermion with momentum } p) \tag{D.0.12}$$

$$\overbrace{\psi^i(x) \bar{\psi}^j(y)} = \int \frac{d^4 l}{(2\pi)^4} \frac{i(\not{l} + m)}{l^2 - m^2 + i\epsilon} e^{-ip(x-y)} \delta^{ij} . \tag{D.0.13}$$

Next, using

$$\int d^4 x e^{i(p-l)x} = (2\pi)^4 \delta(p-l) , \tag{D.0.14}$$

we can perform the integration over x

$$\begin{aligned}
& i \int d^4 x \text{T} [\mathcal{H}_{eff}(x) \mathcal{H}_{eff}(0)] = \\
& i \int \frac{d^4 l}{(2\pi)^4} \bar{c}^i \gamma_\mu (1 - \gamma_5) \frac{i(\not{l} + \not{p} + m_1)}{(l+p)^2 - m_1^2 + i\epsilon} \gamma^\nu (1 - \gamma_5) u^q \\
& \quad \bar{c}^m \gamma_\nu (1 - \gamma_5) \frac{i(\not{l} + m_2)}{l^2 - m_2^2 + i\epsilon} \gamma^\mu (1 - \gamma_5) u^l \delta^{jp} \delta^{nk} \\
& = -4i \int \frac{d^4 l}{(2\pi)^4} \frac{l^\rho l^\sigma + l^\rho p^\sigma}{((l+p)^2 - m_1^2 + i\epsilon)(l^2 - m_2^2 + i\epsilon)} \\
& \quad (\bar{c}^i \gamma_\mu (1 - \gamma_5) \gamma_\rho \gamma^\nu u^q) (\bar{c}^m \gamma_\nu (1 - \gamma_5) \gamma_\sigma \gamma^\mu u^l) \delta^{jp} \delta^{nk} , \tag{D.0.15}
\end{aligned}$$

where all the terms involving m_1, m_2 vanish (easy to check if you rearrange the $(1 - \gamma_5)$ terms) and $p = p_c + p_u$. Taking the imaginary part of Equation (D.0.15) we

get

$$\begin{aligned} \mathcal{T}_{mix}^{ij} &= -4\text{Im} [ig^{\rho\sigma} B_{00} + ip^\rho p^\sigma (B_{11} + B_0)] \delta^{jp} \delta^{nk} \\ &\quad (\bar{c}^i \gamma_\mu (1 - \gamma_5) \gamma_\rho \gamma^\nu u^q) (\bar{c}^n \gamma_\nu (1 - \gamma_5) \gamma_\sigma \gamma^\mu u^l), \end{aligned} \quad (\text{D.0.16})$$

where we have used the notation for the one-loop integrals

$$\int \frac{d^D k}{(2\pi^D)} \frac{1}{((l+p)^2 - m_1^2 + i\epsilon)(l^2 - m_2^2 + i\epsilon)} = B, \quad (\text{D.0.17})$$

$$\int \frac{d^D k}{(2\pi^D)} \frac{k^\mu}{((l+p)^2 - m_1^2 + i\epsilon)(l^2 - m_2^2 + i\epsilon)} = p^\mu B_0, \quad (\text{D.0.18})$$

$$\int \frac{d^D k}{(2\pi^D)} \frac{k^\mu k^\nu}{((l+p)^2 - m_1^2 + i\epsilon)(l^2 - m_2^2 + i\epsilon)} = g^{\mu\nu} B_{00} + p^\mu p^\nu B_{11}. \quad (\text{D.0.19})$$

We can determine the parameters B_0 , B_{00} , and B_{11} in terms of B by contracting Equations (D.0.18) and (D.0.19) with p_μ , $g_{\mu\nu}$ and $p_\mu p_\nu$, a procedure called Passarino-Veltman reduction [184]. We can then write for $D = 4$ ¹⁴

$$B_0 = -\frac{p^2 - m_1^2 + m_2^2}{2p^2} B, \quad (\text{D.0.20})$$

$$B_{00} = -\frac{1}{12p^2} \lambda^2(p^2, m_1^2, m_2^2) B, \quad (\text{D.0.21})$$

$$B_{11} = \frac{1}{p^2} (m_2^2 B - 4B_{00}), \quad (\text{D.0.22})$$

where $\lambda(a, b, c) = \sqrt{a^2 + b^2 + c^2 - 2(ab + bc + ca)}$. Using the equations above as well as

$$\gamma_\nu \gamma_\rho \gamma_\mu (1 - \gamma_5) \otimes \gamma^\mu \gamma^\rho \gamma^\nu (1 - \gamma_5) = 4\gamma_\mu (1 - \gamma_5) \otimes \gamma^\mu (1 - \gamma_5), \quad (\text{D.0.23})$$

$$\gamma_\nu \not{p} \gamma_\mu (1 - \gamma_5) \otimes \gamma^\mu \not{p} \gamma^\nu (1 - \gamma_5) = 4\not{p} (1 - \gamma_5) \otimes \not{p} (1 - \gamma_5), \quad (\text{D.0.24})$$

we can rewrite Equation (D.0.16) including the factor $\frac{G_F^2}{2} (V_{cq_1}^* V_{uq_2})^2$

$$\begin{aligned} \mathcal{T}_{mix}^{ij} &= -4 \frac{G_F^2}{2} (V_{cq_1}^* V_{uq_2})^2 \left[4\text{Im}(iB_{00}) Q_{V-A}^{mix} \right. \\ &\quad \left. + (2p^2 Q_{V-A}^{mix} - 4Q_{S-P}^{pp,mix}) \text{Im}(i(B_{11} + B_0)) \right] \delta^{jp} \delta^{nk} \end{aligned}$$

¹⁴Here we ignore the terms that are real since we are only interested in the imaginary part of the integrals.

$$\begin{aligned}
&= -16 \frac{G_F^2}{2} (V_{cq_1}^* V_{uq_2})^2 \left(Q_{V-A}^{mix} \operatorname{Im} \left(i \left(B_{00} + \frac{p^2}{2} (B_{11} + B_0) \right) \right) \right. \\
&\quad \left. - Q_{S-P}^{pp,mix} \operatorname{Im} (i (B_{11} + B_0)) \right) \delta^{jp} \delta^{nk} \\
&= -2 \frac{G_F^2}{3} (V_{cq_1}^* V_{uq_2})^2 \left[\frac{(m_1^2 - m_2^2)^2 - p^2(2p^2 - m_1^2 - m_2^2)}{p^2} Q_{V-A}^{mix} \right. \\
&\quad \left. - \frac{2(2(m_1^2 - m_2^2)^2 - p^2(p^2 + m_1^2 + m_2^2))}{p^4} Q_{S-P}^{pp,mix} \right] \operatorname{Im}(iB) \delta^{jp} \delta^{nk},
\end{aligned} \tag{D.0.25}$$

where we define

$$Q_{V-A}^{mix} = (\bar{c}^i \gamma_\mu (1 - \gamma_5) u^l) (\bar{c}^m \gamma^\mu (1 - \gamma_5) u^q), \tag{D.0.26}$$

$$Q_{S-P}^{pp,mix} = (\bar{c}^i \not{p} (1 - \gamma_5) u^l) (\bar{c}^m \not{p} (1 - \gamma_5) u^q). \tag{D.0.27}$$

To create these operators we have additionally used the Fierz transformation

$$(\bar{q}_1 q_2)_{V-A} (\bar{q}_3 q_4)_{V-A} = (\bar{q}_1 q_4)_{V-A} (\bar{q}_3 q_2)_{V-A}. \tag{D.0.28}$$

The operator $Q_{S-P}^{pp,mix}$ can be expanded (ignoring the colour indices) as

$$\begin{aligned}
Q_{S-P}^{pp,mix} &= (\bar{c} \not{p}_c (1 - \gamma_5) u) (\bar{c} \not{p}_c (1 - \gamma_5) u) + (\bar{c} (1 + \gamma_5) \not{p}_u u) (\bar{c} \not{p}_c (1 - \gamma_5) u) \\
&+ (\bar{c} \not{p}_c (1 - \gamma_5) u) (\bar{c} (1 + \gamma_5) \not{p}_c u) + (\bar{c} (1 + \gamma_5) \not{p}_u u) (\bar{c} (1 + \gamma_5) \not{p}_u u) \\
&= -m_c^2 (\bar{c} (1 - \gamma_5) u) (\bar{c} (1 + \gamma_5) u) + m_c m_u (\bar{c} (1 + \gamma_5) u) (\bar{c} (1 - \gamma_5) u) \\
&+ m_c m_u (\bar{c} (1 - \gamma_5) u) (\bar{c} (1 + \gamma_5) u) - m_u^2 (\bar{c} (1 + \gamma_5) u) (\bar{c} (1 + \gamma_5) u) \\
&= -m_c^2 Q_{S-P}^{mix},
\end{aligned} \tag{D.0.29}$$

where we have used the equation of motion for fermions and we have neglected the up-quark mass. Using the result from [185] for $\operatorname{Im}(iB)$ we find

$$\begin{aligned}
\mathcal{T}_{mix}^{ij} &= \frac{G_F^2}{24\pi} (V_{cq_1}^* V_{uq_2})^2 m_c^2 \frac{\lambda(1 + \tilde{x}, z_1, z_2)}{(1 + \tilde{x})^2} \times \\
&\quad \left[\left\{ (z_1 - z_2)^2 - (1 + \tilde{x})(2(1 + \tilde{x}) - z_1 - z_2) \right\} Q_{V-A}^{mix} \right. \\
&\quad \left. + 2 \left\{ \frac{2(z_1 - z_2)^2}{1 + \tilde{x}} - (1 + \tilde{x} + z_1 + z_2) \right\} Q_{S-P}^{mix} \right] \delta^{jp} \delta^{nk},
\end{aligned} \tag{D.0.30}$$

where $Q_{S-P}^{mix} = (\bar{c}^i(1-\gamma_5)u^l)(\bar{c}^m(1-\gamma_5)u^q)$ and we have used the notation $z_i = m_i^2/m_c^2$ and $1 + \tilde{x} = p^2/m_c^2 = 1 + 2\frac{p_c p_u}{m_c^2} + \mathcal{O}(p_u^2)$

Each quark propagator will give us a product of delta tensors indicating the flow of colour to the external quarks. We have three different possibilities for operator insertions: $Q_1 \otimes Q_1$, $Q_1 \otimes Q_2$ and $Q_2 \otimes Q_2$ ($Q_1 \otimes Q_2$ and $Q_2 \otimes Q_1$ give identical results).

- For $Q_1 \otimes Q_1$ we have in total a factor $\delta^{jp}\delta^{nk}\delta^{ij}\delta^{kl}\delta^{pq}\delta^{mn} = \delta^{iq}\delta^{km}$ creating the operators

$$\tilde{Q} = (\bar{c}^i\gamma_\mu(1-\gamma_5)u^k)(\bar{c}^k\gamma^\mu(1-\gamma_5)u^i), \quad (\text{D.0.31})$$

$$\tilde{Q}_S = (\bar{c}^i(1-\gamma_5)u^k)(\bar{c}^k(1-\gamma_5)u^i). \quad (\text{D.0.32})$$

- For $Q_2 \otimes Q_2$ we get $\delta^{jp}\delta^{nk}\delta^{ij}\delta^{kl}\delta^{mq}\delta^{ln} = \delta^{kk}\delta^{il}\delta^{qm} = N_C\delta^{il}\delta^{qm}$ which creates the operators

$$Q = (\bar{c}^i\gamma_\mu(1-\gamma_5)u^i)(\bar{c}^m\gamma^\mu(1-\gamma_5)u^m), \quad (\text{D.0.33})$$

$$Q_S = (\bar{c}^i(1-\gamma_5)u^i)(\bar{c}^m(1-\gamma_5)u^m). \quad (\text{D.0.34})$$

- For $Q_1 \otimes Q_2$ we get $\delta^{jp}\delta^{nk}\delta^{ij}\delta^{kl}\delta^{mq}\delta^{pn} = \delta^{il}\delta^{qm}$ giving the Q, Q_S operators again. We also get a factor 2 from symmetry by including the identical contribution from $Q_2 \otimes Q_1$.

We can write now the full result for $\Gamma_{12}^{q_1 q_2}$ (using $Q = \tilde{Q}$ through Fierz transformation)¹⁵

$$\begin{aligned} \Gamma_{12}^{q_1 q_2} &= \frac{1}{2M_D} \frac{G_F^2}{24\pi} (V_{cq_1}^* V_{uq_2})^2 m_c^2 \frac{\lambda(1 + \tilde{x}, z_1, z_2)}{(1 + \tilde{x})^2} \times \\ &\left[w_1(\tilde{x}, z_1, z_2) \left(3C_2^2 + 2C_1C_2 + C_1^2 \right) Q \right. \\ &\left. + 2w_2(\tilde{x}, z_1, z_2) \left(\left(3C_2^2 + 2C_1C_2 \right) Q_S + C_1^2 \tilde{Q}_S \right) \right], \quad (\text{D.0.35}) \end{aligned}$$

¹⁵Here we define $\Gamma_{12}^{q_1 q_2}$ slightly different than Equation (3.4.24), i.e. $\Gamma_{12} = \sum_{q_1 q_2} \Gamma_{12}^{q_1 q_2}$.

where

$$w_1(\tilde{x}, z_1, z_2) = (z_1 - z_2)^2 - (1 + \tilde{x})(2(1 + \tilde{x}) - z_1 - z_2) , \quad (\text{D.0.36})$$

$$w_2(\tilde{x}, z_1, z_2) = \frac{2(z_1 - z_2)^2}{1 + \tilde{x}} - (1 + \tilde{x} + z_1 + z_2) . \quad (\text{D.0.37})$$

The leading order contribution of the above expression is obtained by setting $\tilde{x} = 0$. To get the dimension-seven contribution from Equation (D.0.35) we expand the coefficients to first order in \tilde{x} and discard higher order terms. Then, we identify the subleading operators

$$\begin{aligned} \tilde{x} Q &= 2 \frac{p_c p_u}{m_c^2} (\bar{c}^i \gamma_\mu (1 - \gamma_5) u^i) (\bar{c}^m \gamma^\mu (1 - \gamma_5) u^m) \\ &= \frac{1}{m_c^2} (\bar{c}^i \overleftarrow{D}^\rho \gamma_\mu (1 - \gamma_5) D_\rho u^i) (\bar{c}^m \gamma^\mu (1 - \gamma_5) u^m) \\ &= R_2 , \end{aligned} \quad (\text{D.0.38})$$

$$\begin{aligned} \tilde{x} Q_S &= 2 \frac{p_c p_u}{m_c^2} (\bar{c}^i (1 - \gamma_5) u^i) (\bar{c}^m (1 - \gamma_5) u^m) \\ &= \frac{1}{m_c^2} (\bar{c}^i \overleftarrow{D}^\rho (1 - \gamma_5) D_\rho u^i) (\bar{c}^m (1 - \gamma_5) u^m) \\ &= R_3 , \end{aligned} \quad (\text{D.0.39})$$

where we have used the equations of motion to express the momentum operators as covariant derivatives acting on the fields. In an identical way we derive $\tilde{R}_{2,3}$ from \tilde{Q}, \tilde{Q}_S respectively. As mentioned in Section 3.4 the operators Q, Q_S and \tilde{Q}_S are not independent and a linear combination of them (see Equation (3.4.15)) yields the subleading operator R_0 . This relation is used to eliminate either Q_S or \tilde{Q}_S from the dimension-six result.

Moving to the lifetime calculations, we will start with the Weak Exchange diagram. The calculation of WE, PI and WA topologies has an extra factor of 2 due to the symmetric contribution we get by swapping 0 and x in the time-ordered product. This symmetry is not present in mixing as the initial and final states are different.

Similarly to mixing we can write

$$\begin{aligned}
& T \left[\mathcal{H}_{eff}(x) \mathcal{H}_{eff}(0) \right] \Big|_{WE} = \\
& 2 : \bar{c}^i(x) \Gamma_\mu \overline{q_1^j(x) \bar{q}_2^k(x) \Gamma^\mu u^l(x) \bar{q}_1^m(0) \Gamma_\nu c^n(0) \bar{u}^p(0) \Gamma^\nu q_2^q(0)} : \\
& = 2 \bar{c}^i(x) \gamma_\mu (1 - \gamma_5) \overline{q_1^j(x) \bar{q}_1^m(0)} \gamma_\nu (1 - \gamma_5) c^n(0) \\
& \quad \bar{u}^p(0) \gamma^\nu (1 - \gamma_5) \overline{q_2^q(x) \bar{q}_2^k(x)} \gamma_\mu (1 - \gamma_5) u^l(x) \\
& = 2 \bar{c}^i \gamma_\mu (1 - \gamma_5) \int \frac{d^4 k}{(2\pi)^4} \frac{i(k + m_1)}{k^2 - m_1^2 + i\epsilon} \gamma_\nu (1 - \gamma_5) c^n \\
& \quad \bar{u}^p \gamma^\nu (1 - \gamma_5) \int \frac{d^4 l}{(2\pi)^4} \frac{i(l + m_2)}{l^2 - m_2^2 + i\epsilon} \gamma^\mu (1 - \gamma_5) u^l \\
& \quad e^{i(p_c + p_u - k + l)} \delta^{jm} \delta^{qk} , \tag{D.0.40}
\end{aligned}$$

and by using Equations (D.0.11) – (D.0.14) we get

$$\begin{aligned}
& i \int d^4 x T \left[\mathcal{H}_{eff}(x) \mathcal{H}_{eff}(0) \right] \Big|_{WE} = \\
& 2i \int \frac{d^4 l}{(2\pi)^4} \bar{c}^i \gamma_\mu (1 - \gamma_5) \frac{i(l + \not{p} + m_1)}{(l + p)^2 - m_1^2 + i\epsilon} \gamma_\nu (1 - \gamma_5) c^n \\
& \quad \bar{u}^p \gamma^\nu (1 - \gamma_5) \frac{i(l + m_2)}{l^2 - m_2^2 + i\epsilon} \gamma^\mu (1 - \gamma_5) u^l \delta^{jm} \delta^{qk} \\
& = -8i \int \frac{d^4 l}{(2\pi)^4} \frac{l^\rho l^\sigma + p^\rho l^\sigma}{((l + p)^2 - m_1^2 + i\epsilon)(l^2 - m_2^2 + i\epsilon)} \\
& \quad (\bar{c}^i \gamma_\mu (1 - \gamma_5) \gamma_\rho \gamma_\nu c^n) (\bar{u}^p \gamma^\nu (1 - \gamma_5) \gamma_\sigma \gamma^\mu u^l) \delta^{jm} \delta^{qk} . \tag{D.0.41}
\end{aligned}$$

Taking the imaginary part of Equation (D.0.41) and using Equations (D.0.17) – (D.0.22) and (D.0.28) we get

$$\begin{aligned}
\mathcal{T}_{WE}^{ij} & = -32 \frac{G_F^2}{2} (V_{cq_1}^* V_{uq_2})^2 \left(Q_{V-A}^u \text{Im} \left(i \left(B_{00} + \frac{p^2}{2} (B_{11} + B_0) \right) \right) \right. \\
& \quad \left. - Q_{S-P}^{pp,u} \text{Im} (i (B_{11} + B_0)) \right) \delta^{jm} \delta^{qk} \\
& = -\frac{4G_F^2}{3} (V_{cq_1}^* V_{uq_2})^2 \left[\frac{(m_1^2 - m_2^2)^2 - p^2(2p^2 - m_1^2 - m_2^2)}{p^2} Q_{V-A}^u \right. \\
& \quad \left. - \frac{2(2(m_1^2 - m_2^2)^2 - p^2(p^2 + m_1^2 + m_2^2))}{p^4} Q_{S-P}^{pp,u} \right] \text{Im}(iB) \delta^{jm} \delta^{qk}
\end{aligned}$$

$$\begin{aligned}
&= \frac{G_F^2}{12\pi} \left(V_{cq_1}^* V_{uq_2} \right)^2 \frac{\lambda(1 + \tilde{x}, z_1, z_2)}{(1 + \tilde{x})^2} \times \\
&\quad \left[m_c^2 \left\{ (z_1 - z_2)^2 - (1 + \tilde{x})(2(1 + \tilde{x}) - z_1 - z_2) \right\} Q_{V-A}^u \right. \\
&\quad \left. - 2 \left\{ \frac{2(z_1 - z_2)^2}{1 + \tilde{x}} - (1 + \tilde{x} + z_1 + z_2) \right\} Q_{S-P}^{pp,u} \right] \delta^{jm} \delta^{qk} , \quad (D.0.42)
\end{aligned}$$

where for a general colour structure and spectator quark q we define

$$Q_{V-A}^q = (\bar{c} \gamma_\mu (1 - \gamma_5) q) (\bar{q} \gamma^\mu (1 - \gamma_5) c) , \quad (D.0.43)$$

$$Q_{S-P}^{pp,q} = (\bar{c} \not{p} (1 - \gamma_5) q) (\bar{q} \not{p} (1 - \gamma_5) c) . \quad (D.0.44)$$

Considering now all the possible Wilson coefficient combinations we get the following contributions

- For $Q_1 \otimes Q_1$ we have in total a factor $\delta^{ij} \delta^{jm} \delta^{mn} \delta^{lk} \delta^{kq} \delta^{qp} = \delta^{in} \delta^{lp}$ creating the operators

$$O_1' = (\bar{c}^i \gamma_\mu (1 - \gamma_5) u^l) (\bar{u}^l \gamma^\mu (1 - \gamma_5) c^i) , \quad (D.0.45)$$

$$O_2'^{pp} = (\bar{c}^i \not{p} (1 - \gamma_5) u^l) (\bar{u}^l (1 + \gamma_5) \not{p} c^i) . \quad (D.0.46)$$

- For $Q_2 \otimes Q_2$ we have in total a factor $\delta^{il} \delta^{kj} \delta^{jm} \delta^{mq} \delta^{qk} \delta^{np} = N_C \delta^{il} \delta^{np}$ creating the operators

$$O_1 = (\bar{c}^i \gamma_\mu (1 - \gamma_5) u^i) (\bar{u}^l \gamma^\mu (1 - \gamma_5) c^l) , \quad (D.0.47)$$

$$O_2^{pp} = (\bar{c}^i \not{p} (1 - \gamma_5) u^i) (\bar{u}^l (1 + \gamma_5) \not{p} c^l) . \quad (D.0.48)$$

- For $Q_1 \otimes Q_2$ we get $\delta^{ij} \delta^{jm} \delta^{mq} \delta^{qk} \delta^{kl} \delta^{np} = \delta^{il} \delta^{np}$ creating the operators O_1 and O_2^{pp} . We also get a factor 2 from symmetry by including the identical contribution from $Q_2 \otimes Q_1$.

So far we are proceeding as in the previous computation. For lifetimes, however, we want to express the results in terms of the colour-singlet and colour-octet operators

instead of the colour rearranged ones. To do so we use Equation (2.1.10) and write

$$O'_1 = 2T_1 + \frac{1}{N_C} O_1, \quad (\text{D.0.49})$$

$$O_2'^{pp} = 2T_2^{pp} + \frac{1}{N_C} O_2^{pp}, \quad (\text{D.0.50})$$

where $T_1 = (\bar{c}\gamma_\mu(1-\gamma_5)t^\alpha u)(\bar{u}\gamma^\mu(1-\gamma_5)t^\alpha c)$ and $T_2^{pp} = (\bar{c}\not{p}(1-\gamma_5)t^\alpha u)(\bar{u}(1+\gamma_5)t^\alpha \not{p}c)$.

Putting everything together we can write for WE

$$\begin{aligned} \Gamma_{WE}^{q_1 q_2} &= \frac{1}{2M_D} \frac{G_F^2 |V_{cq_1}^* V_{uq_2}|^2}{12\pi} \frac{\lambda(1 + \tilde{x}, z_1, z_2)}{(1 + \tilde{x}^2)} \times \left\{ \left(\frac{1}{N_C} C_1^2 + 2C_1 C_2 + N_C C_2^2 \right) \right. \\ &\quad \left[m_c^2 w_1(\tilde{x}, z_1, z_2) O_1 - 2w_2(\tilde{x}, z_1, z_2) O_2^{pp} \right] \\ &\quad \left. + 2C_1^2 \left[m_c^2 w_1(\tilde{x}, r_1, r_2) T_1 - 2w_2(\tilde{x}, z_1, z_2) T_2^{pp} \right] \right\}, \quad (\text{D.0.51}) \end{aligned}$$

where $w_1(\tilde{x}, z_1, z_2)$ and $w_2(\tilde{x}, z_1, z_2)$ are defined in Equations (D.0.36) and (D.0.37)

For the Pauli Interference we start with

$$\begin{aligned} &T \left[\mathcal{H}_{eff}(x) \mathcal{H}_{eff}(0) \right] \Big|_{PI} = \\ &2 : \bar{c}^i(x) \Gamma_\mu \overbrace{q_1^j(x) \bar{q}_2^k(x) \Gamma^\mu u^l(x) \overbrace{q_1^m(0) \Gamma_\nu c^n(0) \bar{u}^p(0) \Gamma^\nu q_2^q(0)} : \\ &= 2 \bar{c}^i \gamma_\mu (1 - \gamma_5) \int \frac{d^4 k}{(2\pi)^4} \frac{i(\not{k} + m_1)}{k^2 - m_1^2 + i\epsilon} \gamma_\nu (1 - \gamma_5) c^n \\ &\quad \bar{q}_2^k \gamma^\mu (1 - \gamma_5) \int \frac{d^4 l}{(2\pi)^4} \frac{i(\not{l} + m_u)}{l^2 - m_u^2 + i\epsilon} \gamma^\nu (1 - \gamma_5) q_2^q \\ &\quad e^{i(p_c - p_{q_2} - k - l)} \delta^{jm} \delta^{lp}, \quad (\text{D.0.52}) \end{aligned}$$

Next, we integrate this over x and k to get

$$\begin{aligned} &i \int d^4 x \text{T} \left[\mathcal{H}_{eff}(x) \mathcal{H}_{eff}(0) \right] \Big|_{PI} = \\ &2i \int \frac{d^4 l}{(2\pi)^4} \bar{c}^i \gamma_\mu (1 - \gamma_5) \frac{i(\not{l} - \not{p} + m_1)}{(l - p)^2 - m_1^2 + i\epsilon} \gamma_\nu (1 - \gamma_5) c^n \\ &\quad \bar{q}_2^k \gamma^\mu (1 - \gamma_5) \frac{i(\not{l} + m_u)}{l^2 - m_u^2 + i\epsilon} \gamma^\nu (1 - \gamma_5) q_2^q \delta^{jm} \delta^{lp} \end{aligned}$$

$$\begin{aligned}
&= -8i \int \frac{d^4 l}{(2\pi)^4} \frac{l^\rho l^\sigma - p^\rho l^\sigma}{((l-p)^2 - m_1^2 + i\epsilon)(l^2 - m_u^2 + i\epsilon)} \\
&(\bar{c}^i \gamma_\mu (1 - \gamma_5) \gamma_\rho \gamma_\nu c^n) (\bar{q}_2^k \gamma^\mu (1 - \gamma_5) \gamma_\sigma \gamma^\nu q_2^q) \delta^{jm} \delta^{lp} . \quad (D.0.53)
\end{aligned}$$

In PI we have a different Dirac structure from before. In order to simplify it we use

$$\gamma_\nu \gamma_\rho \gamma_\mu (1 - \gamma_5) \otimes \gamma^\nu \gamma^\rho \gamma^\mu (1 - \gamma_5) = 16 \gamma_\mu (1 - \gamma_5) \otimes \gamma^\mu (1 - \gamma_5) , \quad (D.0.54)$$

$$\gamma_\nu \not{p} \gamma_\mu (1 - \gamma_5) \otimes \gamma^\nu \not{p} \gamma^\mu (1 - \gamma_5) = 4p^2 \gamma_\mu (1 - \gamma_5) \otimes \gamma^\mu (1 - \gamma_5) . \quad (D.0.55)$$

The one-loop integral in Equation (D.0.53) is a little different from before. The $l^\rho l^\sigma$ part of it gives the same result as Equations (D.0.22) and (D.0.21) despite having $(l-p)^2$ in the denominator. On the other hand, the $p^\rho l^\sigma$ part has a different sign from Equation (D.0.20) but it comes with an overall minus, so the sign difference is countered. Thus, we get

$$\begin{aligned}
\mathcal{T}_{PI}^{ij} &= 32 \frac{G_F^2}{2} |V_{cq_1}^* V_{uq_2}|^2 \left[\text{Im} \left(4iB_{00} + p^2 (iB_{11} + iB_0) \right) Q_{V-A}^{q_2} \right] \\
&= \frac{G_F^2}{2\pi} |V_{cq_1}^* V_{uq_2}|^2 m_c^2 \frac{\lambda(1 + \tilde{x}, z_1, z_u)}{(1 + \tilde{x})} \left[(1 + \tilde{x} - z_1 - z_u) Q_{V-A}^{q_2} \right] \delta^{jm} \delta^{lp} , \quad (D.0.56)
\end{aligned}$$

where we have also used Equation (D.0.28). Similar to before we check all operator insertions

- For $Q_1 \otimes Q_1$ we have in total a factor $\delta^{ij} \delta^{jm} \delta^{mn} \delta^{kl} \delta^{lp} \delta^{pq} = \delta^{in} \delta^{kq}$ creating the operator

$$O'_1 = (\bar{c}^i \gamma_\mu (1 - \gamma_5) q_2^k) (\bar{q}_2^k \gamma^\mu (1 - \gamma_5) c^i) . \quad (D.0.57)$$

- For $Q_2 \otimes Q_2$ we have in total a factor $\delta^{il} \delta^{lp} \delta^{pn} \delta^{kj} \delta^{jm} \delta^{mq} = \delta^{in} \delta^{kq}$ creating the operator O'_1 again
- For $Q_1 \otimes Q_2$ we get $\delta^{ij} \delta^{jm} \delta^{mq} \delta^{kl} \delta^{lp} \delta^{pq} = \delta^{iq} \delta^{kn}$ creating the operator

$$O_1 = (\bar{c}^i \gamma_\mu (1 - \gamma_5) q_2^i) (\bar{q}_2^k \gamma^\mu (1 - \gamma_5) c^i) . \quad (D.0.58)$$

We also get a factor 2 from symmetry by including the $Q_2 \otimes Q_1$ contribution.

Using again Equation (2.1.10) we get PI

$$\begin{aligned} \Gamma_{PI}^{q_1 u} &= \frac{1}{2M_D} \frac{G_F^2}{2\pi} |V_{cq_1}^* V_{uq_2}|^2 m_c^2 \frac{\lambda(1 + \tilde{x}, z_1, z_u)}{(1 + \tilde{x})} (1 + \tilde{x} - z_1 - z_u) \\ &\quad \left[\left(\frac{1}{N_C} (C_1^2 + C_2^2) + 2C_1 C_2 \right) O_1 + 2(C_1^2 + C_2^2) T_1 \right]. \end{aligned} \quad (D.0.59)$$

Finally if we look at the Weak Annihilation topology we write

$$\begin{aligned} &T \left[\mathcal{H}_{eff}(x) \mathcal{H}_{eff}(0) \right] \Big|_{WA} = \\ &2 : \bar{c}^i(x) \Gamma_\mu q_1^j(x) \overbrace{\bar{q}_2^k(x) \Gamma^\mu u^l(x) \bar{q}_1^m(0) \Gamma_\nu c^n(0) \bar{u}^p(0) \Gamma^\nu q_2^q(0)} : \\ &= -2 \bar{c}^i \gamma_\mu (1 - \gamma_5) q_1^j \text{Tr} \left[\gamma^\mu (1 - \gamma_5) \int \frac{d^4 k}{(2\pi)^4} \frac{i(\not{k} + m_2)}{k^2 - m_2^2 + i\epsilon} \gamma^\nu (1 - \gamma_5) \right. \\ &\quad \left. \int \frac{d^4 l}{(2\pi)^4} \frac{i(\not{l} + m_u)}{l^2 - m_u^2 + i\epsilon} \right] \bar{q}_1^m \gamma_\nu (1 - \gamma_5) c^n e^{i(p_c + p_{q_1} + k - l)} \delta^{kq} \delta^{lp}, \end{aligned} \quad (D.0.60)$$

where the trace over the spinor indices and minus sign come from the fermion loop.

Performing the integral over x and k we get

$$\begin{aligned} &i \int d^4 x T \left[\mathcal{H}_{eff}(x) \mathcal{H}_{eff}(0) \right] \Big|_{WA} = \\ &-2 \bar{c}^i \gamma_\mu (1 - \gamma_5) q_1^j i \int \frac{d^4 l}{(2\pi)^4} \text{Tr} \left[\gamma^\mu (1 - \gamma_5) \frac{i(\not{l} + \not{p} + m_2)}{(l + p)^2 - m_2^2 + i\epsilon} \right. \\ &\quad \left. \gamma^\nu (1 - \gamma_5) \frac{i(\not{l} + m_u)}{l^2 - m_u^2 + i\epsilon} \right] \bar{q}_1^m \gamma_\nu (1 - \gamma_5) c^n \delta^{kq} \delta^{lp} \\ &= 4i \int \frac{d^4 l}{(2\pi)^4} \frac{l^\rho l^\sigma + p^\rho l^\sigma}{((l + p)^2 - m_2^2 + i\epsilon)(l^2 - m_u^2 + i\epsilon)} \\ &\quad (\bar{c}^i \gamma_\mu (1 - \gamma_5) q_1^j) (\bar{q}_1^m \gamma_\nu (1 - \gamma_5) c^n) \text{Tr} \left[\gamma^\mu (1 - \gamma_5) \gamma_\rho \gamma^\nu \gamma_\sigma \right] \delta^{kq} \delta^{lp}. \end{aligned} \quad (D.0.61)$$

Taking the imaginary part of the one-loop integral and computing the trace we obtain

$$\begin{aligned} \mathcal{T}_{WA}^{ij} &= -32 \frac{G_F^2}{2} |V_{cq_1}^* V_{uq_2}|^2 \times \\ &\quad \text{Im} \left[\left(B_{00} + \frac{p^2}{2} (B_{11} + B_0) \right) Q_{V-A}^{q_1} - (B_{11} + B_0) Q_{S-P}^{pp, q_1} \right] \delta^{kq} \delta^{lp} \end{aligned}$$

$$\begin{aligned}
&= \frac{G_F^2}{12\pi} |V_{cq_1}^* V_{uq_2}|^2 \frac{\lambda(1 + \tilde{x}, z_1, z_2)}{(1 + \tilde{x})^2} \times \\
&\quad \left[m_c^2 \left\{ (z_1 - z_2)^2 - (1 + \tilde{x})(2(1 + \tilde{x}) - z_1 - z_2) \right\} Q_{V-A}^{q_1} \right. \\
&\quad \left. - 2 \left\{ \frac{2(z_1 - z_2)^2}{1 + \tilde{x}} - (1 + \tilde{x} + z_1 + z_2) \right\} Q_{S-P}^{pp, q_1} \right] \delta^{kq} \delta^{lp} .
\end{aligned} \tag{D.0.62}$$

As we can see we have reproduced the same result as in WE (up to the deltas). This is not an accident as the two structures are connected via a Fierz transformation. As we will see though after considering the colour flow the final results differ.

- For $Q_1 \otimes Q_1$ we have in total a factor $\delta^{ij} \delta^{lp} \delta^{pq} \delta^{qk} \delta^{kl} \delta^{mn} = N_C \delta^{ij} \delta^{mn}$ creating the operators

$$O'_1 = (\bar{c}^i \gamma_\mu (1 - \gamma_5) q_1^i) (\bar{q}_1^m \gamma^\mu (1 - \gamma_5) c^m) , \tag{D.0.63}$$

$$O_2'^{pp} = (\bar{c}^i \not{p} (1 - \gamma_5) q_1^i) (\bar{q}_1^m (1 + \gamma_5) \not{p} c^m) . \tag{D.0.64}$$

- For $Q_2 \otimes Q_2$ we have in total a factor $\delta^{il} \delta^{lp} \delta^{pn} \delta^{jk} \delta^{kq} \delta^{qm} = \delta^{in} \delta^{jm}$ creating the operators

$$O'_1 = (\bar{c}^i \gamma_\mu (1 - \gamma_5) q_1^m) (\bar{q}_1^m \gamma^\mu (1 - \gamma_5) c^i) , \tag{D.0.65}$$

$$O_2'^{pp} = (\bar{c}^i \not{p} (1 - \gamma_5) q_1^m) (\bar{q}_1^m (1 + \gamma_5) \not{p} c^i) . \tag{D.0.66}$$

- For $Q_1 \otimes Q_2$ we get $\delta^{ij} \delta^{mq} \delta^{qk} \delta^{kl} \delta^{lp} \delta^{pn} = \delta^{ij} \delta^{mn}$ creating the operators O_1 and $O_2'^{pp}$. We also get a factor 2 from symmetry by including the identical contribution from $Q_2 \otimes Q_1$.

Using Equation (2.1.10) we put everything together for WA

$$\begin{aligned}
\Gamma_{WA}^{uq_2} &= \frac{1}{2M_D} \frac{G_F^2 |V_{cq_1}^* V_{uq_2}|^2}{12\pi} \frac{\lambda(1 + \tilde{x}, z_1, z_2)}{(1 + \tilde{x})^2} \times \left\{ \left(N_C C_1^2 + 2C_1 C_2 + \frac{1}{N_C} C_2^2 \right) \right. \\
&\quad \left[w_1(\tilde{x}, z_1, z_2) m_c^2 O_1 - 2w_2(\tilde{x}, z_1, z_2) O_2'^{pp} \right] \\
&\quad \left. + 2C_2^2 \left[w_1(\tilde{x}, r_1, r_2) m_c^2 T_1 - 2w_2(\tilde{x}, z_1, z_2) T_2'^{pp} \right] \right\} ,
\end{aligned} \tag{D.0.67}$$

The expressions of Equations (D.0.51), (D.0.59) and (D.0.67) can be expanded to give the exact dimension-six and dimension-seven results. For dimension-six we can simply set $\tilde{x} = 0$ and $p^2 = m_c^2$ ignoring effects from small momenta. To include dimension-seven contributions we expand the coefficients in \tilde{x} keeping terms of order $\mathcal{O}(\tilde{x}^1)^{16}$. We still need to expand the operators¹⁷ O_2^{pp} and T_2^{pp} . Their expansion is identical so we will show only for $O_2^{q,pp}$

$$\begin{aligned}
 O_2^{q,pp} &= (\bar{c}\not{p}(1 - \gamma_5)q)(\bar{q}(1 + \gamma_5)\not{p}c) \\
 &= (\bar{c}\not{p}_c(1 - \gamma_5)q)(\bar{q}(1 + \gamma_5)\not{p}_c c) + (\bar{c}\not{p}_c(1 - \gamma_5)q)(\bar{q}\not{p}_q(1 - \gamma_5) c) \\
 &+ (\bar{c}(1 + \gamma_5)\not{p}_q q)(\bar{q}(1 + \gamma_5)\not{p}_c c) + (\bar{c}(1 + \gamma_5)\not{p}_q q)(\bar{q}\not{p}_q(1 - \gamma_5) c) \\
 &= m_c^2(\bar{c}(1 - \gamma_5)q)(\bar{q}(1 + \gamma_5)c) - m_c m_q(\bar{c}(1 - \gamma_5)q)(\bar{q}(1 - \gamma_5)c) \\
 &- m_c m_q(\bar{c}(1 + \gamma_5)q)(\bar{q}(1 + \gamma_5)c) + \mathcal{O}(m_q^2) \\
 &= m_c^2(O_2^q - 2P_1^q) + \mathcal{O}(m_q^2) , \tag{D.0.68}
 \end{aligned}$$

where O_1^q and P_1^q are defined in Equations (4.2.22) and (4.2.44). Similarly we get

$$T_2^{pp} = m_c^2(T_1^q - 2S_1^q) + \mathcal{O}(m_q^2) . \tag{D.0.69}$$

The final dimension-seven operators arise from $\tilde{x} O_1^q$ and $\tilde{x} O_2^q$

$$\begin{aligned}
 \tilde{x} O_1^q &= 2\frac{p_c p_q}{m_c^2}(\bar{c}\gamma_\mu(1 - \gamma_5)q)(\bar{q}\gamma^\mu(1 - \gamma_5)c) \\
 &= \frac{1}{m_c^2}(\bar{c}\overleftarrow{D}^\rho\gamma_\mu(1 - \gamma_5)D_\rho q)(\bar{q}\gamma^\mu(1 - \gamma_5)c) = \frac{1}{m_c}P_2^q , \tag{D.0.70}
 \end{aligned}$$

$$\begin{aligned}
 \tilde{x} O_2^q &= 2\frac{p_c p_q}{m_c^2}(\bar{c}(1 - \gamma_5)q)(\bar{q}(1 + \gamma_5)c) \\
 &= \frac{1}{m_c^2}(\bar{c}\overleftarrow{D}^\rho(1 - \gamma_5)D_\rho q)(\bar{q}(1 + \gamma_5)c) = \frac{1}{m_c}P_3^q , \tag{D.0.71}
 \end{aligned}$$

where P_2 and P_3 are also defined in Equations (4.2.45) and (4.2.46).

So far we have performed these calculations in QCD. To get the expressions for

¹⁶Note that $\tilde{x} = \frac{2p_c p_q}{m_c}$ for WE and WA since $p = p_c + p_q$ but $\tilde{x} = -\frac{2p_c p_q}{m_c}$ for PI where $p = p_c - p_q$

¹⁷Note that from this point on we will use the fact that an operator and its hermitian conjugate have the same matrix element and therefore we add a factor 2.

WE, PI and WA in HQET we need to make some adjustments. First of all, we decompose $p^\mu = m_c v^\mu + k^\mu \pm p_q^{\mu 18}$ where v^μ and k^μ are the hadron velocity and the residual momentum as introduced in Section 2.1.2. Then $\tilde{x} = 2\frac{v \cdot iD}{m_c} \pm 2\frac{v \cdot p_q}{m_c}$ where we have replaced k^μ with iD since the derivative acting on h_v returns only the k part of the momentum. Next we expand the QCD quark field as in Equation (2.1.65) to get¹⁹

$$c = h_v \left(1 + \frac{i\cancel{D}}{2m_c} \right) + \mathcal{O}(1/m_c^2) . \quad (\text{D.0.72})$$

We are also using Equation (2.1.68) to write

$$\begin{aligned} (\bar{c}\Gamma_\mu q)(\bar{q}\Gamma_\nu c) &\simeq (\bar{h}_v\Gamma_\mu)(\bar{q}\Gamma_\nu h_v) + \frac{1}{2m_c} \left((\bar{h}_v(-i\overleftarrow{\cancel{D}})\Gamma_\mu q)(\bar{q}\Gamma_\nu h_v) + (\bar{h}_v\Gamma_\mu q)(\bar{q}\Gamma_\nu(i\cancel{D})h_v) \right) \\ &+ \frac{1}{m_c} i \int dx \text{T}\{(\bar{h}_v\Gamma_\mu q)(\bar{q}\Gamma_\nu h_v), \mathcal{L}_1(x)\} + \mathcal{O}(1/m_c^2) , \end{aligned} \quad (\text{D.0.73})$$

where the \simeq sign indicates that the LHS is evaluated in QCD states while the RHS in HQET²⁰ and \mathcal{L}_1 contains the $1/m_c$ corrections of the HQET Lagrangian. Now we expand $O_2^{q,pp}$ as

$$\begin{aligned} O_2^{q,pp} &= \left(\bar{c}(m_c\psi - i\overleftarrow{\cancel{D}} + \not{p}_q)(1 - \gamma_5)q \right) \left(\bar{q}(1 + \gamma_5)(m_c\psi + i\overleftarrow{\cancel{D}} + \not{p}_q)c \right) \\ &= m_c^2 (\bar{c}\psi(1 - \gamma_5)q) (\bar{q}(1 + \gamma_5)\psi c) + m_c \left(\bar{c}(-i\overleftarrow{\cancel{D}})(1 - \gamma_5)q \right) (\bar{q}(1 + \gamma_5)\psi c) \\ &+ m_c (\bar{c}\psi(1 - \gamma_5)q) (\bar{q}(1 + \gamma_5)(i\cancel{D})c) + m_c (\bar{c}\psi(1 - \gamma_5)q) (\bar{q}(1 + \gamma_5)\not{p}_q c) \\ &+ m_c (\bar{c}\not{p}_q(1 - \gamma_5)q) (\bar{q}(1 + \gamma_5)\psi c) + \mathcal{O}(1/m_c^2) , \end{aligned} \quad (\text{D.0.74})$$

and using Equations (D.0.72), (D.0.73), $(\psi - 1)h_v = h_v$, $(iv \cdot D)h_v = 0$, $(i\cancel{D} - m_q)q = 0$ and the relation $\psi\cancel{D} = -\cancel{D}\psi + 2v \cdot D$ we can write

$$O_2^{q,pp} = m_c^2 \left(\tilde{O}_2^q + \frac{\tilde{R}_2^q}{m_c} + \frac{\tilde{M}_{2,\pi}^q}{m_c} + \frac{\tilde{M}_{2,G}^q}{m_c} - 2\frac{\tilde{P}_1^q}{m_c} \right) , \quad (\text{D.0.75})$$

¹⁸Again here WE and WA come with the plus sign while PI has a minus sign

¹⁹Note that the exponential factor in Equation (2.1.65) is already removed during the HQE so we do not include it here

²⁰We indicate this relation here but for simplicity we will continue using the = sign.

where the HQET operators are defined in Section 4.2. In a similar way we can also write

$$O_1^q = \tilde{O}_1^q + \frac{\tilde{R}_1^q}{m_c} + \frac{\tilde{M}_{1,\pi}^q}{m_c} + \frac{\tilde{M}_{2,G}^q}{m_c}, \quad (\text{D.0.76})$$

$$\tilde{x} \tilde{O}_1^q = \mp 2 \frac{\tilde{P}_2^q}{m_c}, \quad (\text{D.0.77})$$

$$\tilde{x} \tilde{O}_2^q = \mp 2 \frac{\tilde{P}_3^q}{m_c}. \quad (\text{D.0.78})$$

where the minus sign corresponds to WE and WA topologies and the plus to PI. The calculation for the colour-octet operators is exactly identical with the appropriate substitutions.

Bibliography

- [1] PARTICLE DATA GROUP collaboration, P. Zyla et al., *Review of Particle Physics*, *PTEP* **2020** (2020) 083C01.
- [2] BESIII collaboration, M. Ablikim et al., *Measurement of the absolute branching fraction of inclusive semielectronic D_s^+ decays*, 2104.07311.
- [3] F. Herren and M. Steinhauser, *Version 3 of RunDec and CRunDec*, *Comput. Phys. Commun.* **224** (2018) 333–345, [1703.03751].
- [4] M. Kirk, A. Lenz and T. Rauh, *Dimension-six matrix elements for meson mixing and lifetimes from sum rules*, *JHEP* **12** (2017) 068, [1711.02100].
- [5] D. King, A. Lenz and T. Rauh, *$SU(3)$ breaking effects in B and D meson lifetimes*, 2112.03691.
- [6] A. Lenz, M. L. Piscopo and C. Vlahos, *Renormalization scale setting for D -meson mixing*, *Phys. Rev. D* **102** (2020) 093002, [2007.03022].
- [7] C. Vlahos, *Renormalisation scale setting for D -mixing*, *PoS CHARM2020* (2021) 033.
- [8] D. King, A. Lenz, M. L. Piscopo, T. Rauh, A. V. Rusov and C. Vlahos, *Revisiting Inclusive Decay Widths of Charmed Mesons*, 2109.13219.
- [9] P. A. M. Dirac, *The quantum theory of the electron*, *Proc. R. Soc. Lond A* **117** (1928) 610–624.

- [10] R. P. Feynman, *Space-time approach to quantum electrodynamics*, *Phys. Rev.* **76** (Sep, 1949) 769–789.
- [11] R. P. Feynman, *The theory of positrons*, *Phys. Rev.* **76** (Sep, 1949) 749–759.
- [12] R. P. Feynman, *Mathematical formulation of the quantum theory of electromagnetic interaction*, *Phys. Rev.* **80** (Nov, 1950) 440–457.
- [13] J. Schwinger, *On quantum-electrodynamics and the magnetic moment of the electron*, *Phys. Rev.* **73** (Feb, 1948) 416–417.
- [14] J. Schwinger, *Quantum electrodynamics. i. a covariant formulation*, *Phys. Rev.* **74** (Nov, 1948) 1439–1461.
- [15] S. Tomonaga, *On a Relativistically Invariant Formulation of the Quantum Theory of Wave Fields**, *Progress of Theoretical Physics* **1** (08, 1946) 27–42, [<https://academic.oup.com/ptp/article-pdf/1/2/27/24027031/1-2-27.pdf>].
- [16] H. Fritzsch, M. Gell-Mann and H. Leutwyler, *Advantages of the color octet gluon picture*, *Physics Letters B* **47** (1973) 365–368.
- [17] D. J. Gross and F. Wilczek, *Ultraviolet behavior of non-abelian gauge theories*, *Phys. Rev. Lett.* **30** (Jun, 1973) 1343–1346.
- [18] H. D. Politzer, *Reliable perturbative results for strong interactions?*, *Phys. Rev. Lett.* **30** (Jun, 1973) 1346–1349.
- [19] S. A. Bludman, *On the universal Fermi interaction*, *Nuovo Cim.* **9** (1958) 433–445.
- [20] S. L. Glashow, *Partial Symmetries of Weak Interactions*, *Nucl. Phys.* **22** (1961) 579–588.
- [21] S. Weinberg, *A model of leptons*, *Phys. Rev. Lett.* **19** (Nov, 1967) 1264–1266.
- [22] A. Salam, *Weak and Electromagnetic Interactions*, *Conf. Proc. C* **680519** (1968) 367–377.

- [23] P. W. Higgs, *Broken symmetries and the masses of gauge bosons*, *Phys. Rev. Lett.* **13** (Oct, 1964) 508–509.
- [24] F. Englert and R. Brout, *Broken symmetry and the mass of gauge vector mesons*, *Phys. Rev. Lett.* **13** (Aug, 1964) 321–323.
- [25] G. S. Guralnik, C. R. Hagen and T. W. B. Kibble, *Global conservation laws and massless particles*, *Phys. Rev. Lett.* **13** (Nov, 1964) 585–587.
- [26] T. D. Lee and C. N. Yang, *Question of parity conservation in weak interactions*, *Phys. Rev.* **104** (Oct, 1956) 254–258.
- [27] C. S. Wu, E. Ambler, R. W. Hayward, D. D. Hoppes and R. P. Hudson, *Experimental test of parity conservation in beta decay*, *Phys. Rev.* **105** (Feb, 1957) 1413–1415.
- [28] H. YUKAWA, *On the interaction of elementary particles. i*, *Proceedings of the Physico-Mathematical Society of Japan. 3rd Series* **17** (1935) 48–57.
- [29] N. Cabibbo, *Unitary symmetry and leptonic decays*, *Phys. Rev. Lett.* **10** (Jun, 1963) 531–533.
- [30] M. Kobayashi and T. Maskawa, *CP-Violation in the Renormalizable Theory of Weak Interaction*, *Progress of Theoretical Physics* **49** (02, 1973) 652–657, [<https://academic.oup.com/ptp/article-pdf/49/2/652/5257692/49-2-652.pdf>].
- [31] J. Charles, A. Höcker, H. Lacker, S. Laplace, F. R. Le Diberder, J. Malclés et al., *Cp violation and the ckm matrix: assessing the impact of the asymmetric b factories*, *The European Physical Journal C* **41** (May, 2005) 1–131.
- [32] L.-L. Chau and W.-Y. Keung, *Comments on the parametrization of the kobayashi-maskawa matrix*, *Phys. Rev. Lett.* **53** (Nov, 1984) 1802–1805.
- [33] L. Wolfenstein, *Parametrization of the kobayashi-maskawa matrix*, *Phys. Rev. Lett.* **51** (Nov, 1983) 1945–1947.

- [34] S. L. Glashow, J. Iliopoulos and L. Maiani, *Weak interactions with lepton-hadron symmetry*, *Phys. Rev. D* **2** (Oct, 1970) 1285–1292.
- [35] M. Gell-Mann, *A schematic model of baryons and mesons*, *Physics Letters* **8** (1964) 214–215.
- [36] G. Zweig, *An $SU(3)$ model for strong interaction symmetry and its breaking. Version 2*, pp. 22–101. 2, 1964.
- [37] J. E. Augustin, A. M. Boyarski, M. Breidenbach, F. Bulos, J. T. Dakin, G. J. Feldman et al., *Discovery of a narrow resonance in e^+e^- annihilation*, *Phys. Rev. Lett.* **33** (Dec, 1974) 1406–1408.
- [38] J. J. Aubert, U. Becker, P. J. Biggs, J. Burger, M. Chen, G. Everhart et al., *Experimental observation of a heavy particle j* , *Phys. Rev. Lett.* **33** (Dec, 1974) 1404–1406.
- [39] K. G. Wilson and J. Kogut, *The renormalization group and the expansion*, *Physics Reports* **12** (1974) 75–199.
- [40] K. G. Wilson, *Non-lagrangian models of current algebra*, *Phys. Rev.* **179** (Mar, 1969) 1499–1512.
- [41] A. J. Buras, *Weak Hamiltonian, CP violation and rare decays*, in *Les Houches Summer School in Theoretical Physics, Session 68: Probing the Standard Model of Particle Interactions*, pp. 281–539, 6, 1998, [hep-ph/9806471](#).
- [42] G. Buchalla, A. J. Buras and M. E. Lautenbacher, *Weak decays beyond leading logarithms*, *Rev. Mod. Phys.* **68** (1996) 1125–1144, [[hep-ph/9512380](#)].
- [43] S. Fajfer, P. Singer and J. Zupan, *The Radiative leptonic decays $D^0 \rightarrow e^+e^- \gamma, \mu^+ \mu^- \gamma$ in the standard model and beyond*, *Eur. Phys. J. C* **27** (2003) 201–218, [[hep-ph/0209250](#)].
- [44] N. Isgur and M. B. Wise, *Weak decays of heavy mesons in the static quark approximation*, *Physics Letters B* **232** (1989) 113–117.

- [45] H. Georgi, *An Effective Field Theory for Heavy Quarks at Low-energies*, *Phys. Lett. B* **240** (1990) 447–450.
- [46] A. F. Falk, H. Georgi, B. Grinstein and M. B. Wise, *Heavy Meson Form-factors From QCD*, *Nucl. Phys. B* **343** (1990) 1–13.
- [47] M. K. Gaillard and B. W. Lee, *Rare decay modes of the k mesons in gauge theories*, *Phys. Rev. D* **10** (Aug, 1974) 897–916.
- [48] E. Eichten and B. R. Hill, *An Effective Field Theory for the Calculation of Matrix Elements Involving Heavy Quarks*, *Phys. Lett. B* **234** (1990) 511–516.
- [49] E. V. Shuryak, *Hadrons Containing a Heavy Quark and QCD Sum Rules*, *Nucl. Phys. B* **198** (1982) 83–101.
- [50] M. E. Luke, *Effects of subleading operators in the heavy quark effective theory*, *Phys. Lett. B* **252** (1990) 447–455.
- [51] B. Grinstein, *The Static Quark Effective Theory*, *Nucl. Phys. B* **339** (1990) 253–268.
- [52] M. Neubert, *Heavy quark symmetry*, *Phys. Rept.* **245** (1994) 259–396, [hep-ph/9306320].
- [53] T. Mannel, *Heavy-quark effective field theory*, *Reports on Progress in Physics* **60** (oct, 1997) 1113–1172.
- [54] I. I. Y. Bigi, M. A. Shifman and N. Uraltsev, *Aspects of heavy quark theory*, *Ann. Rev. Nucl. Part. Sci.* **47** (1997) 591–661, [hep-ph/9703290].
- [55] M. Neubert, *Symmetry breaking corrections to meson decay constants in the heavy quark effective theory*, *Phys. Rev. D* **46** (1992) 1076–1087.
- [56] A. V. Manohar and M. B. Wise, *Heavy quarks*, p. 44–76. Cambridge Monographs on Particle Physics, Nuclear Physics and Cosmology. Cambridge University Press, 2000. 10.1017/CBO9780511529351.003.

- [57] M. A. Shifman, *Theory of weak inclusive decays and lifetimes of heavy hadrons*, in *27th International Conference on High-energy Physics*, 7, 1994, hep-ph/9409359.
- [58] J. Chay, H. Georgi and B. Grinstein, *Lepton energy distributions in heavy meson decays from QCD*, *Phys. Lett. B* **247** (1990) 399–405.
- [59] I. I. Y. Bigi, M. A. Shifman, N. G. Uraltsev and A. I. Vainshtein, *QCD predictions for lepton spectra in inclusive heavy flavor decays*, *Phys. Rev. Lett.* **71** (1993) 496–499, [hep-ph/9304225].
- [60] B. Blok, L. Koyrakh, M. A. Shifman and A. I. Vainshtein, *Differential distributions in semileptonic decays of the heavy flavors in QCD*, *Phys. Rev. D* **49** (1994) 3356, [hep-ph/9307247].
- [61] I. I. Y. Bigi, N. G. Uraltsev and A. I. Vainshtein, *Nonperturbative corrections to inclusive beauty and charm decays: QCD versus phenomenological models*, *Phys. Lett.* **B293** (1992) 430–436, [hep-ph/9207214].
- [62] A. Lenz, *Lifetimes and heavy quark expansion*, *Int. J. Mod. Phys. A* **30** (2015) 1543005, [1405.3601].
- [63] V. A. Novikov, M. A. Shifman, A. I. Vainshtein and V. I. Zakharov, *Calculations in external fields in quantum chromodynamics: Technical review*, *Fortsch. Phys.* **32** (Aug, 1983) 585. 74 p.
- [64] M. A. Shifman, *Lectures on heavy quarks in quantum chromodynamics*, in *Theoretical Advanced Study Institute in Elementary Particle Physics (TASI 95): QCD and Beyond*, pp. 409–514, 10, 1995, hep-ph/9510377.
- [65] I. I. Y. Bigi, M. A. Shifman, N. G. Uraltsev and A. I. Vainshtein, *Sum rules for heavy flavor transitions in the SV limit*, *Phys. Rev.* **D52** (1995) 196–235, [hep-ph/9405410].

- [66] B. M. Dassing, T. Mannel and S. Turczyk, *Inclusive semi-leptonic B decays to order $1/m_b^4$* , *JHEP* **03** (2007) 087, [hep-ph/0611168].
- [67] K. G. Wilson, *Confinement of quarks*, *Phys. Rev. D* **10** (Oct, 1974) 2445–2459.
- [68] P. Colangelo and A. Khodjamirian, *QCD sum rules, a modern perspective*, hep-ph/0010175.
- [69] M. Bordone, B. Capdevila and P. Gambino, *Three loop calculations and inclusive Vcb*, *Phys. Lett. B* **822** (2021) 136679, [2107.00604].
- [70] U. Nierste, *Three Lectures on Meson Mixing and CKM phenomenology*, in *Heavy quark physics. Proceedings, Helmholtz International School, HQP08, Dubna, Russia, August 11-21, 2008*, pp. 1–38, 2009, 0904.1869.
- [71] A. Lenz and G. Wilkinson, *Mixing and CP violation in the charm system*, 2011.04443.
- [72] V. Weisskopf and E. P. Wigner, *Calculation of the natural brightness of spectral lines on the basis of Dirac's theory*, *Z. Phys.* **63** (1930) 54–73.
- [73] HFLAV collaboration, Y. S. Amhis et al., *Averages of b-hadron, c-hadron, and τ -lepton properties as of 2018*, 1909.12524.
- [74] LHCb collaboration, R. Aaij et al., *Physics case for an LHCb Upgrade II - Opportunities in flavour physics, and beyond, in the HL-LHC era*, 1808.08865.
- [75] M. Ablikim et al., *Future Physics Programme of BESIII*, *Chin. Phys.* **C44** (2020) , [1912.05983].
- [76] BELLE-II collaboration, W. Altmannshofer et al., *The Belle II Physics Book*, *PTEP* **2019** (2019) 123C01, [1808.10567].

- [77] LHCb collaboration, R. Aaij et al., *Observation of CP Violation in Charm Decays*, *Phys. Rev. Lett.* **122** (2019) 211803, [1903.08726].
- [78] M. Chala, A. Lenz, A. V. Rusov and J. Scholtz, ΔA_{CP} *within the Standard Model and beyond*, *JHEP* **07** (2019) 161, [1903.10490].
- [79] A. Dery and Y. Nir, *Implications of the LHCb discovery of CP violation in charm decays*, *JHEP* **12** (2019) 104, [1909.11242].
- [80] A. Khodjamirian and A. A. Petrov, *Direct CP asymmetry in $D \rightarrow \pi^- \pi^+$ and $D \rightarrow K^- K^+$ in QCD-based approach*, *Phys. Lett. B* **774** (2017) 235–242, [1706.07780].
- [81] H.-N. Li, C.-D. Lü and F.-S. Yu, *Implications on the first observation of charm CPV at LHCb*, 1903.10638.
- [82] Y. Grossman and S. Schacht, *The emergence of the $\Delta U = 0$ rule in charm physics*, *JHEP* **07** (2019) 020, [1903.10952].
- [83] H.-Y. Cheng and C.-W. Chiang, *Revisiting CP violation in $D \rightarrow PP$ and VP decays*, *Phys. Rev. D* **100** (2019) 093002, [1909.03063].
- [84] A. Soni, *Charm CP: ΔA_{CP} and Radiative decays*, in *37th International Symposium on Lattice Field Theory*, 1, 2020, 2001.10014.
- [85] LHCb collaboration, R. Aaij et al., *Observation of the Mass Difference Between Neutral Charm-Meson Eigenstates*, *Phys. Rev. Lett.* **127** (2021) 111801, [2106.03744].
- [86] H. N. Nelson, *Compilation of $D^0 \rightarrow \bar{D}^0$ mixing predictions*, in *Lepton and photon interactions at high energies. Proceedings, 19th International Symposium, LP'99, Stanford, USA, August 9-14, 1999*, 8, 1999, hep-ex/9908021.
- [87] A. A. Petrov, *Charm physics: Theoretical review*, *eConf* **C030603** (2003) MEC05, [hep-ph/0311371].

- [88] M. Beneke, G. Buchalla and I. Dunietz, *Width Difference in the $B_s - \bar{B}_s$ System*, *Phys. Rev. D* **54** (1996) 4419–4431, [[hep-ph/9605259](#)].
- [89] M. Beneke, G. Buchalla, C. Greub, A. Lenz and U. Nierste, *Next-to-leading order QCD corrections to the lifetime difference of $B(s)$ mesons*, *Phys. Lett. B* **459** (1999) 631–640, [[hep-ph/9808385](#)].
- [90] A. Dighe, T. Hurth, C. Kim and T. Yoshikawa, *Measurement of the lifetime difference of B_d mesons: Possible and worthwhile?*, *Nucl. Phys. B* **624** (2002) 377–404, [[hep-ph/0109088](#)].
- [91] M. Beneke, G. Buchalla, A. Lenz and U. Nierste, *CP asymmetry in flavor specific B decays beyond leading logarithms*, *Phys. Lett. B* **576** (2003) 173–183, [[hep-ph/0307344](#)].
- [92] M. Ciuchini, E. Franco, V. Lubicz, F. Mescia and C. Tarantino, *Lifetime differences and CP violation parameters of neutral B mesons at the next-to-leading order in QCD*, *JHEP* **08** (2003) 031, [[hep-ph/0308029](#)].
- [93] A. Lenz and U. Nierste, *Theoretical update of $B_s - \bar{B}_s$ mixing*, *JHEP* **06** (2007) 072, [[hep-ph/0612167](#)].
- [94] A. Bazavov et al., *Short-distance matrix elements for D^0 -meson mixing for $N_f = 2 + 1$ lattice QCD*, *Phys. Rev.* **D97** (2018) 034513, [[1706.04622](#)].
- [95] PARTICLE DATA GROUP collaboration, M. Tanabashi et al., *Review of Particle Physics*, *Phys. Rev. D* **98** (2018) 030001.
- [96] CKMFITTER GROUP collaboration, J. Charles, A. Hocker, H. Lacker, S. Laplace, F. Le Diberder, J. Malcles et al., *CP violation and the CKM matrix: Assessing the impact of the asymmetric B factories*, *Eur. Phys. J. C* **41** (2005) 1–131, [[hep-ph/0406184](#)].

- [97] FLAVOUR LATTICE AVERAGING GROUP collaboration, S. Aoki et al., *FLAG Review 2019: Flavour Lattice Averaging Group (FLAG)*, *Eur. Phys. J. C* **80** (2020) 113, [1902.08191].
- [98] E. Golowich and A. A. Petrov, *Short distance analysis of $D^0 - \bar{D}^0$ mixing*, *Phys. Lett. B* **625** (2005) 53–62, [hep-ph/0506185].
- [99] H. Georgi, *$D - \bar{D}$ mixing in heavy quark effective field theory*, *Phys. Lett. B* **297** (1992) 353–357, [hep-ph/9209291].
- [100] T. Ohl, G. Ricciardi and E. H. Simmons, *$D - \bar{D}$ mixing in heavy quark effective field theory: The Sequel*, *Nucl. Phys. B* **403** (1993) 605–632, [hep-ph/9301212].
- [101] I. I. Bigi and N. G. Uraltsev, *$D^0 - \bar{D}^0$ oscillations as a probe of quark hadron duality*, *Nucl. Phys. B* **592** (2001) 92–106, [hep-ph/0005089].
- [102] M. Bobrowski, A. Lenz and T. Rauh, *Short distance $D - \bar{D}$ mixing*, in *Proceedings, 5th International Workshop on Charm Physics (Charm 2012): Honolulu, Hawaii, USA, May 14-17, 2012*, 8, 2012, 1208.6438.
- [103] T. Jubb, M. Kirk, A. Lenz and G. Tetlalmatzi-Xolocotzi, *On the ultimate precision of meson mixing observables*, *Nucl. Phys.* **B915** (2017) 431–453, [1603.07770].
- [104] H. Umeeda, *Quark-hadron duality for heavy meson mixings in the 't Hooft model*, 2106.06215.
- [105] A. F. Falk, Y. Grossman, Z. Ligeti and A. A. Petrov, *$SU(3)$ breaking and $D^0 - \bar{D}^0$ mixing*, *Phys. Rev. D* **65** (2002) 054034, [hep-ph/0110317].
- [106] H.-Y. Cheng and C.-W. Chiang, *Long-Distance Contributions to $D^0 - \bar{D}^0$ Mixing Parameters*, *Phys. Rev. D* **81** (2010) 114020, [1005.1106].

- [107] H.-Y. Jiang, F.-S. Yu, Q. Qin, H.-n. Li and C.-D. Lü, *D^0 - \bar{D}^0 mixing parameter y in the factorization-assisted topological-amplitude approach*, *Chin. Phys. C* **42** (2018) 063101, [1705.07335].
- [108] E. Golowich, S. Pakvasa and A. A. Petrov, *New Physics contributions to the lifetime difference in $D^0 - \bar{D}^0$ mixing*, *Phys. Rev. Lett.* **98** (2007) 181801, [hep-ph/0610039].
- [109] E. Golowich, J. Hewett, S. Pakvasa and A. A. Petrov, *Implications of $D^0 - \bar{D}^0$ Mixing for New Physics*, *Phys. Rev. D* **76** (2007) 095009, [0705.3650].
- [110] M. Bobrowski, A. Lenz, J. Riedl and J. Rohrwild, *How much space is left for a new family of fermions?*, *Phys. Rev. D* **79** (2009) 113006, [0902.4883].
- [111] BELLE-II collaboration, F. Abudinén et al., *Precise measurement of the D^0 and D^+ lifetimes at Belle II*, 2108.03216.
- [112] K. Chetyrkin and M. Steinhauser, *The Relation between the \overline{MS} -bar and the on-shell quark mass at order α_s^3* , *Nucl. Phys. B* **573** (2000) 617–651, [hep-ph/9911434].
- [113] K. Chetyrkin and M. Steinhauser, *Short distance mass of a heavy quark at order α_s^3* , *Phys. Rev. Lett.* **83** (1999) 4001–4004, [hep-ph/9907509].
- [114] K. Melnikov and T. v. Ritbergen, *The Three loop relation between the \overline{MS} -bar and the pole quark masses*, *Phys. Lett. B* **482** (2000) 99–108, [hep-ph/9912391].
- [115] W. A. Bardeen, A. J. Buras, D. W. Duke and T. Muta, *Deep Inelastic Scattering Beyond the Leading Order in Asymptotically Free Gauge Theories*, *Phys. Rev. D* **18** (1978) 3998.
- [116] I. I. Y. Bigi, M. A. Shifman, N. Uraltsev and A. I. Vainshtein, *High power n of m_b in beauty widths and $n = 5 \rightarrow \infty$ limit*, *Phys. Rev. D* **56** (1997) 4017–4030, [hep-ph/9704245].

- [117] M. Fael, K. Schönwald and M. Steinhauser, *Relation between the $\overline{\text{MS}}$ and the kinetic mass of heavy quarks*, *Phys. Rev. D* **103** (2021) 014005, [2011.11655].
- [118] A. H. Hoang, Z. Ligeti and A. V. Manohar, *B decay and the Upsilon mass*, *Phys. Rev. Lett.* **82** (1999) 277–280, [hep-ph/9809423].
- [119] A. H. Hoang, Z. Ligeti and A. V. Manohar, *B decays in the Upsilon expansion*, *Phys. Rev. D* **59** (1999) 074017, [hep-ph/9811239].
- [120] M. Beneke, *A Quark mass definition adequate for threshold problems*, *Phys. Lett. B* **434** (1998) 115–125, [hep-ph/9804241].
- [121] Q. Ho-kim and X.-Y. Pham, *Exact One Gluon Corrections for Inclusive Weak Processes*, *Annals Phys.* **155** (1984) 202.
- [122] G. Altarelli and S. Petrarca, *Inclusive beauty decays and the spectator model*, *Phys. Lett.* **B261** (1991) 303–310.
- [123] M. B. Voloshin, *QCD radiative enhancement of the decay $b \rightarrow c\bar{c}s$* , *Phys. Rev.* **D51** (1995) 3948–3951, [hep-ph/9409391].
- [124] E. Bagan, P. Ball, V. M. Braun and P. Gosdzinsky, *Charm quark mass dependence of QCD corrections to nonleptonic inclusive B decays*, *Nucl. Phys.* **B432** (1994) 3–38, [hep-ph/9408306].
- [125] E. Bagan, P. Ball, B. Fiol and P. Gosdzinsky, *Next-to-leading order radiative corrections to the decay $b \rightarrow c\bar{c}s$* , *Phys. Lett.* **B351** (1995) 546–554, [hep-ph/9502338].
- [126] A. Lenz, U. Nierste and G. Ostermaier, *Penguin diagrams, charmless B decays and the missing charm puzzle*, *Phys. Rev.* **D56** (1997) 7228–7239, [hep-ph/9706501].
- [127] A. Lenz, U. Nierste and G. Ostermaier, *Determination of the CKM angle gamma and $|V_{ub}/V_{cb}|$ from inclusive direct CP asymmetries and branching*

- ratios in charmless B decays*, *Phys. Rev.* **D59** (1999) 034008, [hep-ph/9802202].
- [128] F. Krinner, A. Lenz and T. Rauh, *The inclusive decay $b \rightarrow c\bar{c}s$ revisited*, *Nucl. Phys.* **B876** (2013) 31–54, [1305.5390].
- [129] A. Czarnecki and K. Melnikov, *Two loop QCD corrections to semileptonic b decays at maximal recoil*, *Phys. Rev. Lett.* **78** (1997) 3630–3633, [hep-ph/9703291].
- [130] A. Czarnecki and K. Melnikov, *Two - loop QCD corrections to semileptonic b decays at an intermediate recoil*, *Phys. Rev.* **D59** (1999) 014036, [hep-ph/9804215].
- [131] T. van Ritbergen, *The Second order QCD contribution to the semileptonic $b \rightarrow u$ decay rate*, *Phys. Lett.* **B454** (1999) 353–358, [hep-ph/9903226].
- [132] K. Melnikov, *$\mathcal{O}(\alpha_s^2)$ corrections to semileptonic decay $b \rightarrow c\bar{\nu}_l$* , *Phys. Lett.* **B666** (2008) 336–339, [0803.0951].
- [133] A. Pak and A. Czarnecki, *Heavy-to-heavy quark decays at NNLO*, *Phys. Rev.* **D78** (2008) 114015, [0808.3509].
- [134] A. Pak and A. Czarnecki, *Mass effects in muon and semileptonic $b \rightarrow c$ decays*, *Phys. Rev. Lett.* **100** (2008) 241807, [0803.0960].
- [135] M. Dowling, A. Pak and A. Czarnecki, *Semi-Leptonic b -decay at Intermediate Recoil*, *Phys. Rev.* **D78** (2008) 074029, [0809.0491].
- [136] R. Bonciani and A. Ferroglia, *Two-Loop QCD Corrections to the Heavy-to-Light Quark Decay*, *JHEP* **11** (2008) 065, [0809.4687].
- [137] S. Biswas and K. Melnikov, *Second order QCD corrections to inclusive semileptonic $b \rightarrow X_c\bar{\nu}_l$ decays with massless and massive lepton*, *JHEP* **02** (2010) 089, [0911.4142].

- [138] M. Brucherseifer, F. Caola and K. Melnikov, *On the $O(\alpha_s^2)$ corrections to $b \rightarrow X_u e \bar{\nu}$ inclusive decays*, *Phys. Lett.* **B721** (2013) 107–110, [1302.0444].
- [139] M. Fael, K. Schönwald and M. Steinhauser, *Third order corrections to the semi-leptonic $b \rightarrow c$ and the muon decays*, 2011.13654.
- [140] M. Czakon, A. Czarnecki and M. Dowling, *Three-loop corrections to the muon and heavy quark decay rates*, *Phys. Rev. D* **103** (2021) L111301, [2104.05804].
- [141] A. Czarnecki, M. Slusarczyk and F. V. Tkachov, *Enhancement of the hadronic b quark decays*, *Phys. Rev. Lett.* **96** (2006) 171803, [hep-ph/0511004].
- [142] B. Blok and M. A. Shifman, *The Rule of discarding $1/N_c$ in inclusive weak decays. 1.*, *Nucl. Phys.* **B399** (1993) 441–458, [hep-ph/9207236].
- [143] B. Blok and M. A. Shifman, *The Rule of discarding $1/N_c$ in inclusive weak decays. 2.*, *Nucl. Phys.* **B399** (1993) 459–476, [hep-ph/9209289].
- [144] I. I. Y. Bigi, B. Blok, M. A. Shifman, N. G. Uraltsev and A. I. Vainshtein, *A QCD 'manifesto' on inclusive decays of beauty and charm*, in *7th Meeting of the APS Division of Particles Fields*, pp. 610–613, 11, 1992, hep-ph/9212227.
- [145] A. Alberti, P. Gambino and S. Nandi, *Perturbative corrections to power suppressed effects in semileptonic B decays*, *JHEP* **01** (2014) 147, [1311.7381].
- [146] T. Mannel, A. A. Pivovarov and D. Rosenthal, *Inclusive semileptonic B decays from QCD with NLO accuracy for power suppressed terms*, *Phys. Lett.* **B741** (2015) 290–294, [1405.5072].
- [147] T. Mannel, A. A. Pivovarov and D. Rosenthal, *Inclusive weak decays of heavy hadrons with power suppressed terms at NLO*, *Phys. Rev.* **D92** (2015) 054025, [1506.08167].

- [148] M. Gremm and A. Kapustin, *Order $1/m_b^3$ corrections to $B \rightarrow X(c)$ lepton anti-neutrino decay and their implication for the measurement of $\bar{\Lambda}$ and λ_1* , *Phys. Rev.* **D55** (1997) 6924–6932, [[hep-ph/9603448](#)].
- [149] T. Mannel and A. A. Pivovarov, *QCD corrections to inclusive heavy hadron weak decays at $\Lambda_{\text{QCD}}^3/m_Q^3$* , *Phys. Rev.* **D100** (2019) 093001, [[1907.09187](#)].
- [150] A. Lenz, M. L. Piscopo and A. V. Rusov, *Contribution of the Darwin operator to non-leptonic decays of heavy quarks*, *JHEP* **12** (2020) 199, [[2004.09527](#)].
- [151] T. Mannel, D. Moreno and A. Pivovarov, *Heavy quark expansion for heavy hadron lifetimes: completing the $1/m_b^3$ corrections*, *JHEP* **08** (2020) 089, [[2004.09485](#)].
- [152] D. Moreno, *Completing $1/m_b^3$ corrections to non-leptonic bottom-to-up-quark decays*, *JHEP* **01** (2021) 051, [[2009.08756](#)].
- [153] P. Gambino and J. F. Kamenik, *Lepton energy moments in semileptonic charm decays*, *Nucl. Phys. B* **840** (2010) 424–437, [[1004.0114](#)].
- [154] M. Fael, T. Mannel and K. K. Vos, *The Heavy Quark Expansion for Inclusive Semileptonic Charm Decays Revisited*, [1910.05234](#).
- [155] M. Beneke, G. Buchalla, C. Greub, A. Lenz and U. Nierste, *The $B^+ - B_d^0$ Lifetime Difference Beyond Leading Logarithms*, *Nucl. Phys.* **B639** (2002) 389–407, [[hep-ph/0202106](#)].
- [156] E. Franco, V. Lubicz, F. Mescia and C. Tarantino, *Lifetime ratios of beauty hadrons at the next-to-leading order in QCD*, *Nucl. Phys.* **B633** (2002) 212–236, [[hep-ph/0203089](#)].
- [157] A. Lenz and T. Rauh, *D-meson lifetimes within the heavy quark expansion*, *Phys. Rev.* **D88** (2013) 034004, [[1305.3588](#)].
- [158] F. Gabbiani, A. I. Onishchenko and A. A. Petrov, *Λ_b lifetime puzzle in heavy quark expansion*, *Phys. Rev. D* **68** (2003) 114006, [[hep-ph/0303235](#)].

- [159] F. Gabbiani, A. I. Onishchenko and A. A. Petrov, *Spectator effects and lifetimes of heavy hadrons*, *Phys. Rev.* **D70** (2004) 094031, [[hep-ph/0407004](#)].
- [160] FERMILAB LATTICE, MILC, TUMQCD collaboration, A. Bazavov et al., *Up-, down-, strange-, charm-, and bottom-quark masses from four-flavor lattice QCD*, *Phys. Rev.* **D98** (2018) 054517, [[1802.04248](#)].
- [161] P. Gambino, A. Melis and S. Simula, *Extraction of heavy-quark-expansion parameters from unquenched lattice data on pseudoscalar and vector heavy-light meson masses*, *Phys. Rev.* **D96** (2017) 014511, [[1704.06105](#)].
- [162] JLQCD collaboration, S. Aoki et al., *Heavy quark expansion parameters from lattice NRQCD*, *Phys. Rev.* **D69** (2004) 094512, [[hep-lat/0305024](#)].
- [163] A. S. Kronfeld and J. N. Simone, *Computation of Lambda-bar and lambda(1) with lattice QCD*, *Phys. Lett.* **B490** (2000) 228–235, [[hep-ph/0006345](#)].
- [164] V. Gimenez, G. Martinelli and C. T. Sachrajda, *A High statistics lattice calculation of lambda(1) and lambda(2) in the B meson*, *Nucl. Phys.* **B486** (1997) 227–244, [[hep-lat/9607055](#)].
- [165] P. Ball and V. M. Braun, *Next-to-leading order corrections to meson masses in the heavy quark effective theory*, *Phys. Rev.* **D49** (1994) 2472–2489, [[hep-ph/9307291](#)].
- [166] M. Neubert, *QCD sum rule calculation of the kinetic energy and chromo interaction of heavy quarks inside mesons*, *Phys. Lett.* **B389** (1996) 727–736, [[hep-ph/9608211](#)].
- [167] D. King, A. Lenz and T. Rauh, *B_s mixing observables and $|V_{td}/V_{ts}|$ from sum rules*, *JHEP* **05** (2019) 034, [[1904.00940](#)].
- [168] R. Bause, M. Golz, G. Hiller and A. Tayduganov, *The new physics reach of null tests with $D \rightarrow \pi \ell \ell$ and $D_s \rightarrow K \ell \ell$ decays*, *Eur. Phys. J. C* **80** (2020) 65, [[1909.11108](#)].

- [169] S. de Boer and G. Hiller, *Flavor and new physics opportunities with rare charm decays into leptons*, *Phys. Rev. D* **93** (2016) 074001, [1510.00311].
- [170] T. Mannel, A. V. Rusov and F. Shahriaran, *Inclusive semitauonic B decays to order $\mathcal{O}(\Lambda_{QCD}^3/m_b^3)$* , *Nucl. Phys.* **B921** (2017) 211–224, [1702.01089].
- [171] V. A. Novikov, M. A. Shifman, A. I. Vainshtein and V. I. Zakharov, *Calculations in External Fields in Quantum Chromodynamics. Technical Review*, *Fortsch. Phys.* **32** (1984) 585.
- [172] M. L. Piscopo, *Higher order corrections to the lifetime of heavy hadrons*, Ph.D. thesis, Siegen U., 2021. 2112.03137. 10.25819/ubsi/10024.
- [173] W. Kilian and T. Mannel, *QCD corrected $1/m_b$ contributions to $B - \bar{B}$ mixing*, *Phys. Lett. B* **301** (1993) 382–392, [hep-ph/9211333].
- [174] T. Mannel, D. Moreno and A. A. Pivovarov, *The Heavy Quark Expansion for the Charm Quark*, 2103.02058.
- [175] H.-Y. Cheng, *Phenomenological Study of Heavy Hadron Lifetimes*, *JHEP* **11** (2018) 014, [1807.00916].
- [176] FERMILAB LATTICE, MILC, TUMQCD collaboration, A. Bazavov et al., *Up-, down-, strange-, charm-, and bottom-quark masses from four-flavor lattice QCD*, *Phys. Rev. D* **98** (2018) 054517, [1802.04248].
- [177] I. I. Bigi, T. Mannel and N. Uraltsev, *Semileptonic width ratios among beauty hadrons*, *JHEP* **09** (2011) 012, [1105.4574].
- [178] N. Uraltsev, *On the chromomagnetic expectation value μ_G^2 and higher power corrections in heavy flavor mesons*, *Phys. Lett. B* **545** (2002) 337–344, [hep-ph/0111166].
- [179] A. F. Falk and M. Neubert, *Second order power corrections in the heavy quark effective theory. 1. Formalism and meson form-factors*, *Phys. Rev. D* **47** (1993) 2965–2981, [hep-ph/9209268].

- [180] I. I. Y. Bigi, M. A. Shifman, N. G. Uraltsev and A. I. Vainshtein, *On the motion of heavy quarks inside hadrons: Universal distributions and inclusive decays*, *Int. J. Mod. Phys. A* **9** (1994) 2467–2504, [[hep-ph/9312359](#)].
- [181] H.-N. Li, H. Umeeda, F. Xu and F.-S. Yu, *D meson mixing as an inverse problem*, 2001.04079.
- [182] A. F. Falk, Y. Grossman, Z. Ligeti, Y. Nir and A. A. Petrov, *The $D^0 - \bar{D}^0$ mass difference from a dispersion relation*, *Phys. Rev. D* **69** (2004) 114021, [[hep-ph/0402204](#)].
- [183] A. Lenz, *Lifetimes and heavy quark expansion*, *Int. J. Mod. Phys. A* **30** (2015) 1543005, [[1405.3601](#)].
- [184] G. Passarino and M. J. G. Veltman, *One Loop Corrections for $e^+ e^-$ Annihilation Into $\mu^+ \mu^-$ in the Weinberg Model*, *Nucl. Phys. B* **160** (1979) 151–207.
- [185] B. A. Kniehl, *Dispersion relations in loop calculations*, *Acta Phys. Polon. B* **27** (1996) 3631–3644, [[hep-ph/9607255](#)].